

DISSERTATION

EVALUATING SOIL PRODUCTIVITY AND CLIMATE CHANGE BENEFITS OF WOODY BIOCHAR SOIL
AMENDMENTS FOR THE US INTERIOR WEST

Submitted by

Matthew Alan Ramlow

Graduate Degree Program in Ecology

In partial fulfillment of the requirements

For the Degree of Doctor of Philosophy

Colorado State University

Fort Collins, Colorado

Summer 2018

Doctoral Committee:

Advisor: M. Francesca Cotrufo

Stephen Ogle

Charles C. Rhoades

Joseph von Fischer

Copyright by Matthew Alan Ramlow 2018

All Rights Reserved

ABSTRACT

EVALUATING SOIL PRODUCTIVITY AND CLIMATE CHANGE BENEFITS OF WOODY BIOCHAR SOIL AMENDMENTS FOR THE US INTERIOR WEST

Managing our lands to provide for today and the future requires sustainable land management practices that enhance productivity while reducing climate impacts. Proponents claim biochar soil amendments offer a comprehensive solution to enhance soil capacity to deliver water and nutrients to plants while decreasing climate impacts through reduced nitrous oxide (N₂O) emissions from fertilizer use and carbon (C) sequestration. This dissertation evaluates such claims for woody biochar applications within the US Interior West; to enhance crop production and reduce N₂O emissions in deficit irrigation agricultural systems, and to support forest road restoration efforts. It also employs laboratory incubations and soil biogeochemical modeling to predict and to better understand the controls on biochar's greenhouse gas mitigation potential. The field studies demonstrate that this woody biochar improved soil moisture content but its enhanced capacity to retain water did not alleviate plant water stress when water inputs were low. Similarly, in forest soils, this woody biochar amendment improved plant available N but at levels that did not impact productivity. In lab incubations this woody biochar reduced N₂O emissions. While this reduction could not be explained by bulk soil mineral N transformations, the soil moisture regime did affect biochar's ability to reduce N₂O emissions. Despite the observed biochar N₂O emission reductions in incubated soils, under field conditions biochar effects on N₂O emissions were inconclusive. When evaluating biochar's C sequestration potential, soil biogeochemical modeling revealed that 59 percent of the biochar C applied will be sequestered in soils after 100 years. Losses from biochar fragmentation and leaching may constitute a considerable proportion of the C losses. Of the applications considered, C sequestration remains the most promising use for biochar soil amendments within the US Interior West.

ACKNOWLEDGEMENTS

This research would not have been possible without support from the many individuals who provided the training, technical assistance, editing and new insights throughout my studies. I am extremely grateful for the guidance provided by my advisor Dr. M. Francesca Cotrufo. I also appreciate the advising I received from my committee members Dr. Stephen Ogle, Dr. Charles C. Rhoades and Dr. Joseph von Fischer along with my collaborators Dr. Andy Robertson, Dr. Erika Foster, Dr. Steve del Grosso and Dr. Keith Paustian.

I could not have completed this work without generous assistance in the laboratory and field. I would like to thank M. Haddix, D. Reuss, G. Beresford, J.R. Hermann, T. Fegel, D. Pierson, S. Mosier, J. Berlejung, S. Uhle, B. Orth, N. Bradley, S. Block, R. Tyler, R. Even, S. Katz, D. Song, J. Zanini, F. Luiz and C. Bliss for their technical support in these studies.

I would like to thank my family and friends for their encouragement both leading up to and during my program. I also would like to thank my partner Sarah who has always been there for me to provide motivation and positivity throughout the process.

TABLE OF CONTENTS

ABSTRACT.....	ii
ACKNOWLEDGEMENTS.....	iii
1. INTRODUCTION.....	1
2. WOODY BIOCHAR’S GREENHOUSE GAS MITIGATION POTENTIAL ACROSS AGRICULTURAL SOILS, FERTILIZATION AND SOIL MOISTUE REGIMES	5
2.1. Introduction	5
2.2. Materials and Methods.....	8
2.2.1. Materials	9
2.2.2. Experimental Design	10
2.2.3. GHG Efflux.....	12
2.2.4. Soil and Biochar Analysis.....	12
2.2.5. Data and Statistical Analysis	13
2.3. Results.....	14
2.3.1. Biochar’s Impact on C Sequestration and GHG Efflux by Soil Types and Fertilization.....	14
2.3.2. Biochar’s Impact on Mineral N Dynamics by Soil Types and Fertilization	18
2.3.3. Biochar’s Impact on GHG Efflux by Soil Moisture Regime.....	21
2.3.4. Biochar’s Impact on Mineral N by Soil Moisture Regime	24
2.3.5. Biochar’s GHG Mitigation Potential	25
2.4. Discussion.....	26
2.4.1. C Sequestration	26
2.4.2. CO ₂ Impacts.....	27
2.4.3. CH ₄ Impacts	27
2.4.4. N ₂ O Impacts	28
2.4.5. Toward Biochar Application as a GHG Mitigation Technology	33
3. BROADCAST WOODY BIOCHAR PROVIDES LIMITED BENEFITS TO DEFICIT IRRIGATION MAIZE IN COLORADO.....	35
3.1. Introduction	35
3.2. Materials and Methods.....	38
3.2.1. Site Description and Experimental Design.....	38
3.2.2. Biochar and Fertilizer Application.....	39
3.2.3. Soil C and Bulk Density Sampling	40

3.2.4.	Soil Moisture Sampling and Water Stress Coefficient	41
3.2.5.	Soil Mineral N Sampling	42
3.2.6.	Maize Biomass and Yield Sampling	42
3.2.7.	Soil GHG Flux Sampling	43
3.2.7.1.	Static Chamber-GC N ₂ O Sampling	43
3.2.7.2.	Automatic Chamber-CRDS GHG Sampling	44
3.2.8.	Data and Statistical Analysis	44
3.3.	Results	45
3.3.1.	Biochar increased soil moisture but did not reduce crop water stress	45
3.3.2.	Biochar did not improve crop yield or biomass	47
3.3.3.	Biochar did not impact soil mineral N availability or crop N uptake	48
3.3.4.	Biochar sequesters C but provides limited GHG benefits from N ₂ O reduction	49
3.4.	Discussion	52
3.4.1.	Biochar effects on soil moisture and soil field capacity	52
3.4.2.	Biochar and deficit irrigation effect on grain and biomass yield	54
3.4.3.	Biochar effects on N availability	55
3.4.4.	Biochar effects on GHG emission reductions and C sequestration	56
3.4.4.1.	Biochar impacts on C sequestration and mobility	56
3.4.4.2.	Biochar impacts on N ₂ O emissions	57
3.5.	Conclusions	58
4.	PROMOTING REVEGETATION AND SOIL CARBON SEQUESTRATION ON DECOMISSIONED FOREST ROADS IN COLORADO, USA: A COMPARATIVE ASSESSMENT OF ORGANIC SOIL AMENDMENTS	60
4.1.	Introduction	60
4.2.	Materials and Methods	65
4.2.1.	Study Site and Experimental Design	65
4.2.2.	Materials	65
4.2.3.	Cover and Biomass	66
4.2.4.	Soil Moisture	66
4.2.5.	Mineral Nitrogen Sampling	67
4.2.6.	Carbon and Nitrogen Mineralization Assays and Soil pH	68
4.2.7.	Soil Total Carbon and Nitrogen and Bulk Density	69
4.2.8.	Statistical Analyses	69
4.3.	Results	70

4.3.1.	Cover and Biomass.....	70
4.3.2.	Soil Moisture	72
4.3.3.	Mineral Nitrogen Availability	74
4.3.4.	Carbon and Nitrogen Mineralization Assays and Soil pH.....	76
4.3.5.	Soil Total Carbon and Nitrogen and Bulk Density	79
4.3.6.	Soil Factors and Processes Influencing Revegetation	81
4.4.	Discussion.....	82
4.4.1.	Soil Amendments’ Impact on Revegetation	82
4.4.1.1.	Organic Fertilizer	82
4.4.1.2.	Wood Strand Mulch	83
4.4.1.3.	Biochar	85
4.4.2.	Importance of Biological Soil Processes for Revegetation.....	86
4.4.3.	Soil Amendments’ Impact on Carbon Sequestration.....	87
4.4.3.1.	Wood Strand Mulch	87
4.4.3.2.	Biochar	88
4.4.4.	Management Implications	88
5.	ESTIMATING BIOCHAR’S CARBON SEQUESTRATION POTENTIAL AND ITS MAJOR CONTROLS	90
5.1.	Introduction	90
5.2.	Materials and Methods.....	95
5.2.1.	Model Structure and Assumptions	95
5.2.2.	Model Simulations	100
5.2.3.	Evaluating Model Sensitivities and Uncertainty	101
5.2.3.1.	Baseline Scenario – Feedstock Decomposition and Stabilization in Soil	102
5.2.3.2.	Biochar Scenario – Biochar Decomposition	102
5.2.3.3.	Biochar Scenario – Biochar Stabilization in Soils.....	104
5.3.	Results.....	104
5.3.1.	Baseline Scenario – Sensitivity to Feedstock Decomposition and Stabilization in Soil.....	106
5.3.2.	Biochar Scenario – Sensitivity to Biochar Decay	107
5.3.3.	Biochar Scenario – Biochar Stabilization in Soils.....	109
5.4.	Discussion.....	109
5.5.	Conclusions	111
6.	CONCLUSION.....	112
	REFERENCES.....	114

APPENDICES	132
Appendix 1. Chapter 2 Supplementary Information.....	132
Appendix 2. Chapter 3 Supplementary Information.....	134
Appendix 3. Chapter 4 Supplementary Information.....	139
Appendix 4. Chapter 5 Supplementary Information.....	142

1. INTRODUCTION

Climate change poses a major threat to the stability of both natural and argoecosystems. Curtailing anthropogenic impacts on Earth's climate system requires a broad suite of technologies, with growing evidence that negative emissions technologies are required to stabilize climate impacts (Fuss *et al.*, 2014). With 24% of global emissions, the agriculture, forestry and other land use sector offers many opportunities to not only mitigate greenhouse gas (GHG) emissions but also sequester carbon (C) (Smith *et al.*, 2014). One C sequestration practice that has received growing attention over the past two decades is the use of biochar soil amendments. Biochar, the solid product of pyrolyzing sustainably-sourced feedstocks, offers a promising strategy with studies showing it can sequesters C in soils, improve soil fertility and reduce nitrous oxide (N₂O) emissions from applying nitrogen (N) to soils (Lehmann *et al.*, 2006; Sohi *et al.*, 2010). While much of the early biochar research focused on identifying and confirming these claims, there is now a need to evaluate and understand their effectiveness in real-world applications if biochar is to be widely adopted as a sustainable land management practice.

Biochar's ability to impact soil function stems from its unique chemical and physical structure. During pyrolysis, the majority of the feedstock is converted to volatiles, light hydrocarbons and condensable organic compounds. The 10 to 40 percent of the feedstock mass remaining is largely transformed into aromatic C compounds with varying degrees of polymerization (Neves *et al.* 2011). This biochar C can be generally characterized by two pools; a small labile fraction and a larger recalcitrant fraction that is more resistant to mineralization (Wang *et al.*, 2016). During pyrolysis, the internal porosity of the feedstock's cellular structure is largely maintained, which controls biochar macro-porosity and additional micro-porosity can develop due to chemical alterations as amorphous C compounds are converted to more crystalline graphene sheets (Gray *et al.*, 2014; Lian *et al.* 2017). Through both this increased

intraporosity of the biochar itself, and increased interporosity between soil particles, due to biochar's irregular shape, biochar can improve soil aeration and retain more water in soils (Liu *et al.*, 2017). Biochar's surface chemistry combined with its high surface area can also play an important role in controlling biochar's polarity and hydrophobicity, which can improve biochar's ion-exchange and water retention capacity (Clough *et al.*, 2013; Gray *et al.*, 2014). While our understanding of biochar properties has greatly evolved over the past decade, the practical benefits resulting from these properties must also be realized in land management applications.

When considering possible applications for biochar, its impacts on soil moisture may provide an important benefit to agroecosystems and ecological restoration practices. Variability in precipitation regimes under climate change coupled with increased demands on water resources requires improvements in agricultural water use efficiency. Irrigation is a major consumer of water resources and innovative new strategies to enhance agricultural water use efficiency are required (Wada & Bierkens, 2014). Biochar's ability to improve soil water retention may allow for irrigation strategies that apply less water while maintaining or even improving productivity. Likewise, biochar may also serve an important role in revegetating sites with low organic matter content and capacity for water retention.

Biochar impacts on N availability and transformation may also provide soil fertility benefits that land managers can utilize. Despite many innovations in agricultural practices, N fertilizer use efficiency remains low with up to 50 to 80 percent of the N applied to croplands lost to the environment (Sharma & Bali, 2018). Such N losses increase reactive N in our landscapes and further exacerbate climate change through emissions of N₂O. Biochar has been shown to alleviate such impacts through its increased ion-exchange capacity allowing for N retention, which may prevent leaching losses or transformation to gaseous N compounds. This could improve agricultural N use efficiency, allowing for decreased N fertilizer application and fewer losses of reactive N, and extend the efficacy of N inputs used in ecological restoration (Biederman & Harpole, 2013).

Perhaps the most established rationale for biochar production and application is its ability to mitigate GHG emissions, primarily by sequestering C in soil. Biochar was first identified as an effective soil amendment due to its long-term stability and potential to sequester C in soils (Glaser *et al.*, 2001). Biochar's biochemical recalcitrance allows for increased C sequestration beyond the soil mineral fraction's capacity to stabilize organic matter, giving it some of the greatest potential for long term soil C sequestration relative to other practices (Griscom *et al.*, 2017). Studies also indicate biochar has great potential to mitigate N₂O emissions coming from fertilizer use (Cayuela *et al.*, 2015), although the mechanism for these effects and widespread demonstration in the field are still not fully realized. Despite over two decades of research on biochar stability it has yet to be widely implemented as a climate change solution with policymakers unsure how to manage uncertainty in estimates for biochar stability (Bach *et al.*, 2016). Biochar's ability to mitigate GHG emissions and sequester C in soil must be critically evaluated and, if it is a viable strategy, quantitative predictions are required to advance the necessary incentives for its adoption.

When considering the full sustainability of biochar applications, one must also consider the context; from the sourcing of biochar feedstocks, to utilization. In the Interior West region of the United States, woody fuels from bark-beetle outbreaks have emerged as a sustainable feedstock that otherwise pose a forest fire risk (Adams, 2013). Within the region, potential biochar applications include enhancing agricultural resource use efficiency, restoration of degraded forest ecosystems or reclamation of acid mine soils. Linking potential benefits from biochar application with the cost for treatment of woody fuels may offer economic incentives if such biochar benefits can be achieved.

The objective of my research is to understand how biochar's impact on water and N influence its ability to enhance productivity, reduce GHG emissions and increase soil C stocks. I address this by evaluating biochar applications relevant to the US Interior West using a woody biochar sourced from beetle-killed

forests. In these applications I explore biochar's impact on productivity and GHG mitigation with the following specific questions:

1. Can biochar's ability to improve soil water retention increase productivity in deficit irrigation agriculture and forest restoration efforts, and why or why not?
2. How does biochar impact soil N availability and transformation in field applications, and how do such impacts on N relate to biochar's effects on productivity or N₂O emission?
3. Does biochar reduce N₂O emissions in deficit irrigation applications and what are the controls on biochar's ability to mitigate N₂O emissions?
4. What is the uncertainty in biochar's C sequestration potential and what are some of the primary factors controlling biochar's ability to sequester C?

I explore these questions using laboratory incubations, field studies and soil biogeochemical models as detailed in the following chapters.

2. WOODY BIOCHAR'S GREENHOUSE GAS MITIGATION POTENTIAL ACROSS AGRICULTURAL SOILS, FERTILIZATION AND SOIL MOISTURE REGIMES¹

2.1. Introduction

Applying biochar, the solid product of organic matter pyrolysis, as an amendment to agricultural soils can provide an integrated strategy to address waste management, bioenergy production, soil fertility and GHG mitigation (Lehmann, 2007). Globally, biochar amendments to soils have an estimated potential to provide 1 to 1.8 Pg CO₂-eq in GHG emission reductions (Paustian *et al.*, 2016). In agricultural applications, biochar amendments have potential to reduce GHG emissions by sequestering C in the biochar applied to soils (i.e., due to slower mineralization of the pyrolyzed biomass to CO₂), increasing soil CH₄ consumption, decreasing soil N₂O emissions and improving soil fertility to decrease the yield-scaled emissions (Brassard *et al.*, 2016; Mandal *et al.*, 2016; Smith, 2016). Understanding biochar's impact on individual GHG fluxes across a range of agricultural soils, fertilization and soil moisture regimes can help target the most promising applications and identify mechanisms responsible for biochar's full GHG mitigation potential in soils.

C sequestration is one of the earliest and most widely established benefits of biochar application (Lehmann *et al.*, 2006), stemming from early research on the persistence of black carbon in Terra Preta soils (Glaser *et al.*, 2001). Biochar's recalcitrant chemical structure (Paris, 2005; Spokas, 2010), ability to promote soil aggregation (Soenne *et al.*, 2014) and interaction with mineral phases and soil organic matter (SOM) all contribute to the stabilization of biochar in soils, thus providing a C sink at the centuries timescale (Lehmann *et al.*, 2007; Preston & Schmidt, 2006). Biochar application may also have indirect effects on native soil organic carbon (SOC), either stimulating or preventing mineralization of

¹ Ramlow, M., Cotrufo, M.F. (2018). "Woody biochar's greenhouse gas mitigation potential across fertilized and unfertilized agricultural soils and soil moisture regimes". *GCB Bioenergy*, **10**, 108-122.

© 2017 Ramlow M & Cotrufo MF. Global Change Biology Bioenergy Published by John Wiley & Sons Ltd
This is an open access article under the terms of the Creative Commons Attribution License, which permits use, distribution and reproduction in any medium, provided the original work is properly cited.

native SOM (Cross & Sohi, 2011; Stewart *et al.*, 2013). A recent meta-analysis of biochar impacts on CO₂ in upland soils shows biochar to have a range of responses depending on soil type but overall no significant effect on priming soil C (Liu *et al.*, 2016).

Research on how biochar impacts CH₄ production and consumption in agricultural soils is less developed. Generally, agricultural CH₄ fluxes are dominated by CH₄ emissions from flooded irrigation systems and manure management, while upland agricultural soils provide a moderate CH₄ sink (Mosier *et al.*, 1998). A recent meta-analysis of biochar's effect on CH₄ emissions and uptake found that biochar has potential to mitigate CH₄ emissions under flood irrigation management regimes but may decrease the CH₄ sink in upland agricultural systems (Jeffery *et al.*, 2016). Possible mechanisms influencing CH₄ uptake include biochar decreasing the ratio of methanogens to methanotrophs (Feng *et al.*, 2012), possibly through pH mediated effects (Jeffery *et al.*, 2016), directly adsorbing CH₄ (Sadasivam & Reddy, 2014) or aerating soils (Karhu *et al.*, 2011).

Agricultural soils are the leading contributor to N₂O emissions in many countries world-wide due to microbial transformation of reactive N added through excessive fertilizer application and promotion of N fixing crops (Bouwman, 1996). In laboratory incubations, biochar has been shown to decrease N₂O efflux on average by 54%, with contrasting effects by soil type (Cayuela *et al.*, 2015; Cayuela *et al.*, 2014), but results from field trials are beginning to challenge such findings (Verhoeven *et al.*, 2017). Numerous mechanisms for biochar N₂O reductions have been proposed, which can be generally categorized as 1) biochar decreasing nitrification or denitrification rates (van Zwieten *et al.*, 2014; Wang *et al.*, 2015), 2) biochar decreasing the N₂O/N₂ product ratio of denitrification (Cayuela *et al.*, 2013; Obia *et al.*, 2015; Xu *et al.*, 2014) or 3) biochar impacting diffusion of N₂O from soils (Cornelissen, *et al.*, 2013; Harter *et al.*, 2016; Quin *et al.*, 2015). While many studies have explored the effects of biochar under anaerobic conditions, which are most favorable to N₂O production (Baggs & Bateman, 2005), research on biochar's ability to reduce N₂O under aerated soils is more limited. Some studies indicate biochar can actually

increase N₂O production under aerobic conditions where nitrification may be the dominant N₂O formation pathway (Sánchez-García, 2014; Wells & Baggs, 2014).

Biochar's effects on GHG emissions vary greatly depending on biochar feedstock (Mandal *et al.*, 2016). Biochar produced from woody feedstocks has higher porosity and surface area, and lower H:C_{org}, O:C_{org}, volatiles and ash contents as compared to other biochars (Enders *et al.*, 2012; Kloss *et al.*, 2012; Ronsse *et al.*, 2013). These characteristics are correlated with increased C stability of biochar (Crombie *et al.*, 2013; Spokas, 2010), increased CH₄ oxidation in upland soils (Brassard *et al.*, 2016) and greater N₂O emission mitigation potential (Cayuela *et al.*, 2015), making woody biochar a prime candidate for GHG mitigation. In many forested regions of the western United States, there is an oversupply of woody fuels that require management, due to mortality from beetle outbreaks, fire suppression efforts and declining timber markets (Adams, 2013; Hicke *et al.*, 2012; Noss *et al.*, 2006). Producing biochar from these woody fuels and applying it to agricultural soils could serve to produce bioenergy, manage residues and reduce emissions from agriculture (Field *et al.*, 2013). A mechanistic understanding of how biochar impacts GHG emission across agricultural soils, in interaction with N availability and across soil moisture regimes, is necessary to implement successful biochar GHG mitigation programs. This study explores the GHG mitigation potential of a beetle-killed pine biochar soil amendment along a gradient of agricultural soil properties, nitrogen (N) fertilization treatments and soil moisture regimes and determines how these edaphic factors influence woody biochar's GHG mitigation potential.

The objectives of this research are to: 1) quantify the full GHG mitigation potential of a woody biochar by identifying the conditions that maximize C sequestration and GHG emission reductions across different agricultural soils, N fertilization levels and soil moisture regimes; 2) assess mineral N dynamics within the bulk soil and on biochar isolates to evaluate how soil properties, N fertilization and soil moisture regime impact biochar's ability to mitigate N₂O efflux. We hypothesize that the C sequestration of biochar provides the greatest potential to mitigate GHG emissions when compared on an annualized

CO₂-eq basis, but this will vary by soil type, with high SOC soil retaining more biochar C. Relative to C sequestration, we expect biochar to have a significantly smaller impact on CO₂ and CH₄ emissions. We hypothesize biochar can provide significant reductions in N₂O emissions but effects will vary by soil properties, fertilization and soil moisture. Of the processes impacting soil N₂O efflux, we expect biochar to decrease N₂O efflux relative to unamended control soils by: 1) reducing net N mineralization, resulting in greater N₂O reductions in soils with more total N; 2) causing surface interactions with mineral N in the soil solution to prevent N transformation, resulting in N retention on biochar isolates and greater percent N₂O reductions in N fertilized treatments; 3) impacting the relative amounts of N undergoing nitrification versus denitrification, with biochar treatments exhibiting more aerobic conditions thus decreasing N₂O production from denitrification under anaerobic soil moisture regimes.

2.2. Materials and Methods

We tested these hypotheses in two lab incubations where biochar's full GHG mitigation potential was measured over a 30 or 60-day period. In experiment 1 (E1), under aerobic conditions we tested how N fertilization and soil properties, including pH, SOM content and soil texture, regulate biochar's impacts on GHG efflux, SOC stocks and mineral N dynamics. In experiment 2 (E2), on one of the fertilized soils across a range of moisture contents, we tested how soil moisture regime regulates biochar's impacts on GHG efflux and mineral N dynamics.

Table 1: Soil properties for the four temperate agricultural soils used in the incubation, including mean annual temperature (MAT) and mean annual precipitation (MAP) for the site, and bulk density (BD), sand (Sa), silt (Si), clay (Cl), total organic carbon (TOC), total inorganic carbon (TIC), total nitrogen (TN) and BET surface area of the soils. Analytical error (n=3) presented in parenthesis, where available.

Site	Land Use	MAT (°C)	MAP (mm)	BD (g/cm ³)	Soil Properties						pH	BET (m ² /g)
					Sa	Si	Cl	TOC (%)	TIC (%)	TN (%)		
Fort Collins, Colorado (CO)	Cultivated maize	9	276	1.06 (±0.02)	35	32	34	0.81 (±0.01)	0.43 (±0.00)	0.13 (±0.00)	7.99 (±0.10)	36.8
Carey, Idaho (ID)	Rangeland	7	278	0.93 (±0.02)	28	54	19	5.69 (±0.12)	0.02 (±0.00)	0.52 (±0.01)	5.86 (±0.12)	11.2
Mandan, North Dakota (ND)	Cultivated wheat	5	402	0.94 (±0.00)	11	60	29	2.38 (±0.01)	0.03 (±0.00)	0.24 (±0.00)	7.27 (±0.06)	20.0
Vernon, Texas (TX)	Cultivated wheat	17	665	1.00 (±0.01)	14	50	36	0.91 (±0.01)	0.03 (±0.01)	0.11 (±0.00)	8.04 (±0.26)	49.4

2.2.1. Materials

The four agricultural soils represent a gradient of pH, SOM content and soil texture (Table 1). Soils were sampled to a 10 cm depth using 4 soil pits per site then consolidating samples into a single air-tight bag. Soil samples were sieved to 2mm, air dried and stored prior to the incubation. Brunauer-Emmett-Teller (BET) surface area analysis was conducted using a single subsample of oven dried soil using a micromeritics BET surface area and porosity analyzer (ASAP 2020; Micromeritics, Norcross, GA). Soil texture was measured on a single 40g subsample of pre-incubated soils using sedimentation columns (Pansu & Gautheyrou, 2006). Soils were also analyzed for pH, inorganic C, and total C and N as described below.

The woody biochar was produced using a beetle-killed lodgepole pine feedstock, under slow pyrolysis, reaching temperatures of 550°C, by Biochar Now (Berthoud, CO). Biochar was crushed and sieved to obtain a 2 to 2.8 mm size fraction that could be fractionated and recovered for analysis post-incubation. Biochar BET surface area and pH were analyzed using the same

Table 2: Biochar production information along with physical and chemical properties.

Description	Biochar Property
Feedstock	Beetle-killed lodgepole pine
Pyrolysis	Slow pyrolysis, 550°C max temp
Particle Size	Sieved to 2.0-2.8mm
Organic C	81.7 g/100 g biochar
H:C	0.70
C:N	255.3
Ash	1.2 g/100g biochar
pH	8.49
BET	111.89 m ² /g biochar

protocol as for the soils. All other biochar analyses were conducted by the Soil Control Lab (Watsonville, CA 95076) in accordance with International Biochar Initiative protocols (Table 2).

2.2.2. Experimental Design

The E1 treatments consisted of the four agricultural soils (CO, ID, ND and TX; Table 1), two N fertilizer rates (unfertilized and fertilized), and two biochar addition rates (0 and 2.5% by weight) in a fully factorial design with four replicates, for each of the three destructive harvests (day 1, day 30 and day 60) (n = 192). An additional destructive harvest was performed on day 7 for all N fertilizer and biochar treatments for the CO and TX soils only (n = 32). A 2.5% biochar application rate was selected to balance tradeoffs between economics and GHG effect size (Roberts *et al.*, 2010). This rate is, depending on the soil bulk density (Table 1) and assuming a 10 cm incorporation depth, equivalent to a 23.3 to 26.5 Mg/ha field application.

Samples were prepared using 50 g air-dried soil (0% biochar treatment) or 50 g air-dried mixture of soil and biochar (2.5% biochar treatment) in specimen cups. For E1, all samples were wetted with an amount of distilled (DI) water calculated to achieve 40% water filled pore space (WFPS) in the unamended control soil, see below, then pre-incubated for 4 days at 25°C in the dark to activate soil microbial activity. The incubation began on the fifth day by wetting the pre-incubated samples with DI water or a NH₄Cl fertilizer solution to achieve 60% WFPS of the control soil. Fertilized samples received

1M NH₄Cl at a rate of 140 µg N/g soil, which, depending on soil bulk density, was equivalent to a 130 to 148 kg/ha field N fertilizer application. The sample cups were placed in an air-tight, quart-size mason jars, with ports for gas sampling, and stored at 25°C in the dark throughout the incubation. GHG efflux was sampled throughout the incubation on the treatments scheduled for harvest on day 60, as described below. Samples were destructively harvested at day 1, 7, 30 and 60 and processed for mineral N, as described below. Soil pH, inorganic C, and total C and N analyses were only performed on the samples harvested at day 60, as described below. Jars were periodically flushed to avoid excessive CO₂ accumulation (>2%) and soil moisture levels were maintained by checking the sample weight to monitor and compensate for evaporative losses.

The soil moisture gradient incubation (E2) was conducted using the N fertilized (1M NH₄Cl at a rate of 140 µg N/g soil) CO soil with treatments consisting of two biochar rates (0 and 2.5% by weight) and four soil moisture levels (40, 60, 80 and 100% WFPS of the control soils, see below) in a fully factorial design with four replicates and one harvest at day 30 (n = 32). Samples were incubated using the same protocol as E1 and wetted to the desired WFPS after the pre-incubation period (note that the dry treatments were pre-incubated to 30% WFPS of the control). Samples were destructively harvested at day 30, and analyzed for mineral N as described below.

Porosity of treatments were calculated assuming a soil particle density of 2.65 g/cm³ and biochar solid C density of 1.6 g/cm³ (Downie *et al.*, 2009). In accordance with the methods used by Quin *et al.* (2015), the porosity of the soil and biochar mixtures were calculated as the composite from the estimated porosities of the components. Soil moisture was added to achieve 40, 60, 80 or 100% WFPS of the control soils, resulting in an estimated WFPS for the biochar treatments of 39.6%, 59.2%, 79.1% and 98.7%, respectively. These treatments are referred to as dry (39.6-40% WFPS), aerobic (59.2-60% WFPS), moderately anaerobic (79.1-80% WFPS) and anaerobic (98.7-100% WFPS) throughout the text.

2.2.3. GHG Efflux

The net CO₂, CH₄ and N₂O fluxes were measured in both E1 and E2 by sampling the headspace gas periodically throughout the incubation (for E1 on day 1, 2, 3, 4, 6, 8, 10, 13, 16, 20, 25, 30, 35, 42, 50, 58; for E2 on day 0.5, 1, 1.5, 3, 4, 5, 6, 8, 10, 12.5, 15, 17, 20, 24, 28). Headspace GHG concentrations were sampled using cavity ring down spectroscopy (CRDS) with a recirculation pump (G2508 CRDS Analyzer; Picarro Inc., Santa Clara, CA). GHG concentrations were adjusted to account for mixing of headspace gas with the gas in the analyzer lines and chamber when sample ports were connected in a closed loop. The equilibrated GHG concentration of ambient air in the lines and chamber was measured prior to mixing with sample headspace. Mixed GHG samples were left to equilibrate for 3 mins before taking measurements. Headspace GHG concentrations were then calculated using a mixing model (eq. 1).

$$[GHG]_h = \frac{n_m[GHG]_m - n_{lc}[GHG]_{lc}}{n_h} \quad (1)$$

Where $[GHG]_h$ is the GHG concentration of the headspace, $[GHG]_{lc}$ is the GHG concentration of the lines and chamber, $[GHG]_m$ is the GHG concentration of the mixed sample, n_h is the mol gas in headspace, n_{lc} is the mol gas in lines and chamber and n_m is the sum of n_h and n_{lc} . GHG efflux was calculated as the difference between GHG concentration of the headspace after flushing, and that measured at the day of the following sampling.

2.2.4. Soil and Biochar Analysis

Upon harvest, each sample was thoroughly mixed before subsampling for analysis of extractable mineral N in bulk soil (10g), extractable mineral N in biochar isolates (10g), pH (5g), and inorganic C, total C and N concentrations (5g). Soil subsamples for mineral N analyses were processed prior to air drying. Soil subsamples for inorganic C, total C and N analyses were ground using mortar and pestle and oven dried at 63°C prior to analysis.

Soil pH was measured in DI water (soil/water ratio, 5:1 by mass) using a pH electrode and stirrer bar (Orion EA940 Expandable ionAnalyzer; Orion Research, Jacksonville, FL). Inorganic C was only measured on the E1 CO soils (the other soil types had <0.1% inorganic C; Table 1) by dissolving samples in 6N HCl +3% ferrous chloride and sampling CO₂ produced using a pressure transducer (Setra 280E; Boxborough, MA) (Sherrod *et al.*, 2003). Total C and N were measured using an elemental analyzer (LECO Tru-SPEC elemental analyzer; Leco Corp., St. Joseph, MI). All analyses for the soils prior to incubation were performed on three lab replicates, while analyses of the E1 day 60 soils were performed on each of the four replicates.

To quantify extractable mineral N concentrations in the bulk soil, a 10g subsample of the bulk soil (E1 day 1, 7, 30 and 60; E2 day 30) was extracted using 2M KCl (soil/KCl ratio, 5:1 by mass), shaken for 1 hour, filtered (Whatman #40 ashless filter paper) and analyzed colorimetrically (Alpkem Flow Solution IV Automated wet chemistry system; O.I. Analytical, College Station, TX) for NH₄⁺ and nitrate (NO₃⁻).

In order to quantify the extractable mineral N within the biochar particles, for the 2.5% biochar treatment samples only, another 10 g subsample was taken (E1 day 1, 7, 30 and 60; E2 day 30), placed on a 2 mm sieve and rinsed with 1 L DI water to isolate the biochar from the bulk soil (as biochar particle size was 2 - 2.8mm). The biochar isolates were then extracted and analyzed for mineral N using the same method as described above. The dry mass of biochar isolates in the extracted subsample was determined by recovering the biochar post extraction, drying overnight at 63°C and weighing, accounting for any KCl residues on the biochar.

2.2.5. Data and Statistical Analysis

Biochar-induced GHG emission reductions and C sequestration was calculated as the difference between biochar and control GHG emissions or SOC stock means, and this difference was then converted to carbon dioxide equivalents (CO₂-eq) using 100-year global warming potentials (Myhre *et al.*, 2013). The

standard error for the GHG emission reductions and C sequestration was calculated using error propagation of the standard error for each treatment. An annualized value for C sequestration was estimated by multiplying the measured biochar-induced C sequestration by a factor estimating the percent biochar C left after 100 years, determined from a regression of the H:C_{org} of the biochar by Zimmerman and Gao ($-74.3 \times (\text{H:C}_{\text{org}}) + 110.2 = 58.2\%$), then dividing by 100 years to annualize (2013).

Treatment effects were analyzed on the following response variables; cumulative CO₂, CH₄, N₂O efflux, SOC, total N, pH, bulk soil NH₄⁺ and NO₃⁻ and biochar isolate NH₄⁺ and NO₃⁻. We used a three factor ANOVA for E1 with fertilizer, amendment and soil as factors, and a two factor ANOVA for E2 with amendment and soil moisture level as factors. We used an ANCOVA to test for significant differences between soil and fertilization treatments on the relationship between N₂O emissions in the biochar versus control soils, by modeling N₂O in the biochar treatments using soil and fertilizer as factors and N₂O in the control treatments as a covariate. Linear and exponential regressions were applied to model cumulative CO₂ emissions by initial SOC content, cumulative N₂O emissions by initial TN content and biochar isolate NO₃⁻ concentrations by bulk soil NO₃⁻ concentrations. For mineral N concentrations, NH₄⁺ concentrations with mean values less than the measurement uncertainty were reported as undetectable. Where response variables were non-parametric, a Box Cox parametric power transformation was applied to transform the data for analysis (Box & Cox, 1964). All statistical analyses were performed in R version 3.3.1 (R Core Team, 2016). Significant differences between treatments were determined where $p < 0.05$. All error bars are reported as the standard error.

2.3. Results

2.3.1. Biochar's Impact on C Sequestration and GHG Efflux by Soil Types and Fertilization

After the 60-day incubation (E1), biochar amendments significantly increased SOC relative to the control soils by 0.84 ± 0.05 , 1.01 ± 0.04 , 1.16 ± 0.16 and 1.21 ± 0.11 g C ($p < 0.001$ for each soil type) for the CO, TX, ID

and ND soils respectively. The soils with the lowest initial SOC content, CO and TX (Table 1), experienced the lowest gain in SOC. In the CO soil, the difference between biochar and control soils at the end of the incubation was less than the C added as biochar (1.02 g C), indicating some mineralization of the biochar added. N fertilization did not affect SOC content, nor did it significantly interact with the biochar treatments or soil type (Table 3).

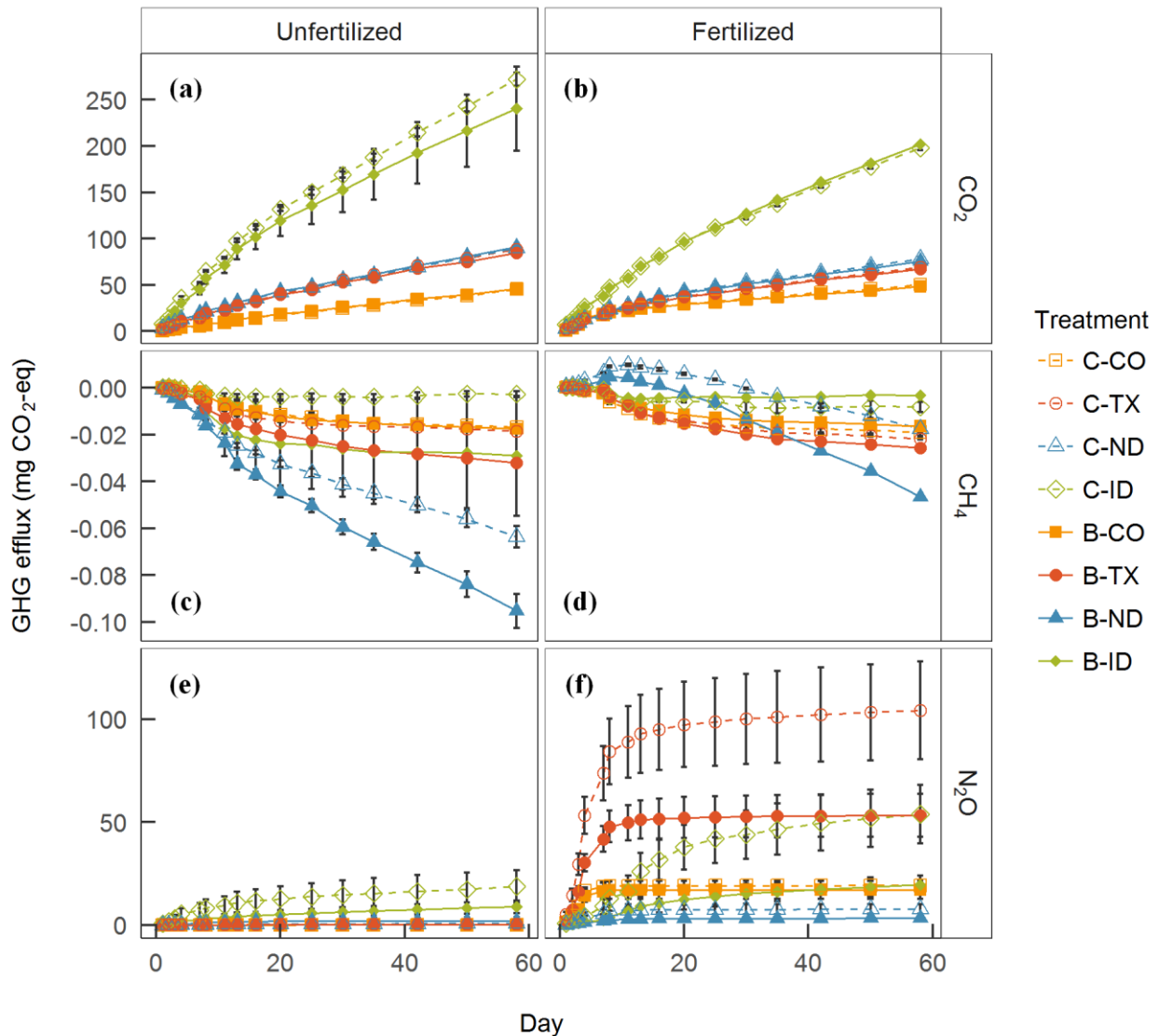


Fig. 1: Cumulative GHG efflux dynamics from biochar (closed shapes) and control (open shapes) treatments for the CO (orange squares), TX (red circles), ND (blue triangles) and ID (green diamonds) soils by nitrogen (N) fertilization (unfertilized, Fig. 1a,c,e; fertilized, Fig. 1b,d,f) and GHG type (CO₂, Fig. 1a,b; CH₄, Fig. 1c,d; N₂O, Fig. 1e,f) over the 60-day incubation (E1). Error bars display standard error.

All samples continued to respire throughout the 60-day incubation with CO₂ emissions never reaching an asymptote (Fig. 1a,b). Soil type significantly affected cumulative CO₂ emissions ($p < 0.001$) with a strong positive correlation between initial SOC content and cumulative CO₂ emissions ($R^2 = 0.83$; $p < 0.001$). However, on a percent initial SOC basis, the TX soil experienced the greatest C loss as CO₂ (5.3%), followed by CO (3.1%), ID (2.6%) and ND (2.1%) soils. N fertilization significantly decreased soil respiration by 18.3% ($p < 0.001$). Overall, biochar amendments did not have a significant impact on soil CO₂ emissions, but there were significant interactions with soil type and fertilization (Table 3). Biochar resulted in a 3.6% decrease in CO₂ in the TX soils ($p = 0.03$) and a 0.6% decrease in the fertilized treatments ($p = 0.04$), but the other soils and unfertilized treatments showed no significant biochar effects on respiration (Fig. 1a,b).

Table 3: Model of the response of soil organic carbon (SOC) and greenhouse gas emissions (CO₂, CH₄ and N₂O) to biochar (B), fertilization (F) and soil type (S) treatments in Experiment 1 (see text for details). Degree of freedom (df) F and p-values from a three factor ANOVA are reported, with significant values ($p < 0.05$) bolded.

Effect	df	SOC		CO ₂		CH ₄		N ₂ O	
		F	p	F	p	F	p	F	p
B	1	4.72E³	<0.01	0.92	0.34	70.75	<0.01	37.22	<0.01
F	1	0.02	0.89	360.53	<0.01	120.36	<0.01	1.16E³	<0.01
S	3	2.14E³	<0.01	6.63E³	<0.01	405.90	<0.01	141.77	<0.01
B x F	1	0.65	0.42	3.88	0.05	5.61	0.02	3.92	0.05
B x S	3	767.64	<0.01	2.83	0.05	50.55	<0.01	3.04	0.04
F x S	3	0.81	0.49	109.20	<0.01	125.99	<0.01	118.41	<0.01
B x F x S	3	0.23	0.88	1.54	0.22	0.61	0.62	1.82	0.16

All treatments experienced net CH₄ uptake in E1 but with relatively low cumulative uptake (-2.80 ± 0.37 to -0.08 ± 0.07 $\mu\text{g CH}_4$), especially when reported on a CO₂-eq basis (<95 $\mu\text{g CO}_2\text{-eq}$ uptake per sample). Biochar overall increased CH₄ uptake by 48.6% ($p < 0.001$), but with significant interactions with soil type and fertilization (Table 3). Across soils, biochar increased CH₄ by 154.3% in the ID soil ($p = 0.01$), 60.0% in the ND soil ($p < 0.001$) and 43.3% in the TX soil ($p < 0.001$) but had no impact on the CO soil. Between N fertilization treatments, biochar showed greater potential to increase CH₄ uptake by 57.4% in the

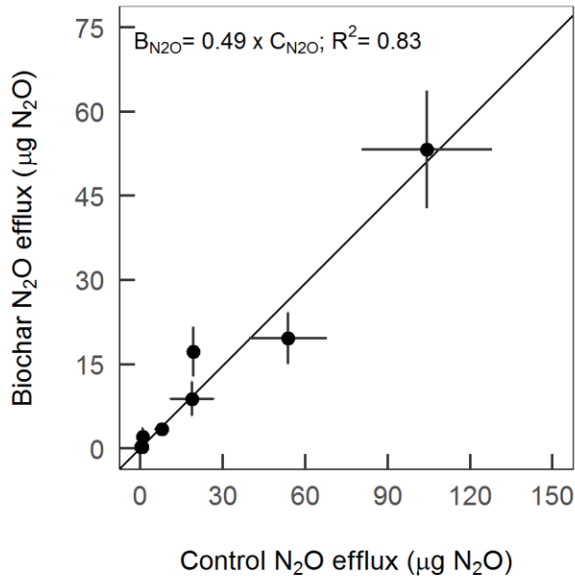


Fig. 2: Relationship between cumulative N₂O efflux in the control soils to cumulative N₂O efflux in biochar soils across treatments over the course of the 60-day incubation (E1). Error bars display standard error.

unfertilized treatments ($p < 0.001$) compared to 38.3% increase in uptake under the fertilized treatments ($p = 0.001$) (Fig. 1c,d). Fertilization had the opposite effect, overall reducing CH₄ uptake by 39.0% ($p < 0.001$).

N₂O efflux was also significantly impacted by biochar amendments, fertilization and soil type, and their binary interactions in E1 (Table 3), with cumulative emissions ranging from 0.7 ± 0.1 to 349.9 ± 159.8 µg N₂O (Fig. 1e,f). The fertilized treatments experienced the greatest N₂O efflux with 3.2% to 0.1% of the fertilizer added being emitted as N₂O-N. In the fertilized treatments, the TX soil exhibited the greatest N₂O production in both the control and biochar treatments followed by the ID soil, while the CO and ND soils had moderate levels of N₂O production (Fig. 1f). N₂O efflux in the unfertilized control treatments were reduced relative to the fertilized treatments and followed a more predictable trend with an exponential correlation between N₂O efflux and initial total N ($R^2 = 0.82$; $p < 0.001$). Biochar amendments decreased N₂O efflux in the fertilized ID, ND, TX and CO soils by 63.6% ($p = 0.04$), 56.5% ($p = 0.03$), 48.9% ($p = 0.26$) and 10.8% ($p = 0.63$), respectively. In the unfertilized soils, biochar

amendments led to a decrease of 59.8% ($p < 0.001$), 57.0% ($p < 0.001$), 52.9% ($p = 0.08$) and 8.5% ($p = 0.56$) in the ND, TX, ID and CO soils, respectively. N_2O efflux in the biochar treatments exhibited a linear relationship with N_2O efflux in the control treatment ($R^2=0.81$; $p < 0.001$), and there was no significant effect of soil ($p=0.46$) or fertilizer ($p=0.16$) on this relationship (Fig. 2).

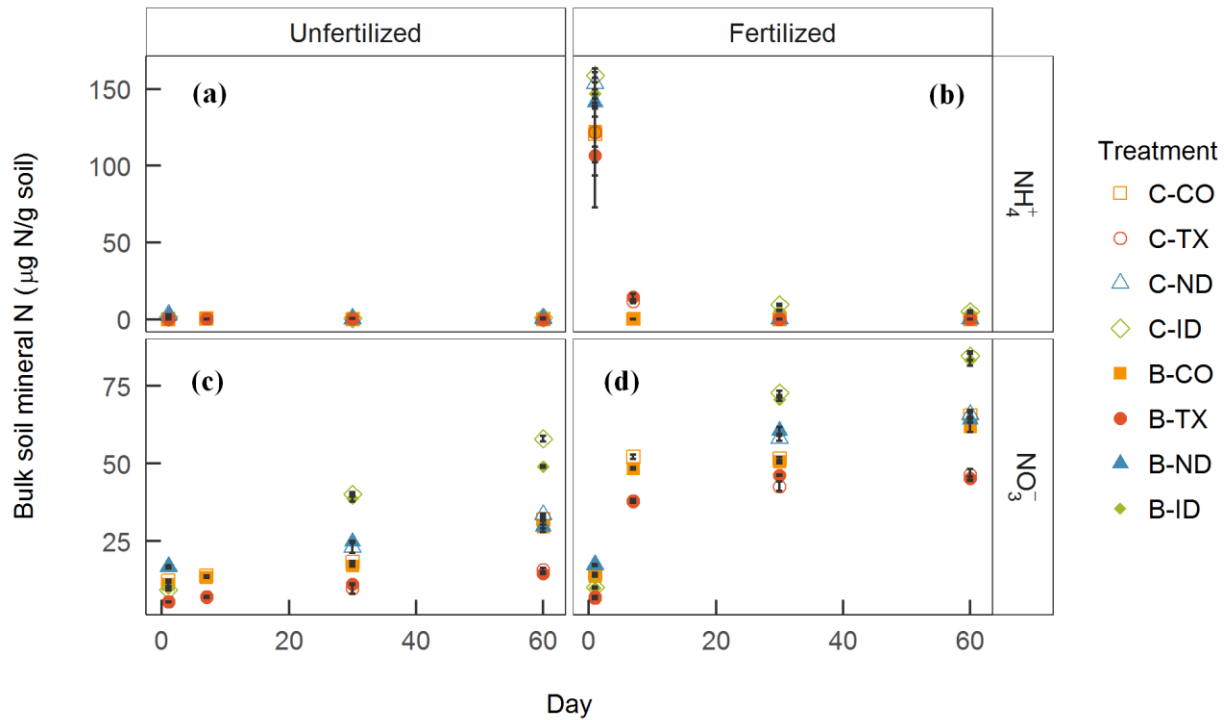


Fig. 3: Soil mineral nitrogen (N) extracted from the bulk soil for biochar (closed shapes) and control (open shapes) treatments for the CO (orange squares), TX (red circles), ND (blue triangles) and ID (green diamond) soils by nitrogen (N) fertilization (unfertilized, Fig. 3a,c; fertilized, Fig. 3b,d) and mineral N type (ammonium (NH_4^+), Fig. 3a,b; nitrate (NO_3^-), Fig. 3c,d) measured over the course of the 60-day incubation (E1). Error bars display standard error.

2.3.2. Biochar's Impact on Mineral N Dynamics by Soil Types and Fertilization

NH_4^+ concentrations in the unfertilized soils were low throughout the incubation with NH_4^+ only detected in the day 1 ID and ND soils, then decreasing to 0 by day 60 (Fig. 3a). NO_3^- concentrations in the unfertilized treatments gradually rose throughout the incubation with a net increase of 10.3 ± 0.6 , 16.8 ± 0.6 , 20.0 ± 0.4 and 48.7 ± 0.9 μg NO_3^- -N / g soil, in the TX, ND, CO and ID control soils, respectively (Fig. 3c). In the fertilized treatments, where 140 μg NH_4^+ -N / g soil was added, the day 1 soils captured

this NH_4^+ addition, then concentrations decreased to 0 by the end of the incubation in all soils except for the ID soil (Fig. 3b). Over the 60-day incubation NO_3^- concentrations increased even more than the unfertilized treatments (Fig. 3c,d), with a net increase of 39.8 ± 1.7 , 48.4 ± 1.4 , 50.8 ± 1.0 and 74.5 ± 1.4 $\mu\text{g NO}_3^- \text{N} / \text{g soil}$, in the TX, ND, CO and ID control soils, respectively. The additional accumulation of $\text{NO}_3^- \text{N}$ in the fertilized treatments relative to the unfertilized treatments can account for 18.4 to 24.4% of the $\text{NH}_4^+ \text{N}$ added, indicating the NH_4Cl fertilizer underwent other transformation pathways.

Biochar treatments exhibited similar dynamics as control treatments where NH_4^+ decreased to 0 for all but the ID soils. Across soil types, in both the fertilized and unfertilized treatments at day 60, biochar reduced bulk soil NO_3^- relative to the control by 3.0% ($p=0.01$) and 11.6% ($p<0.001$), respectively. However, such differences in bulk soil NO_3^- were not significant across soil types at day 1 or day 30. Only the CO soils showed consistent reductions in NO_3^- concentrations relative to the control soils throughout the incubation, with some of the unfertilized soils also indicating biochar reduced NO_3^- at day 60 in the unfertilized treatments (Fig. 3c; Table 4).

Table 4: Effect size and p-values for the difference between NO_3^- extracted from the bulk soil in the biochar treatments relative to the control treatments by fertilization treatments, soil types and day sampled, with significant values ($p < 0.05$) bolded.

Soil	Unfertilized			Fertilized		
	Day 1	Day 30	Day 60	Day 1	Day 30	Day 60
CO	-1.19 (p=0.01)	-1.32 (p=0.04)	-2.49 (p=0.01)	-1.09 (p=0.04)	-1.01 (p=0.47)	-3.74 (p=0.02)
TX	0.06 (p=0.81)	1.47 (p=0.23)	-1.09 (p=0.06)	0.34 (p=0.25)	3.57 (p<0.01)	-1.37 (p=0.30)
ND	-0.15 (p=0.80)	1.84 (p=0.65)	-3.86 (p<0.01)	-0.18 (p=0.78)	2.57 (p=0.10)	-1.59 (p=0.34)
ID	0.44 (p=0.28)	-1.30 (p=0.25)	-8.99 (p<0.01)	-0.19 (p=0.64)	-2.04 (p=0.25)	-1.30 (p=0.51)

Mineral N dynamics on the biochar isolates displayed similar trends as mineral N in the bulk soils (Fig. 4). In the unfertilized soils NH_4^+ concentrations on biochar isolates were below the detection limit for all treatments. In the fertilized treatment, NH_4^+ recovery on biochar isolates could account for 0.8 to 1.1 % of the total NH_4^+ measured in the day 1 fertilized treatments.

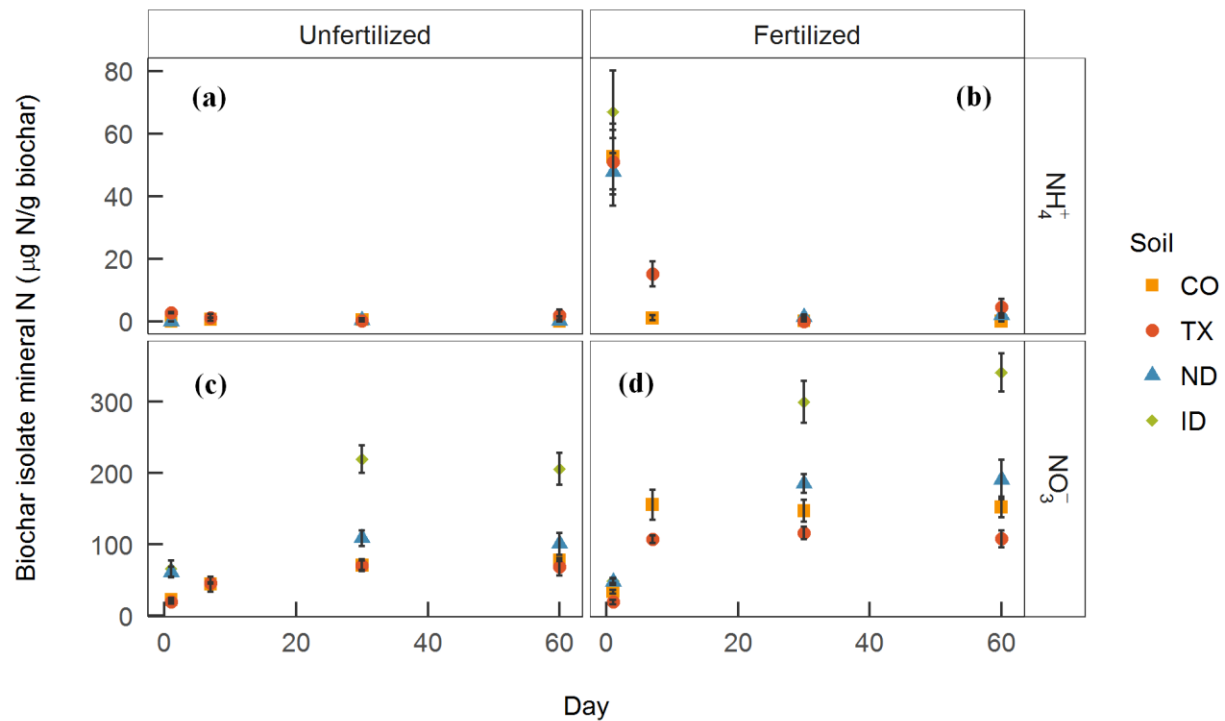


Fig. 4: Soil mineral nitrogen (N) extracted from biochar isolates in biochar treatments for the CO (orange squares), TX (red circles), ND (blue triangles) and ID (green diamonds) soils by nitrogen (N) fertilization (unfertilized, Fig. 4a,c; fertilized, Fig. 4b,d) and mineral N type (ammonium (NH_4^+), Fig. 4a,b; nitrate (NO_3^-), Fig. 4c,d) measured over the course of the 60-day incubation (E1). Error bars display standard error.

However, by day 60 in the fertilized there was little evidence for NH_4^+ retention on biochar isolates with NH_4^+ concentrations dropping to less than $4.49 \pm 2.57 \mu\text{g NH}_4^+\text{-N / g biochar}$. Given the small biochar addition rate such NH_4^+ would not have been detectable in the bulk soil extracts.

NO_3^- concentrations on biochar isolates were significantly higher than bulk soil on a per mass basis, therefore NO_3^- concentrations on biochar isolates were compared on a per surface area basis. NO_3^- concentrations by bulk soil could predict NO_3^- concentrations on biochar isolates following a linear relationship ($R^2 = 0.84$; $p < 0.001$). NO_3^- recovery on biochar isolates accounted for 7.0%, 8.5%, 9.3% and 12.4% of the total NO_3^- extracted from bulk soils across the CO, ND, TX and ID soils, respectively. Compared to biochar's percent surface area for each soil type, 7.2%, 12.5%, 5.5% and 20.4% of the total surface area in the CO, ND, TX and ID soils, respectively (calculated using BET surface areas; Table 1),

Table 5: Model of the response of GHG emissions (CO₂, CH₄ and N₂O) to biochar (B) and soil moisture (W) treatments in Experiment 2. Degree of freedom (df), F and P-values from a two factor ANOVA with significant values (p < 0.05) bolded.

Effect	df	CO ₂		CH ₄		N ₂ O	
		F	p	F	p	F	p
B	1	32.20	<0.01	5.53	0.03	29.19	<0.01
W	3	33.88	<0.01	1.75	0.18	144.89	<0.01
B x W	3	17.97	<0.01	2.62	0.07	33.90	<0.01

biochar isolates retained less NO₃⁻ per surface area in the higher SOM ND and ID soils, and similar NO₃⁻ per surface area in the CO and TX soils.

Soil total N was not significantly impacted by biochar amendments, but fertilization significantly increased total N in the TX, ND and CO soils (Table A1). Biochar and fertilization significantly altered pH with interactions by soil type (Table A1), where biochar increased pH by 1.1% (p < 0.001) and fertilization decreased pH by 6.5% (p < 0.001) across treatments. Biochar significantly increased pH in the unfertilized ID and ND soils, which had a lower initial pH (Table 1), by 1.5% (p = 0.004) and 2.9% (p = 0.003), respectively. In the ID soil, which was the only acidic soil used in this study, biochar increased pH also in the fertilized treatment by 1.9% (p < 0.001).

2.3.3. Biochar's Impact on GHG Efflux by Soil Moisture Regime

In E2, the soil moisture and biochar treatments, as well as their interaction, significantly affected GHG efflux, with some exceptions for CH₄ (Fig. 5; Table 5). In the control soils along the soil moisture gradient, soil respiration peaked in the aerobic treatment then declined in the anaerobic treatments. In the biochar soils, soil respiration continued to increase up to the moderately

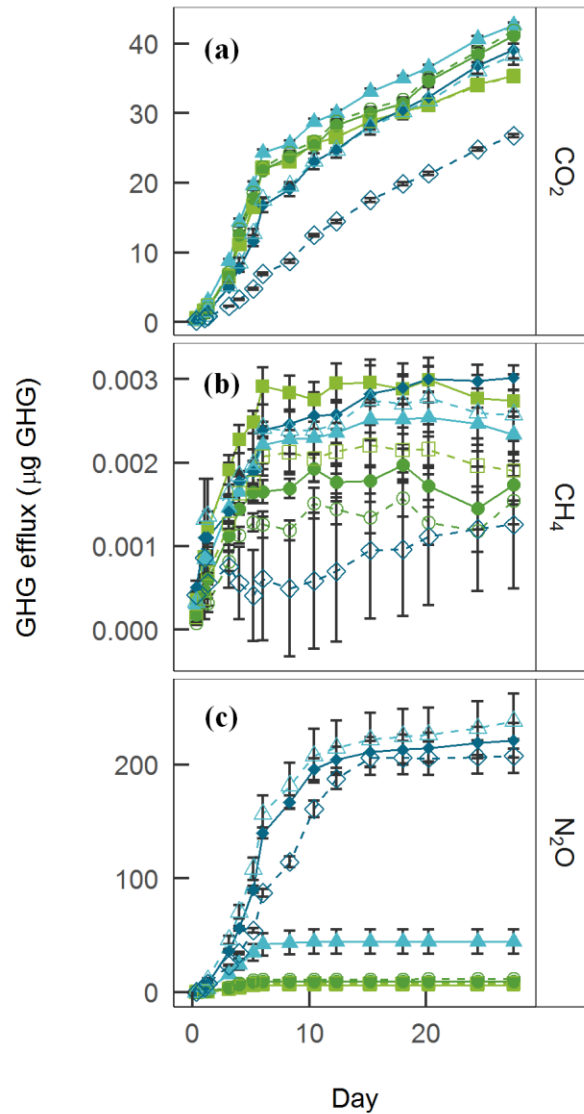


Fig. 5: Cumulative GHG efflux dynamics from biochar (solid shapes) and control (open shapes) treatments for each of the four soil moisture levels (dry (light green squares), aerobic (dark green circles), moderately anaerobic (light blue triangles) and anaerobic (dark blue diamonds) by GHG type (CO_2 , Fig. 5a; CH_4 , Fig. 5b; N_2O , Fig. 5c), measured over the 28-day fertilized CO soil incubation (E2). Error bars display standard error.

anaerobic treatment and only slightly decreased in the anaerobic treatment. Such interactions resulted in biochar significantly increasing soil respiration by $11.1\pm\%$ in the moderately anaerobic treatment ($p=0.01$) and 46.1% in the anaerobic treatment ($p < 0.001$). CH_4 dynamics in this incubation resulted in small (0.04 ± 0.02 to $0.09\pm 0.004 \mu\text{g CH}_4$) but net CH_4 emissions from soil. Biochar amendments led to a 138.6% increase in CH_4 efflux ($p = 0.003$) in the anaerobic

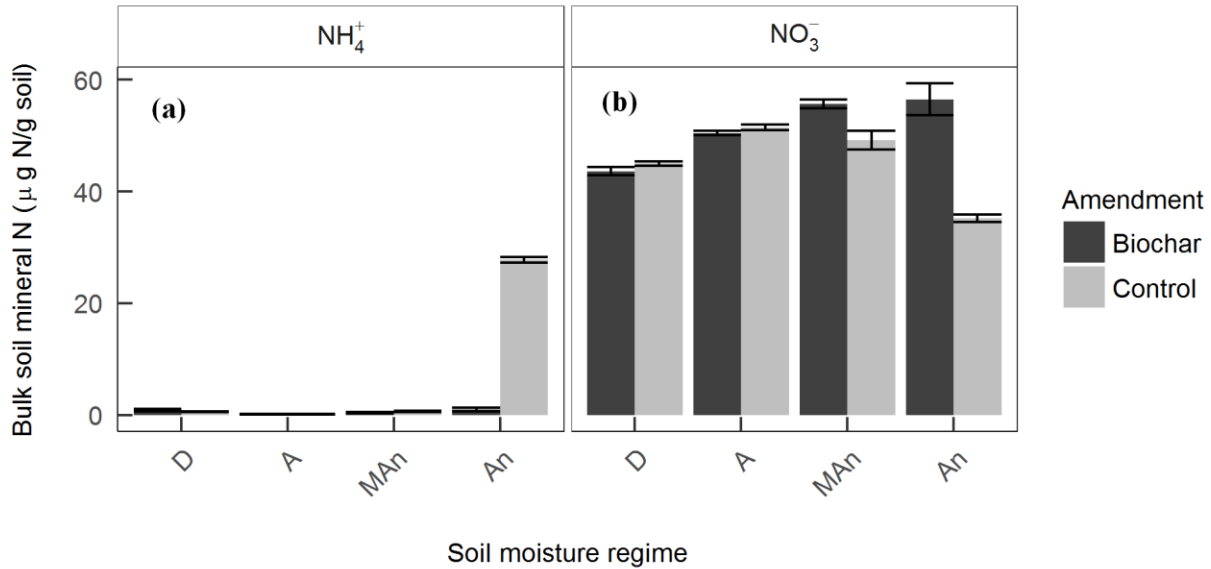


Fig. 6: Bulk soil mineral nitrogen (N) from the biochar and control soils separated by mineral N type (ammonium (NH_4^+), Fig. 6a; nitrate (NO_3^-), Fig. 6b) across the four soil moisture regimes (dry (D), aerobic (A), moderately anaerobic (MAn) and anaerobic (An), see text for details) measured at the end of the 28-day, fertilized, CO soil incubation (E2). Error bars display standard error.

Treatment, but had no impact on CH_4 at any of the other soil moisture levels. Surprisingly, water content did not significantly affect CH_4 fluxes, which however suffered in this experiment from high within treatment variability (Fig. 5b; Table 5). The soil moisture gradient also highlighted the large impact soil moisture, biochar and their interactions have on N_2O (Fig. 5c; Table 5). In the control soils, the anaerobic treatments resulted in significantly greater N_2O emissions than the dry and aerobic treatments (Fig. 5c). In the moderately anaerobic treatment, biochar amendments resulted in the largest reduction in N_2O emissions relative to the control both in magnitude and percent change ($649.40 \pm 88.63 \mu\text{g N}_2\text{O}$, 86.9% decrease; $p < 0.01$). In the anaerobic treatment, N_2O efflux from the biochar amended soils was not significantly different from the control soils ($p = 0.74$).

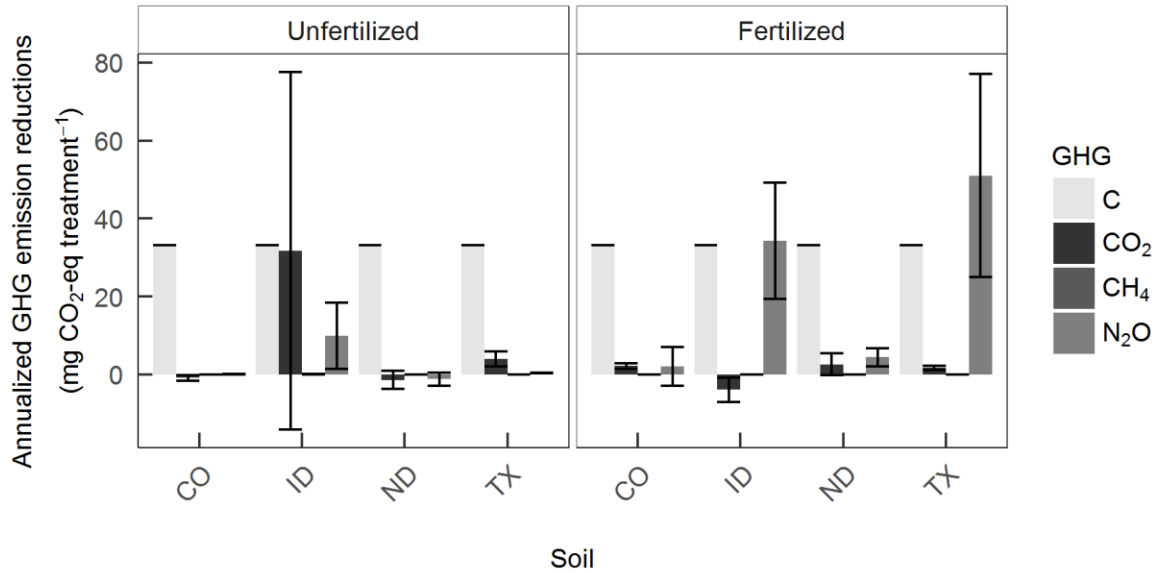


Fig. 7: Biochar-induced GHG emission reductions by GHG or C sequestration (annualized CO₂ equivalents) across the four soil types by nitrogen (N) fertilization (unfertilized Fig. 7a; fertilized Fig. 7b) measured at the end of the 60-day incubation (E1), per experimental unit (50g soil:biochar mixture 100:2.5). Error bars display standard error.

2.3.4. Biochar's Impact on Mineral N by Soil Moisture Regime

At the end of the 30-day soil moisture incubation, NH₄⁺ concentrations were below detection limits in all treatments (0 to 0.93±0.33 µg NH₄⁺-N / g soil) except for the anaerobic control treatment where 27.87±0.51 µg NH₄⁺-N / g soil remained (Fig. 6a). In the control treatments, bulk soil NO₃⁻ concentrations initially increased along the soil moisture gradient up to the aerobic treatment, but then began to decrease under the more anaerobic soil moisture regimes. Biochar NO₃⁻ dynamics differed from the control soil across the soil moisture gradient, where concentrations steadily increased as soils became more anaerobic (Fig. 6b). This resulted in biochar increasing NO₃⁻ by 13.1% (p = 0.002) in the moderately anaerobic treatment and 60.7% (p < 0.001) in the anaerobic treatment. Mineral N dynamics on the biochar isolates in E2 followed similar patterns as in E1. NH₄⁺ concentrations on biochar isolates were below detection limit for all moisture levels (Fig. A1a). NO₃⁻ concentrations on biochar isolates exhibited slightly different dynamics from bulk soil where NO₃⁻ extracted increased until the moderately anaerobic treatments but decreased in the aerobic treatment (Fig. A1b).

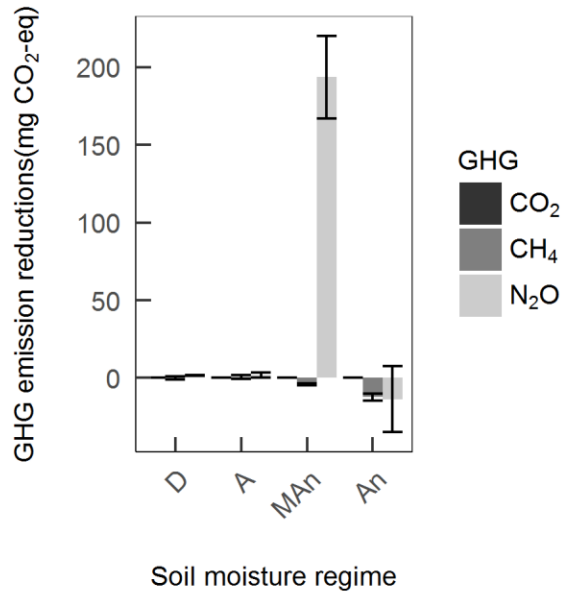


Fig. 8: Biochar-induced GHG emission reductions by GHG (CO₂ equivalents) per experimental unit (50g soil:biochar mixture 100:2.5), across the four soil moisture regimes (dry (D), aerobic (A), moderately anaerobic (MAn) and anaerobic (An), see text for details) measured at the end of the 28-day, fertilized, CO soil incubation (E2). Error bars display standard error.

2.3.5. Biochar's GHG Mitigation Potential

Overall, in our study, woody biochar's annualized C sequestration provided the greatest average GHG benefit of 23.6 ± 5.2 mg CO₂-eq per 50 g soil/soil + biochar treatment followed closely by biochar's N₂O reductions in the fertilized treatments of 22.9 ± 12.8 mg CO₂-eq per treatment. Biochar's ability to reduce CO₂ emissions across treatments and N₂O in the unfertilized treatments were both negligible at 1.2 ± 2.4 and 2.2 ± 3.0 mg CO₂-eq per treatment, respectively, with the high variance highlighting uncertainty in biochar's ability to mitigate GHG efflux in unfertilized soils. Biochar did significantly improve CH₄ uptake but the GHG reduction were orders of magnitude lower at 10.2 ± 6.2 μg CO₂-eq per treatment. Biochar's full GHG mitigation potential showed marked differences by soil type and fertilization especially for N₂O (Fig. 7), which emphasizes the importance of understanding controls on biochar's ability to mitigate N₂O. Depending on fertilization and soil environmental conditions (assuming predominately aerobic conditions), scaling the results from this incubation indicate that biochar amendments showed potential to mitigate soil CO₂ emissions from 0.39 to 1.49 Mg CO₂-eq ha⁻¹ at a 25 Mg ha⁻¹ biochar application rate

or 14.8 to 59.7 kg CO₂-eq ha⁻¹ (Mg biochar)⁻¹ reduction. GHG mitigation potential from E2 highlighted biochar's significant GHG mitigation potential for N₂O under moderately anaerobic conditions. By contrast, under anaerobic conditions biochar induced an increase in GHG emissions from increased CO₂ efflux (Fig. 8).

2.4. Discussion

To maximize biochar's GHG mitigation potential from bioenergy to agricultural systems, it is important to understand biochar's effect on individual GHG fluxes and C sequestration, then target biochar applications to achieve the greatest net GHG emission reduction. Similar to other studies measuring woody biochar impacts on different GHG emission reductions, this study showed the greatest GHG mitigation potential in C sequestration and N₂O emission reductions (Thomazini *et al.*, 2015; Stewart *et al.*, 2013; Zheng *et al.*, 2012). These incubations highlight the magnitude of biochar's effect on mitigating different GHGs, rather than simply the percent change. Across different agricultural soils, biochar application for GHG mitigation show the most promise for C sequestration and reducing N₂O emissions in fertilized soils, while impacts on CO₂ priming and CH₄ show to be minimal.

2.4.1. C Sequestration

Increased SOC in the biochar treatments relative to the control confirmed that much of the biochar C added was retained throughout the 60 day incubation, but with less of an increase in the lower SOC soils. The CO soil showed evidence of biochar C mineralization with the difference between biochar and control SOC being only 82% of the biochar C added. The reduced effect of biochar C additions in these low SOC soils suggests that the labile components of biochar may be more readily mineralized by soils with greater C turnover, as evidenced by these soils' cumulative CO₂ emissions also comprising a greater proportion of their initial SOC. Studies exploring biochar-derived CO₂ similarly find that biochar C is a more abundant microbial substrate in low SOC soils (Stewart *et al.*, 2013).

2.4.2. CO₂ Impacts

Biochar's ability to positively or negatively prime native SOM is one concern researchers have identified when considering biochar's full GHG mitigation potential (Liu *et al.*, 2016). Biochar has been predicted to stimulate decomposition of native SOC due to inputs of labile biochar C or microbial protection from predators stimulating mineralization (Cross & Sohi, 2011). Negative priming could also occur through direct sorption of labile organic matter on biochar or within biochar-mineral fractions (Lu *et al.*, 2014; Singh *et al.*, 2014). As found in similar lab incubations (Liu *et al.*, 2016), this study demonstrated that across four different agricultural soils with various SOM, pH and texture there was no evidence of biochar inducing increased CO₂ emissions. Two of the soils with lower SOC exhibited biochar decreasing CO₂ efflux, suggesting biochar functional groups may interact with labile SOM to decrease mineralization (Jiang *et al.*, 2016; Pignatello *et al.*, 2006). However, on a CO₂-eq basis these emissions from priming are minimal comprising only 5.1% of the annualized C sequestration. Methodologies to quantify biochar's GHG mitigation potential should address the potential effects of priming but estimations from the literature (Liu, *et al.*, 2016) can be used to streamline monitoring requirements.

2.4.3. CH₄ Impacts

This woody biochar showed potential to increase the CH₄ sink in upland agricultural soils by 48.6% depending on fertilization and soil type (E1). This result contrasts findings of the recent Jeffery *et al.* (2016) biochar CH₄ meta-analysis which found biochar decreases the CH₄ sink in upland soils. In this aerobic incubation, biochar's ability to increase CH₄ uptake was greater in the unfertilized treatment as compared to the fertilized soils, which may indicate NH₄⁺ is competitively excluding CH₄ at binding sites preventing CH₄ oxidation (Bedard & Knowles, 1989). However, biochar's CH₄ mitigation potential for upland agricultural soils must be viewed in the context of the magnitude of change in addition to percent change. Upland agricultural systems are generally observed to be a CH₄ sink with capacities around 0.03 to 0.20 mg CH₄ m⁻² per day (Powlson *et al.*, 1997). Applying the 48.6% increase in CH₄ uptake

achieved in this incubation to that range, biochar would only have potential to annually increase CH₄ uptake by 1.8 to 12.1 kg CO₂-eq/ha, less than 2.6% of the annualized C sequestration potential. Biochar application to upland agricultural systems therefore provides limited net GHG mitigation from increasing CH₄ uptake relative to other GHGs.

Along the soil moisture gradient in the fertilized CO soils (E2), biochar led to an increase in soil CH₄ efflux ($p=0.03$), again contrasting the trend of decreased CH₄ in flooded systems (Jeffery *et al.*, 2016). Increases in CH₄ has also been found in numerous other studies citing mechanisms such as inputs of labile C from biochar under anaerobic conditions stimulating CH₄ production (Zhang *et al.*, 2013) and reduced CH₄ oxidation from changes in microbial community composition (Spokas *et al.*, 2009; Yu *et al.*, 2013). However, further exploration of different biochars in saturated soils may provide larger magnitudes of CH₄ emission reduction that could serve as a viable GHG mitigation strategy (Jeffery *et al.*, 2016; Feng *et al.*, 2012).

2.4.4. N₂O Impacts

Relative to impacts on other GHG emissions, this woody biochar shows the greatest GHG mitigation potential in reducing N₂O in fertilized soils. The interactions between biochar and SOM, soil pH, soil texture, fertilization and soil moisture on mineral N dynamics and N₂O efflux can help inform the mechanisms by which biochar impacts N₂O efflux. Hypotheses for biochar's ability to reduce N₂O include effects on nitrification and denitrification rates (He *et al.*, 2016; Wang *et al.*, 2015), sorption of mineral N to the biochar (Case *et al.*, 2012; Sohi *et al.*, 2010; van Zwiiten *et al.*, 2014) and impacts on soil aeration (Augustenborg *et al.*, 2011; Mukerjee *et al.*, 2014; Rogovska *et al.*, 2011). These incubations primarily tested hypotheses related to nitrification and denitrification rates, biochar reducing N mineralization, preventing N transformation via sorption of mineral N, impacting soil redox and the resulting N transformation processes, as evidenced by mineral N dynamics in soils.

We found that:

1. Woody biochar did not reduce N₂O emissions by reducing net N mineralization and nitrification

Biochar has been hypothesized to decrease N₂O by reducing net N mineralization and the available NH₄⁺, thus reducing nitrification rates and subsequent N₂O production (He *et al.*, 2016; Wang *et al.*, 2015). We evaluated this impact in the unfertilized treatments by comparing biochar's impact on net mineralization and nitrification, and N₂O efflux. For the unfertilized soils, the positive correlation between soil total N and N₂O production combined with negligible NH₄⁺ concentrations and accumulation of NO₃⁻ throughout the incubation, confirms that N mineralization and subsequent nitrification is the primary control on N₂O production. Biochar significantly reduced N₂O efflux in the ID and TX unfertilized soils with minimal effects in the CO soil. However, at day 30, only the CO soil exhibited reduced NO₃⁻ availability in the biochar treatment relative to the control, indicating a reduction in net mineralization and nitrification. CO₂ data confirms that biochar did not significantly impact soil respiration across treatments further substantiating the claim that biochar did not significantly decrease mineralization. While the unfertilized treatments did experience a significant decrease in NO₃⁻ by day 60 (Fig. 3c; Table 4), 67% to 100% of the N₂O was produced by day 30 with a clear biochar reduction in N₂O across treatments (Fig. 1e,f).

In the fertilized treatments, a similar pattern emerged where biochar amendments only significantly decreased NO₃⁻ concentrations in the CO soils, yet biochar significantly reduced N₂O emissions in the ND and ID soils. In the fertilized treatments, the increase in NO₃⁻-N could only account for 19.1 to 24.7% of the NH₄⁺-N added across treatment, indicating gross N immobilization, or possibly other N losses through denitrification or NH₃ volatilization also may have occurred. Even though other NH₄⁺ consumption pathways besides nitrification were present, NO₃⁻ accumulation within the biochar and control treatments remained the same in all but the CO soils indicating biochar did not reduce

nitrification rates. Therefore, in this study, across both soil types and fertilization, biochar's N₂O emission reductions cannot be explained by biochar's impact on N mineralization and nitrification.

2. Woody biochar did not reduce N₂O emissions by reducing mineral N availability

N sorption processes on biochar surfaces is another commonly cited mechanism for biochar's ability to reduce soil N₂O efflux (Case *et al.*, 2012; Sohi *et al.*, 2010; Thomazini *et al.*, 2015; van Zwieten *et al.*, 2010). Leachate studies have demonstrated that biochar surfaces can retain mineral N, potentially through surface reactions that prevent microbial transformations. In our study, NH₄⁺ recovery from both the bulk soil and biochar isolates was minimal after day 1, with no retention of extractable NH₄⁺ on biochar isolates. Extractable NO₃⁻ recovered on biochar isolates also exhibited a strong correlation relative to the NO₃⁻ concentrations of the bulk soil. This indicates that sorption processes impacting nitrification are not required to explain extractable N recovered on the biochar surfaces, and mineral N dynamics within the bulk soil can account for mineral N dynamics on biochar isolates. Other studies confirm that biochar does have significant potential to sorb NH₄⁺, but sorption is primarily mediated through cation exchange processes (Cui, 2016; Zeng, 2013), where mineral N would still be accessible to microbial transformation. Physical adsorption with interior biochar pores has also been shown to be an important mechanism for the adsorption capability of biochar (Nguyen *et al.*, 2017; Zhang *et al.*, 2012). Biochar sorption of mineral N did not prevent nitrification on biochar isolates and this mechanism cannot account for reduced N₂O efflux.

3. Woody biochar consistently reduced N₂O emissions relative to control treatments regardless of soil type or fertilization rate

One of the clearest patterns emerging from the aerobic incubation was the consistency of N₂O emissions in the biochar treatments relative to the controls (Fig. 2). Neither fertilization nor soil type significantly impacted this relationship suggesting that soil properties or substrate availability may have a limited

impact on the percent reductions from biochar amendments. This finding confirms the findings of Thomazini *et al.* (2015) who found a similar relationship between biochar and control N₂O across ten different soil types. Our study extends the trend to fertilized treatments with greater N₂O production. This implies the relative reduction achieved by the biochar may be driven more by biochar properties rather than by the soil properties.

Biochar's ability to impact gaseous diffusion of N₂O from soil could provide one possible mechanism for the consistent percent N₂O reductions across treatments. Diffusion of N₂O from soils is an often-overlooked process, which could reduce N₂O independent of N₂O production (Blagodatsky & Smith, 2012). Harter *et al.* (2016) demonstrated biochar's ability to entrap N₂O in water-filled pores under anaerobic soil conditions. Similarly, under a range of aerobic WFPS in sterilized soils, Quin *et al.* (2015) showed significant sorption of N₂O to biochar treated soils. This may serve as a temporary mechanism to limit N₂O efflux by slowing diffusion and increasing the likelihood of N₂O being fully reduced to N₂ by denitrifying microbial communities within anaerobic microsites. Cornelissen *et al.* (2013) developed N₂O sorption isotherms for woody biochars showing their large capacity for N₂O sorption. Applying this woody biochar's BET surface area to the curves they developed indicates a maximum sorption capacity of roughly 40 cm³ N₂O / g biochar or 98.2 mg N₂O for the biochar treatment, well above the max N₂O emissions in this experiment (Cornelissen *et al.*, 2013). Biochar N₂O sorption thus provides one possible explanation for the consistent trend across soil type and fertilization observed in these aerobic incubations.

4. Woody biochar reduced N₂O by aerating soil under moderately anaerobic conditions, thus reducing denitrification rates

Biochar treatments may also have differing impacts on N₂O production as soils transition from predominantly aerobic to anaerobic conditions. Woody biochar is characterized by containing residual

macropores which while, in this study only contributed 3.8% to the total porosity of the soil, may be more effective at retaining air-filled pores than other soil pores (Sun *et al.*, 2012). Such biochar residual macropores exhibit much lower pore connectivity than bulk soil pores thus may more readily retain air-filled pore space reducing the prevalence of anaerobic microsites within the soil matrix (Schnee *et al.*, 2016; Sun *et al.*, 2013). Biochar porosity can retain air even when soils are fully saturated due to hydrophobic effects depending on biochar functional groups (Gray *et al.*, 2014). N₂O production from denitrification can be significantly more than N₂O production from nitrification, thus shifts to a more aerobic soil environment induced by biochar porosity could potentially reduce the rates of denitrification within soils.

The fertilized CO soils incubated across a soil moisture gradient (E2) demonstrated that soil moisture significantly impacts biochar's N₂O mitigation potential and the greatest potential is at moderately anaerobic soil moisture levels (Fig. 8). In the control soils, N₂O production from the moderately anaerobic and anaerobic treatments was far greater than the dry and aerobic treatments, indicating that N₂O contributions from denitrification dominate N₂O production in this CO soil (Bateman and Baggs, 2005; Linn & Doran; 1984). In the moderately anaerobic treatments, biochar showed an 86.9% reduction in N₂O efflux which could be explained by a shift from moderately anaerobic conditions to a more aerobic soil environment where denitrification would be reduced. This shift towards less denitrification in the moderately anaerobic biochar treatment was confirmed by higher NO₃⁻ concentrations at day 30, suggesting decreased NO₃⁻ consumption through denitrification. Further evidence for biochar inducing a more aerobic soil environment in the moderately anaerobic treatments comes from biochar significantly increasing the cumulative CO₂ efflux relative to the control soil, another aerobic process.

In the anaerobic soil moisture treatments the control soil retained 23% of the NH₄⁺ added (Fig. 6a), likely due to the limited O₂ availability for nitrification. The biochar treatments however saw no NH₄⁺

remaining after 30 days and higher levels of NO_3^- indicating nitrification was not O_2 limited, potentially due to O_2 retention within the biochar pores. Biochar's ability to better retain air-filled pore space than bulk soil pores may have supplied enough O_2 for nitrification but under predominately anaerobic conditions did not prevent denitrification resulting in no significant difference between biochar and control N_2O efflux. The additional air-filled pore space from biochar may have reduced anaerobic zones within the soil where N_2O would be fully reduced to N_2 , resulting in biochar treatments exhibiting no change or a potential increase in N_2O relative to the control. Soil moisture level and the prevailing redox status within the soil show large potential to influence biochar's ability to reduce N_2O and future research must consider these dynamics especially when modeling field condition with variable soil redox.

2.4.5. Toward Biochar Application as a GHG Mitigation Technology

If biochar is pursued as a climate-smart technology to reduce the GHG footprint of bioenergy and agricultural systems, biochar applications show the greatest GHG emission reduction potential by sequestering C and reducing N_2O emissions in fertilized soils. Research should be directed toward developing and testing models that can consider the multiple interacting mechanisms highlighted above of how biochar impacts the soil environment, such as the new biochar module within the Agricultural Production Systems sIMulator software (Archontoulis *et al.*, 2016). Modeling efforts should test the mechanisms where biochar demonstrates the greatest GHG emission reduction potential, specifically those related to biochar's impact on mineral N dynamics and biochar C stabilization, and utilize research from lab incubations to help explain dynamics in field studies. Field studies and data sharing will be critical for developing and parameterizing such biochar models and identifying if such mechanisms are artifacts of lab incubations or carry over to field results (Verhoeven *et al.*, 2017). Biochar research should also focus on understanding the temporal dynamics of these various mechanisms and if biochar can provide sustained annual GHG emission reductions or just short-lived effects, thus impacting the full

GHG emission reduction potential over the lifetime of the biochar. If the “biochar solution” is to provide significant GHG mitigation potential, research efforts must shift to applying lessons learned from mechanistic studies to the field and identify applications that can deliver the greatest GHG emission reductions.

3. BROADCAST WOODY BIOCHAR PROVIDES LIMITED BENEFITS TO DEFICIT IRRIGATION MAIZE IN COLORADO²

3.1. Introduction

Agriculture is one of the most vulnerable sectors to changing temperature and precipitation regimes, yet also contributes to the problem itself generating 24% of GHG emissions globally (Smith & Bustamante, 2014). In the context of climate change, identifying agricultural practices that improve water and nutrient management while decreasing GHG impacts is essential for developing sustainable agricultural systems. Dryland and irrigated systems are especially sensitive to changes in precipitation and the resulting impacts on water supply, thus promoting water-use efficiency in agricultural practices is critical in managing these increasingly limited water resources (Kang *et al.*, 2009). Increasing soil organic matter is one strategy to help improve the available water capacity of soils (Hudson, 1994), to help manage crop water stress while also providing climate benefits through C sequestration. Soil moisture regime also interacts with soil N cycling to impact crop productivity, affecting N availability, transformation and losses (Gonzalez-Dugo *et al.*, 2010). Sustainable agricultural practices must consider interactions with soil water dynamics to maximize fertilizer N delivery to crops while minimizing environmental losses from N leaching or gaseous N production, including the important GHG, N₂O. Biochar soil amendments are one agricultural technology with potential to deliver improved water and N retention while decreasing GHG emissions (Atkinson *et al.*, 2010), but few field studies have evaluated biochar's agronomic and environmental benefits in combination with reducing irrigation inputs (Foster *et al.*, 2016; Kangoma *et al.*, 2017).

With shifting climate patterns and growing demands on water supplies, producers in arid to semi-arid climates must consider new strategies for water conservation and increasing water productivity.

² This chapter is currently in review in *Agriculture, Ecosystems and the Environment* as a manuscript authored by Ramlow, M., Foster, E., del Grosso, S., and Cotrufo, M.F.

Irrigation systems are generally designed to supply water to match the demands of evapotranspiration (Allen *et al.*, 1998). With increasing competition for water resources and variable water supply, farmers may resort to deficit irrigation strategies to maintain yields while decreasing irrigation water use. Deficit irrigation strategies might include not irrigating crops during the early vegetative growth phases, which are less sensitive to water stress, or reducing total irrigation water throughout the growing season (Geerts & Raes, 2009; Sudar *et al.*, 1981). Soil amendments, such as biochar, offer opportunities for improving water productivity by potentially increasing water storage while reducing evaporative losses. Biochar's porous structure has been shown to increase the water holding capacity of soils (Ali *et al.*, 2017; de Melo Carvalho *et al.*, 2014; Omondi *et al.*, 2016), but this effect varies with soil texture, with more heavily textured soils showing diminished effects (Dan *et al.*, 2015). Combining strategies of deficit irrigation while increasing water storage through biochar amendments may minimize crop water stress and reduce total water inputs.

Changes to soil moisture due to irrigation and soil organic matter management will also influence N availability, including soil N transformation and delivery to the crops (Barakat *et al.*, 2016; Gonzalez-Dugo *et al.*, 2010). N requirements are largely supplied through passive water uptake into roots, therefore higher irrigation has been shown to significantly increase N use efficiency across cropping systems (Aulakh & Malhi, 2005). Modeling studies also suggest that soils with greater water holding capacity have greater potential for improved N use efficiency (Asseng *et al.*, 2001). Soil moisture levels and dynamics not only impacts crop N uptake but also microbial N cycling, as soil water content controls N diffusion, mineralization, immobilization, nitrification and denitrification (Barakat *et al.*, 2016). Biochar may alter mineral N availability through its high ion exchange capacity (Gai *et al.*, 2014), direct impacts on microbial N transformation (Clough *et al.*, 2013; Nguyen *et al.*, 2017) and interactions with soil hydraulic properties affecting mineral N transport through (Sun *et al.*, 2015). Previous research demonstrated that biochar reduces mineral N leaching in irrigated systems (Gai *et al.*, 2014), but the

dynamics for mineral N transport and transformation with biochar addition in deficit irrigation systems requires further study.

Lab incubations have shown that biochar can substantially reduce N₂O emissions by 54% across studies (Cayuela *et al.*, 2014; Cayuela *et al.*, 2015), yet the degree to which biochar mitigates N₂O emissions under field conditions remains uncertain (Verhoeven *et al.*, 2017). Exploring interactions with irrigation regimes may help resolve some of those outstanding discrepancies. Assessing the impact of management practices on N₂O emissions in the field presents numerous challenges due to extensive temporal and spatial variability (Parkin & Venterea, 2010). Soil moisture is a key control on soil redox status, which moderates nitrification and denitrification rates, the two primary sources of N₂O in soils (Baggs & Bateman, 2005; Linn & Doran, 1984), although other N transformation processes may also contribute to N₂O production (Butterbach-Bahl *et al.*, 2013). Deficit irrigation regimes with different soil moisture dynamics may alter biochar's impact on N₂O emissions. Some field studies indicate that soil moisture moderates biochar's ability to reduce N₂O, but more research is needed to understand these impacts (Angst *et al.*, 2014; Saarnio *et al.*, 2013; Scheer *et al.*, 2011).

In addition to N₂O reduction, biochar also reduces GHGs by sequestering C in soils. Biomass pyrolysis generates a condensed aromatic C structure that is more resistant to microbial decomposition, allowing for C sequestration in soils on the century to millennia timescales (Spokas, 2010). When sourced from sustainable feedstocks, biochar has potential to deliver significant GHG benefits up to 12% of global anthropogenic CO₂-eq emission annually (Woolf *et al.*, 2010). Biochar's effects on the priming of native soil organic matter must also be considered when calculating its full impact on GHG emissions, but a recent meta-analysis suggests such effects are minimal (Wang *et al.*, 2016).

Here we assessed both the agronomic and environmental benefits of a beetle-killed pine biochar soil amendment relative to unamended soils under conventional and deficit irrigation management in a

maize production system. This study explored three agronomic and environmental benefits biochar may provide across different irrigation regimes: 1) improved soil water retention, 2) reduced mineral N losses, and 3) increased GHG benefits. We hypothesize that in irrigated maize biochar will:

- 1) Increase soil water retention throughout the growing season, translating to yield benefits under deficit irrigation;
- 2) Mobilize nutrients in the rooting zone and decrease N leaching through the soil profile leading to improved crop N uptake, with less of an effect in deficit irrigation due to less mineral N leaching;
- 3) Provide significant GHG benefits by sequestering C in soils and reducing N₂O emissions, with less of an effect in deficit irrigation due to lower N₂O emissions.

3.2. Materials and Methods

3.2.1. Site Description and Experimental Design

We tested biochar's impact on soil moisture dynamics, mineral N availability and GHG benefits in a maize system with irrigation manipulation at the Agricultural Research Development and Education Center in northeastern CO (40°39'6" N; 104°59'57" W). The site receives 27.3 cm precipitation annually with a mean annual temperature of 8.9°C (CoAgMet weather station, 1993-2016 annual average, retrieved 2017). The 2016 field season (April to October) recorded a mean temperature of 15.9°C (ranging from -4.9 to 37.0°C) and received 14.1 cm precipitation, in addition to the irrigation treatments described below (CoAgMet weather station, retrieved 2017). The soil at the site is a Fort Collins loam (mesic Aridic Haplustalfs; NRCS, 2017) with a clay loam texture (34.7% sand, 31.6% silt, 33.7% clay), 1.19 g cm⁻³ bulk density, pH 7.99 (5:1 water:soil, w/w), 1.49% C, and 0.12% N.

The experiment was a randomized block design with four blocks, three irrigation treatments (Full, Limited and Drought irrigation) and two soil amendments (biochar and control), for a total of 24 plots.

Experimental plots were 4.5 x 4.5 m, each planted with six rows of Dupont® Pioneer maize hybrid (P9697A). Irrigation treatments included Full irrigation (irrigation amounts designed to meet crop requirements (50.8 cm)), Limited irrigation (stopping irrigation during the non-essential growth phases V5 to V10 (42.5 cm; Table 6)), and Drought irrigation (half the rate of the Full irrigation treatment (25.4 cm)). Irrigation was applied weekly as specified in Table 6. Such irrigation treatments were applied each year starting with the 2014 growing season, as described in Foster *et al.* (2016). Within each irrigation treatment, we established two soil amendment treatments: 1) a coarse-sized, slow pyrolysis woody biochar treatment, and 2) a no amendment control.

Table 6: Crop phenology and management throughout the growing season

Date	Crop Phenology	Management
13 May		Fertilizer application
23 May		Planting
24 May		Herbicide application
3 June	Emergence	Begin irrigation
7 June	V1	
23 June	V6	Limited irrigation: irrigation stopped
8 July	V9	Limited irrigation: irrigation resumes
12 July		Herbicide application
29 July	VT	
2 Aug	R1	
21 Sept		Biomass sample harvest
29 Sept	R6	

3.2.2. Biochar and Fertilizer Application

The woody biochar was produced using a beetle-killed lodgepole pine feedstock, under slow pyrolysis, reaching temperatures of 550°C, sieved to the chip size fraction (>3 mm) by Biochar Now (Berthoud, CO). Biochar treatments were applied in April 2015 at a rate of 25 Mg ha⁻¹ to the surface of the plots (equivalent to a 2.1% by mass application rate), then tilled using a disc tiller to a 10 cm depth (control plots were also tilled). Biochar characterization was conducted by Hazen Research, Inc. (Golden, CO 80403) in accordance with International Biochar Initiative protocols (Table 7). BET surface area analysis (Table 7) was conducted using a micromeritics BET surface area and porosity analyzer (ASAP 2020;

Micromeritics, Norcross, GA, USA), as described in Ramlow & Cotrufo (2017). All treatments received a banded fertilizer applied at a depth of 25 cm on May 13th, 2016. The fertilizer solution was a urea ammonium nitrate liquid fertilizer applied at a rate of 98.6 N - 34.7 P - 1.7 Zn kg ha⁻¹, based on plant requirements and previous soil nutrient levels. Planting occurred on May 23, 2016 with recommended herbicide treatments (Roundup® PowerMAX at 2.3 L ha⁻¹) the following day.

Table 7: Biochar production information along with physical and chemical properties as characterized by an ultimate analysis, pH and bulk density measurements and BET surface area analysis.

Description	Biochar Property
Feedstock	Beetle-killed lodgepole pine
Pyrolysis	Slow pyrolysis, 550°C max temp
Particle Size	Sieved to >3mm
Organic C	86.2 %
H:C _{org}	0.35 molar ratio
C:N	478.8 mass ratio
Ash	1.1 %
pH	8.49
Bulk Density	0.11 g cm ⁻³
Porosity	0.93
BET surface area	111.89 m ² /g biochar

3.2.3. Soil C and Bulk Density Sampling

Soils were sampled after biochar application (May 27, 2015) and at the end of the 2016 growing season (Sept. 27, 2016) to a 30 cm depth using a 7 cm-diameter soil corer and were separated at a 0-10 and 10-30 cm soil depth for determining soil bulk density, and total C. Additionally, periodically throughout the 2016 growing season, 3 soil samples per plot were taken with a 2 cm-diameter soil auger to a 10 cm depth, and composited by plot for gravimetric water content (GWC) determination. Soil samples were stored in plastic bags in a cooler, transported to the lab, sieved to 2 mm, sampled for GWC and then left to air dry. Coarse biochar particles (>2 mm) were physically separated on all soil samples. Soil and coarse biochar GWC was determined on a ~15g subsample by oven-drying overnight at 105°C. For total C measurements, oven-dried soils were pulverized and analyzed on a LECO True-Spec CN analyzer (Leco

Corp., St. Joseph, MI, USA). Total C in the coarse biochar particles was determined from their C concentration (Table 7) and dry weight.

3.2.4. Soil Moisture Sampling and Water Stress Coefficient

Volumetric water content was sampled weekly throughout the 2016 growing season using a time domain reflectrometer (TDR), measuring to a depth of 10 cm. Field capacity for each plot was determined on Sept. 9, 2016 by saturating a 20 cm² section of the plot, wetting soils 3 times waiting 90 minutes to allow for drainage before the next sample. We took TDR measurements and soil cores (as described above) initially and after each of the three wetting events within the saturated zone to develop a calibration curve between TDR and GWC measurements. Field capacity was then measured the subsequent day to allow for sufficient drainage after saturation (Veihmeyer & Hendrickson, 1949). GWC and TDR readings were compared to develop a linear regression to calibrate and convert TDR readings to GWC ($R^2=0.68$, $p<0.001$) (Fig. A2).

Soil porosity was estimated from the field soil bulk density, assuming a soil particle density of 2.65 g cm⁻³ and biochar particle density of 1.6 g cm⁻³ (Brewer *et al.*, 2009). The porosities of biochar amended soils were calculated using the method of Quin *et al.* (2015), where the composite porosity was estimated from the soil and biochar components. Water-filled pore space (WFPS) was then estimated as volumetric water content divided by the soil porosity. To evaluate soil water content in relation to crop water demands, we calculated the water stress coefficient, K_s , throughout the growing season. K_s values less than 1 indicate increasing crop water stress, or the degree to which soil moisture has dropped below the management allowable depletion, the maximum soil water depletion acceptable between irrigation applications. K_s was calculated using the following equations from FAO 56 (eq. 2; Allen *et al.*, 1998), assuming a single uniform soil layer:

$$K_s = \frac{TAW - SWD}{TAW * (1 - MAD)} = \frac{(\theta_{FC} - \theta_{WP}) - (\theta_{FC} - \theta)}{(\theta_{FC} - \theta_{WP}) * (1 - MAD)} \quad (2)$$

We applied a management allowable depletion (MAD) of 0.5 for maize cropping systems (Allen *et al.*, 1998). Soil water depletion (SWD) was estimated with plot level measurements of gravimetric field capacity (θ_{FC}) and gravimetric soil moisture content (θ) for each sampling day. To calculate total available water (TAW), we applied the same θ_{FC} values and a wilting point (θ_{WP}) of 8.98% GWC, determined from web soil survey data for the site (NRCS, 2017), to all plots assuming no impacts of biochar on the wilting point (Abel *et al.*, 2013; Andrenelli *et al.*, 2016; Hardie *et al.*, 2014; Sun *et al.* 2013).

3.2.5. Soil Mineral N Sampling

Available mineral N was assessed using ion exchange resin bags (Binkley & Matson, 1983). For each time interval, resin bags were buried at a 25cm depth within each of the four central rows of the six-row plot where fertilizer was banded. Resin bags were deployed in the field for a period of 3 weeks in June (June 14th to July 6th), July (July 7th to July 27th) and August (July 28th to Aug 16th). At the end of the deployment period, resin bags were recovered and stored in plastic bags within a cooler. Resins were then removed from the bags and extracted for mineral N analysis. Extracts were performed on each subsample using 100mL 2M KCl, shaken for 1 hour, filtered and analyzed colorimetrically (Alpkem Flow Solution IV Automated wet chemistry system; O.I. Analytical, College Station, TX) for ammonium (NH_4^+) and nitrate (NO_3^-). Available mineral N detected in resin bags was converted to a per area basis assuming resin bags intercepted the soil solution over a 5cm effective diameter (Binkley, 1984).

3.2.6. Maize Biomass and Yield Sampling

Crop phenology was recorded throughout the growing season (Table 6). We measured plant biomass and grain yield once plants had reached physiological maturity. We harvested a 2 m section of the row in each plot measuring the wet biomass in the field and collecting three plants per plot for additional analysis. Plants were dried at 70°C then weighed. Dry biomass measurements included stalk, leaves, cob

and grain. Kernels were dried at 105°C, ground and analyzed for C and N content on a LECO True-Spec CN analyzer (Leco Corp., St. Joseph, MI, USA). Grain N uptake was calculated as the grain N content multiplied by the grain yield. The harvest index was calculated as the dry mass of grain divided by total plant biomass.

3.2.7. Soil GHG Flux Sampling

We measured N₂O fluxes over the entire growing season using a static chamber - gas chromatography (GC) system to capture spatial variability, and an automatic chamber - cavity ring down spectroscopy (CRDS) system to capture temporal variability in GHG fluxes across treatments. Static chambers were installed in each plot (n=24) whereas automatic chambers were deployed in one plot per treatment (n=6).

3.2.7.1. Static Chamber-GC N₂O Sampling

Vented non-steady state closed chambers built from rectangular aluminum pans (29 cm x 50 cm x 10.2 cm, 14.79 L) covered by a thin foam layer with reflective surfaces were used for static chambers (Livingston & Hutchinson, 1995). Collars and chambers were fitted with rubber seals and clamped together during deployment to prevent gaseous losses. The rectangular collars were installed perpendicular to the row to cover both the in-row and between-row gas fluxes (Parkin & Venterea, 2010). N₂O samples were collected weekly starting April 14th, 2016 through Sept 22nd, 2016, with more intensive sampling following fertilizer application. N₂O samples were taken by inserting a 25-mL syringe through the sampling port at 0, 15, 30 and 45 mins after the chamber was sealed (Parkin & Venterea, 2010). Gas samples were transferred from the 25-mL syringe to 12-mL pre-evacuated glass vials with butyl rubber septa, then transported to the USDA Agricultural Research Service laboratory in Fort Collins for GC analysis. Within two weeks of sampling, N₂O concentrations were measured on a fully automated GC equipped with an electron capture detector for measuring N₂O concentrations. Fluxes were

calculated using the linear increase in concentration over the four time points, as CRDS data indicated that fluxes increased linearly (see below). Cumulative N₂O emissions were calculated using trapezoidal integration of the daily N₂O fluxes (Parkin & Venterea, 2010).

3.2.7.2. Automatic Chamber-CRDS GHG Sampling

The automatic cylindrical chambers used in this study (15.2 cm diameter, 1.97 L) had an integrated venting system (eosAC, Eosense, Dartmouth, NS, Canada). Chambers were connected, using 20-30 m of 2 mm inner diameter PVC gas lines, to a multiplexer unit with a recirculation pump (eosMX, Eosense, Dartmouth, NS, Canada), which controlled chamber deployment and gas flow into the GHG analyzer (G2508 CRDS Analyzer; Picarro Inc., Santa Clara, CA). The six automatic chambers were positioned in-row between plants and deployed in series for 30 min with a 5-min flushing period between deployments. The unit was operational from April 19, 2016 to Sept 28, 2016 with occasional down periods due to field operations, electrical outages or temporary equipment malfunctions. The equipment was housed in a wooden shed outfitted with an air-conditioning unit to maintain suitable operating conditions. GHG fluxes were computed using the Eoanalyze software (Eosense, Dartmouth, NS, Canada), setting a 3-min deadband and applying a linear regression to N₂O fluxes and exponential regression to CO₂ fluxes, as such regressions minimized the error in the flux calculation.

3.2.8. Data and Statistical Analysis

Biochar induced N₂O emission reductions were calculated as the difference between biochar and control treatments then converted to CO₂-eq using global warming potentials from the IPCC 5th assessment report (Myhre *et al.*, 2013). The standard error for the N₂O emission reductions were calculated using error propagation. Irrigation water-use efficiency was calculated as the grain yield divided by the irrigation water applied. Yield-scaled N₂O emissions were calculated as the cumulative N₂O emissions divided by the grain yield. All response variables were modeled using a linear mixed effect model with

biochar amendment and irrigation (and date, for mineral N and soil C analysis) as fixed effects and block (and date for average water content analysis) as a random effect when block was a significant factor. Where block effects were not significant, a two-factor linear model of amendment and irrigation was applied. Where model residuals were non-parametric, exponential or logarithmic transformations were applied to the response variables to achieve a normal distribution. Models were then evaluated using analysis of variance and pairwise comparisons. Linear regressions were applied to evaluate the relationship between average Ks during vegetative growth stages and biomass yield, and average Ks during reproductive growth stages and grain yield, fitting an intercept of 0 to the model. All statistics were performed in R version 3.3.2 (R Core Team, 2016).

3.3. Results

3.3.1. Biochar increased soil moisture but did not reduce crop water stress

Both biochar ($p < 0.001$) and irrigation treatments ($p = 0.005$) had a significant impact on soil moisture over the growing season (Fig. 9). Over the growing season, the biochar amendment increased GWC across treatments by 9.7%, and specifically by 7.9%, 7.7% and 12.9% in the Full, Limited irrigation, and Drought treatment, respectively. Upon application, biochar amendments decreased the bulk density of the control soils from $1.19 \pm 0.02 \text{ g cm}^{-3}$ to $1.01 \pm 0.03 \text{ g cm}^{-3}$ ($p < 0.001$), resulting in biochar increasing total soil porosity from 55% in the control soils to 62% in biochar amended soils upon application. Despite the apparent losses of biochar C over the study (as described in section 3.4), bulk density within the biochar plots did not significantly change over time. Soil WFPS varied between 7.4% and 53.1% throughout the growing season, with biochar amendments significantly increasing the average WFPS ($28.6\% \pm 0.5$) relative to the control ($26.5\% \pm 0.4$; $p = 0.001$) (Fig. A3).

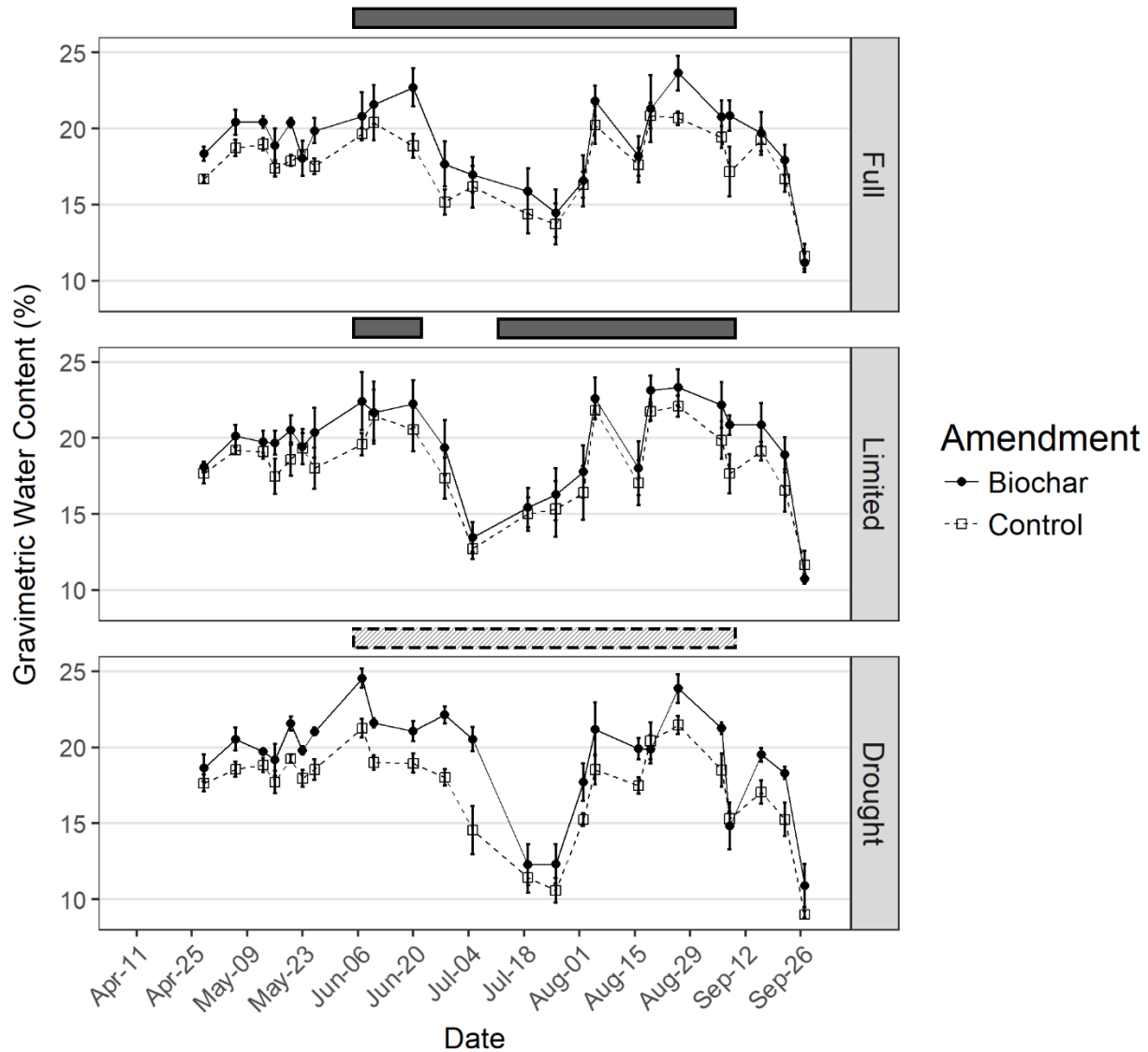


Fig. 9: Gravimetric water content dynamics throughout the 2016 growing season in the biochar (closed circles) and control (open squares) treatments, across the three irrigation regimes (Full, Limited and Drought). Bars above the plots represent the period of weekly irrigation water application with darker shading representing conventional irrigation rates and lighter shading indicating half such rates. Data are presented as means \pm 1 SE (n=4).

Biochar treatments increased soil field capacity (21.7% GWC) relative to the control (20.2%, $p=0.004$), with no effect of irrigation treatment. Across all treatments, maize experienced greater water stress during the reproductive phases as indicated by the water stress coefficient, K_s , where values less than 1 indicate increasing crop water stress. During the vegetative phases the average K_s value was 0.95, while during the reproductive phases it averaged 0.92 ($p=0.002$; Fig. 10). Irrigation regime significantly impacted water stress ($p<0.001$) where over the growing season the Drought treatments experienced

the lowest K_s values averaging 0.91, while Limited irrigation and Full irrigation treatments were subject to moderate water stress at 0.94 and 0.96, respectively (Fig. 10). Biochar amendments did not impact the water stress coefficient over the growing season.

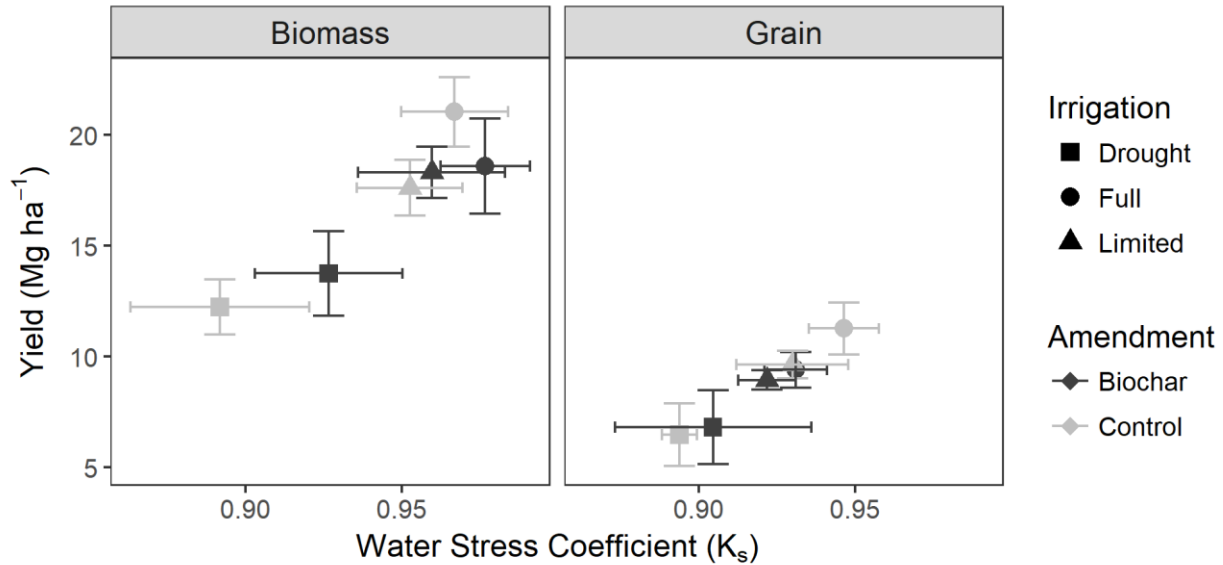


Fig. 10: Relationship between the average water stress coefficient during the vegetation growth phases (left panel) and reproductive growth phases (right panel) and the corresponding yield (biomass yield, left panel; grain yield, right panel) by soil amendment (biochar, black; control, light grey) and irrigation treatments (Full, squares; Limited, circles; and Drought, triangles; see text for details). Data are presented as means \pm 1 SE (n=4).

3.3.2. Biochar did not improve crop yield or biomass

Biochar amendments had no significant impact on field-scaled maize biomass, grain yield or harvest index, with the latter being on average 0.51 ± 0.05 , across all treatments. Irrigation treatments did impact both yield ($p=0.001$) and biomass ($p<0.001$) but not harvest index. Relative to the Full irrigation treatment, the Drought treatment had 36% lower grain yield ($p<0.001$). The Limited irrigation treatment did not significantly affect yields or irrigation water-use efficiency relative to the Full. Irrigation had similar impacts on maize biomass. Relative to the Full irrigation treatment, the Drought treatment resulted in a 34% decrease in biomass ($p<0.001$), while there was no significant reduction in biomass within the Limited irrigation treatment. Biomass yield was best predicted relative to the average water stress coefficient during the vegetative growth phases (slope = 17.95, $R^2=0.95$, $p<0.001$; Fig. 10) while

grain yield was correlated to the average K_s values during the reproductive growth phases (slope = 9.54, $R^2=0.93$, $p<0.001$; Fig. 10).

3.3.3. Biochar did not impact soil mineral N availability or crop N uptake

Biochar amendments had no significant impact on either NH_4^+ or NO_3^- extracted from resin bags deployed throughout the growing season (Fig. 11). Irrigation treatments, month of the growing season, and their interactions did significantly impact NH_4^+ ($p < 0.001$, $p < 0.001$, $p=0.01$, respectively) and NO_3^- (all $p < 0.001$). Across all treatments, the available NH_4^+ significantly decreased from June to August (Fig. 11). In June, all irrigation treatments had similar NH_4^+ concentrations. In July and August, NH_4^+ availability in the Drought treatment was 93% and 98% (both $p < 0.001$) less than the Full irrigation treatments, while the Limited irrigation treatments contained similar NH_4^+ levels as the Full. In contrast, NO_3^- availability increased over the three months in all treatments, except for the Full irrigation plots where August recorded the lowest NO_3^- levels (Fig. 11). In June, all irrigation treatments showed distinct NO_3^- availability (relative to Full irrigation, Limited irrigation NO_3^- experienced a 34% decrease and Drought a 95% decrease). In July, only the Drought treatment exhibited a 76% decrease in NO_3^- relative to the Full irrigation plots. In August, there were no significant differences in NO_3^- between irrigation treatments. Grain N uptake was not impacted by irrigation regime or biochar amendments, averaging $114.7 \pm 6.3 \text{ kg N ha}^{-1}$.

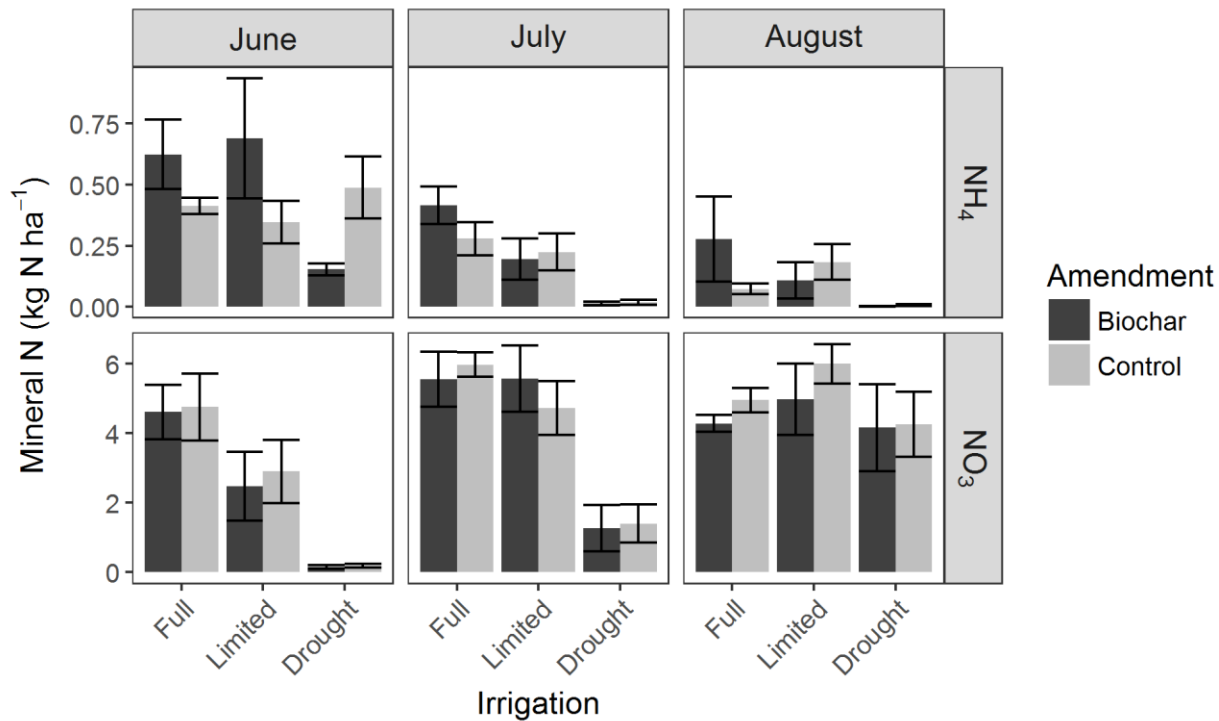


Fig. 11: Available mineral N (ammonium (NH₄⁺), top panels; nitrate (NO₃⁻), bottom panels) in the soil solution at 25 cm depth sampled by month in the biochar amended (black) and control (light grey) treatments, across the three irrigation regimes (Full, Limited and Drought). All treatments received a urea ammonium nitrate fertilizer May 13, 2018 banded at a similar depth. Data are presented as means ± 1 SE (n=4).

3.3.4. Biochar sequesters C but provides limited GHG benefits from N₂O reduction

Biochar amendments significantly increased soil C both at the initial soil sampling after biochar application (May 27th, 2015) and the conclusion of the study (Sept 27th, 2016), but to a much lesser extent (Fig. 12). Irrigation regime had no impact on soil C. After sixteen months biochar treatments exhibited a 6.3 Mg ha⁻¹ increase in total C relative to the control ($p < 0.001$), equivalent to a 7.3 Mg ha⁻¹ or 0.6% by mass biochar application rate. At the 10-30 cm depth, total C remained constant over time and by treatment, with no significant change in soil C by date, amendment or irrigation. The coarse biochar C fraction decreased from 18.6 to 5.2 Mg C ha⁻¹ over the sixteen-month study period. At the 0-10 cm depth, biochar treatments significantly increased the soil C fraction by 0.92% C at the initial soil sampling ($p < 0.001$), but showed no difference in soil C content relative to the control at the final sampling date. In the biochar treatments some of the soil C fraction consisted of biochar particles

fragmented into soil particulate organic matter. Biochar treatments did not significantly impact average CO₂ fluxes, as sampled by the automatic chamber-CRDS measurements (Fig. A4)

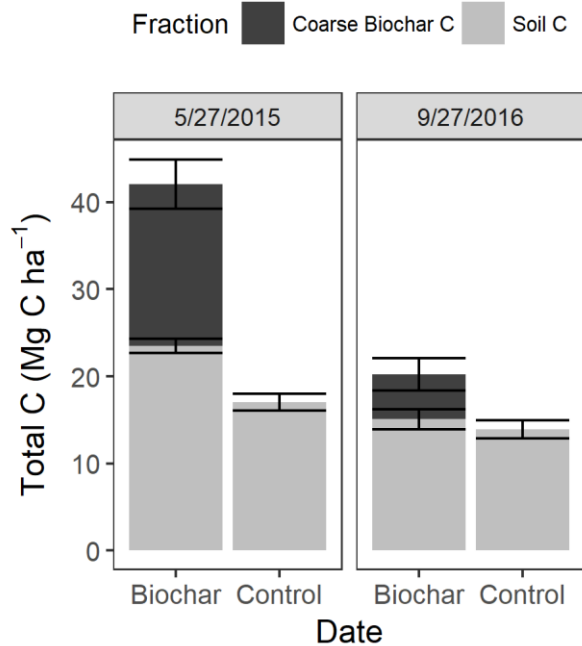


Fig. 12: Total C at the 0-10 cm depth in the biochar and control treatments separated by the coarse biochar C (black) and soil C (light gray) sampled after biochar application (5/27/2016) and at the end of year two (9/27/2016). There was no biochar effect on total C at the 10-30 cm depth. Data are presented as means \pm 1 SE (n=4).

N₂O fluxes are reported using the results from the spatially replicated static chamber-GC measurements (Fig. 13), while automatic chamber-CRDS measurements (Fig. A5) were used to evaluate N₂O flux temporal variability. Automatic chamber-CRDS N₂O fluxes confirmed that the weekly static chamber-GC measurements caught the primary N₂O peaks throughout the field season (with peaks defined as N₂O fluxes exceeding one standard deviation above mean). Automatic chamber-CRDS also verified that static chamber-GC fluxes measured in the AM hours were representative of fluxes over the full day.

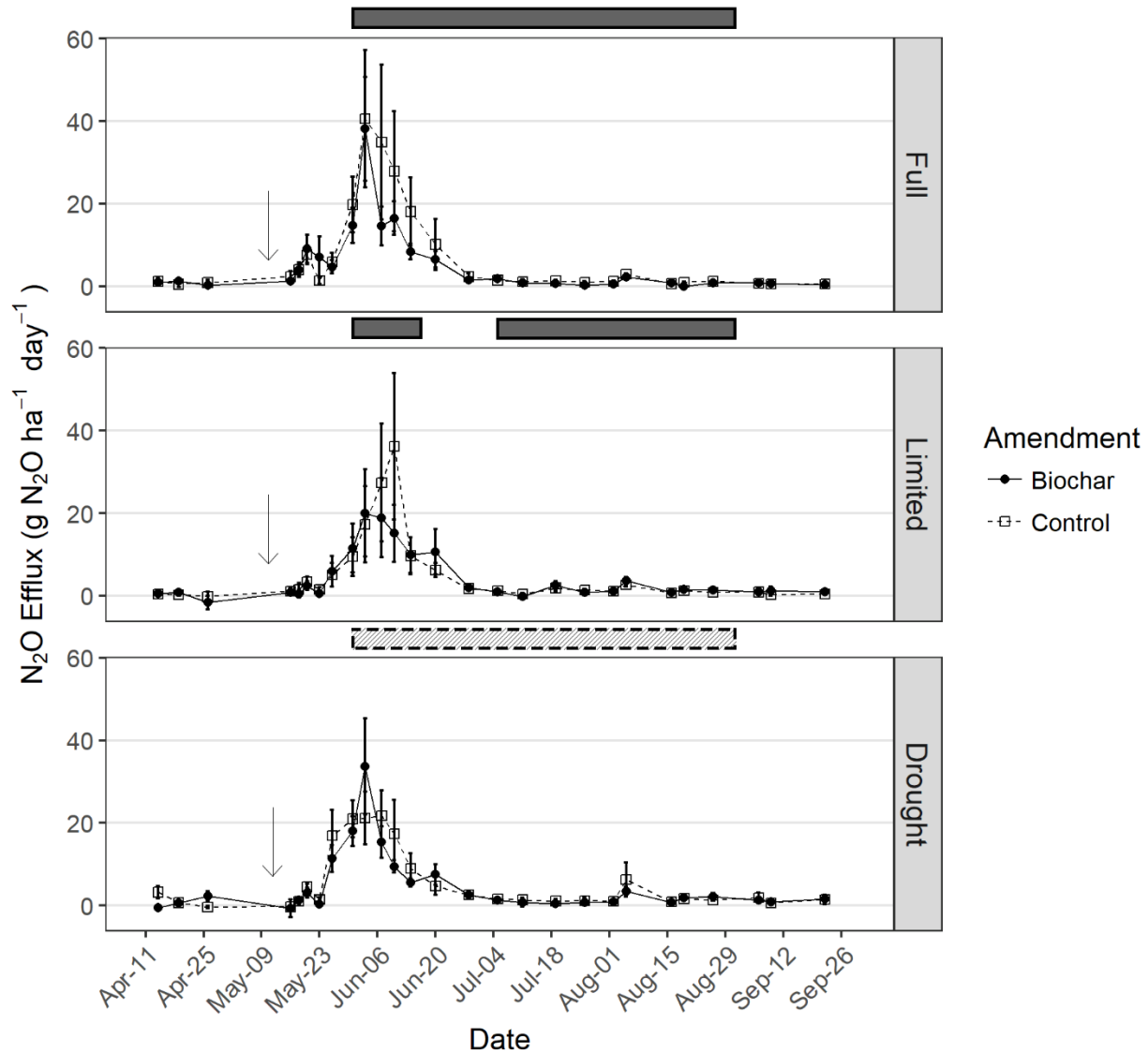


Fig. 13: Nitrous oxide fluxes sampled using static chambers and gas chromatography across all plots throughout the growing season in the biochar (closed circles) and control (open squares) treatments, across the three irrigation regimes (Full, Limited and Drought). Arrows indicate fertilizer application, while bars above the plots represent the period of weekly irrigation water application with darker shading representing conventional irrigation rates and lighter shading indicating half such rates. Data are presented as means \pm 1 SE (n=4).

N₂O fluxes peaked three weeks (June 3rd) after N fertilizer application, dropping below 13.5 g N₂O ha⁻¹ day⁻¹ (one standard deviation above the mean N₂O flux) by June 20th and remaining below that threshold for the remainder of the field season (Fig. 13). Mean cumulative N₂O emissions over the growing season ranged from 0.52 to 0.81 kg N₂O ha⁻¹ across treatments with the coefficient of variation (CV) ranging from 33% to 81% (Fig. 14). In the biochar and control treatments, mean cumulative N₂O-N emissions

over the growing season comprised 0.36% and 0.43% of the mineral N fertilizer applied. There was no statistically significant impact of either biochar or irrigation treatments on cumulative N₂O emissions (Fig 14). Similarly, biochar did not significantly affect yield-scaled N₂O emission but trended toward decreased yield-scaled emissions across treatments (Fig. A6).

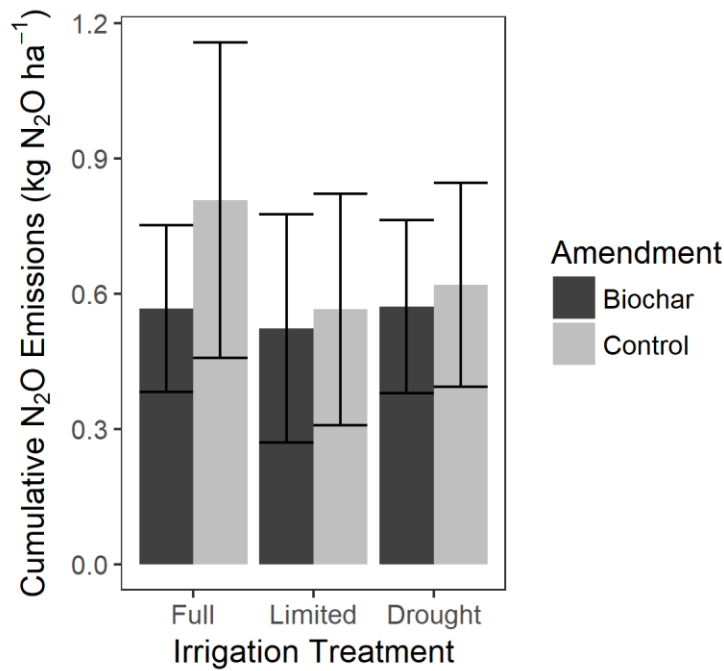


Fig. 14: Cumulative nitrous oxide emissions interpolated over the 2016 growing season (April 14 to Sept 22) using static chamber data in the biochar (black) and control (light grey) treatments, across the three irrigation regimes (Full, Limited and Drought). Data are presented as means ± 1 SE (n=4).

3.4. Discussion

3.4.1. Biochar effects on soil moisture and soil field capacity

Biochar amendments significantly increased soil water content and field capacity in this study, which can largely be attributed to the 15% decrease in soil bulk density, increasing the total porosity of the soil (Basso *et al.*, 2013; Suliman *et al.*, 2017). However, numerous factors regulate the degree to which biochar impacts soil water retention, including soil texture, biochar pore size distribution and biochar surface chemistry (Gray *et al.*, 2014; Omondi *et al.*, 2016; Sun *et al.*, 2012). Biochar amendments show

the greatest improvement in available water content in sandier soils (Dan *et al.*, 2015; Omondi *et al.*, 2016), however, in this clay loam soil, biochar amendments still resulted in a 7.5% increase in field capacity. The increased water content at higher matric potentials (i.e. field capacity) is largely driven by biochar's increased macro-porosity (Sun *et al.*, 2013). Biochar's macro-porosity is well correlated with feedstock selection due to retention of the cellular structure of the feedstock (Gray *et al.*, 2014). Woody biomass, composed of tracheids or vessels, retains much of this tubular structure during pyrolysis and results in greater biochar macro-porosity (Sun *et al.*, 2012). At lower matric potentials, where water content is largely regulated by micro- and nano-porosity, biochar surface chemistry becomes a greater control due to the hydrophobic or hydrophilic nature of surface functional groups (Gray *et al.*, 2014). Many studies indicate biochar has no impact on soil wilting point at the 2.1% application rate used in this study (Abel *et al.*, 2013; Andrenelli *et al.*, 2016; Hardie *et al.*, 2014; Sun *et al.* 2013). However, some research indicates a small biochar-induced increase in the wilting point of the soil of 0.28% VWC for each percent increase in the biochar application rate (Suliman *et al.*, 2017; Bruun *et al.*, 2014). Thus, with minimal impacts on the wilting point and increased field capacity, biochar can increase soil available water content (Abel *et al.*, 2013; Andrenelli *et al.*, 2016; Bruun *et al.*, 2014; Suliman *et al.*, 2017).

Biochar may increase water retention throughout the field season but its agronomic value is better reflected in its ability to decrease crop water stress. The water stress coefficient K_s is a widely used proxy for crop water stress, based on the available water in the rooting zone relative to crop water demands from evapotranspiration (Allen *et al.*, 1998). K_s was higher during the vegetative stages (V1-VT; Table 6) resulting in less water stress compared to the reproductive stages (R3-R4) when water is critical for grain filling (Payero *et al.*, 2009). The Drought treatments experienced the lowest K_s values indicating increased stress. This stress was not significantly alleviated by the increased water content in the biochar treatment (Fig. 10). As the water stress coefficient is a function of both the current soil

moisture and water deficit, it better assesses crop water requirements relative to water available in the soil profile. While biochar increased the field capacity, it also increased the available water content, which is proportionally related to management allowable depletion. Thus, biochar treatments required higher water contents to satisfy crop demands resulting in insignificant changes to K_s . Woody biochar may improve water retention, but without specifically tailoring the irrigation timing and amounts to account for such impacts, soil moisture may still drop below the management allowable depletion and continue to result in crop water stress.

3.4.2. Biochar and deficit irrigation effect on grain and biomass yield

Drought irrigation treatments, where irrigation was reduced by 50%, resulted in greater water stress and lower yields during both the vegetative and reproductive growth phases (Fig. 10). The Limited irrigation treatments, where irrigation was stopped during vegetative growth stages, did not impact yields, highlighting one strategy to improve irrigation water-use efficiency (Foster *et al.*, 2016; Geerts & Raes, 2009). However, the modest water savings from the Limited irrigation treatment (8.3 cm) did not significantly increase irrigation water-use efficiency relative to the Full irrigation treatment. Grain yields are less impacted by such Limited irrigation treatments, because maize tends to be more sensitive to water stress during the reproductive growth phases as grain fill occurs (Payero *et al.*, 2009).

Despite water retention improvements, neither grain nor biomass yields in either deficit irrigation treatments were significantly improved by the biochar amendment. The two deficit irrigation treatments did reduce mineral N availability in the soil (Fig. 11) or impact grain N uptake, indicating N limitation did not drive the reduction in yields under deficit irrigation treatments. A similar biochar induced increase in soil moisture without yield impacts has been shown in maize (Haider *et al.*, 2017), sunflower (Pfister & Saha, 2016), and other cropping systems (Tammeorg *et al.*, 2014). Haider *et al.* found similar results of increased water content but no yield impacts in a 4-year field study (2017) yet in

a similar pot study, they saw a yield impact correlated to increased soil moisture (2014). Across treatments, the average water stress coefficient proved to be well correlated with yields. Fig. 10 illustrates how biochar's minor improvement in K_s only slightly increased the relevant yield in accordance with the regression. In this study, the standard deficit irrigation treatments (i.e. a temporary drought period or severely reduced irrigation amounts) were not tailored to biochar's improved water holding capacity, resulting in periods of crop water stress. By better monitoring such periods of crop water stress and managing deficit irrigation treatments with biochar's improved water retention, producers may be able to reduce water inputs while maintaining yields.

Other hydraulic factors beyond water holding capacity or the water stress coefficient may also influence the system. Despite the majority of water uptake in maize occurring at a depth of 5 to 20 cm (Asbjornsen *et al.*, 2008), soil moisture dynamics below the 10 cm sampling depth may have been impacted by increased water retention in the upper soil layers. A recent meta-analysis indicates biochar generally increases soil saturated hydraulic conductivity, which could influence soil water dynamics deeper in the profile potentially altering root growth and root water uptake (Omondi *et al.*, 2016). Future research of biochar effects on soil moisture dynamics along the soil profile may help explain why the increased soil moisture in the upper soil layers did not result in yield benefits for deficit irrigation treatments.

3.4.3. Biochar effects on N availability

Despite hypotheses of biochar's increased surface area and cation exchange capacity improving N retention and delivery to crops (Clough *et al.*, 2013), in this maize system, we found biochar had no impact on mineral N availability in the rooting zone (Fig. 11) or grain N uptake. These results confirm findings in similar temperate maize systems where no improvement in N uptake with biochar amendments were observed (Güereña *et al.*, 2013; Haider *et al.*, 2017), while others reported a pine

wood biochar improved maize yields at higher fertilization rates (Brantley *et al.*, 2015). While numerous studies cite biochar's ability to decrease N leaching (Nguyen *et al.*, 2017), an average 4.2% of fertilizer N applied was intercepted in this clay loam soil by the ion exchange resins over the 3-week period they were deployed. Such interception of mineral N is low relative to the global 15% average loss of fertilizer N to NO_3^- leaching in maize systems (Zhou & Butterbach-Bahl, 2014). This low movement of mineral N through the soil profile indicates no significant mineral N leaching for biochar to alleviate.

3.4.4. Biochar effects on GHG emission reductions and C sequestration

3.4.4.1. Biochar impacts on C sequestration and mobility

While much of the biochar was recovered in the coarse particulate fraction at the end of the study, there was a surprising loss of $21.9 \text{ Mg C ha}^{-1}$ from the system, with 61% of the loss from the coarse biochar C fraction and 39% from the soil C fraction. Biochar particles at the surface may be increasingly susceptible to wind erosion when soil GWC < 15% (Silva *et al.*, 2015). Wind erosion may explain the significant loss of biochar C in both fractions at this field site. In this study 37% of days experienced wind speeds greater than 5 m s^{-1} , a threshold sufficient to move larger biochar particle sizes >0.6 mm (Silva *et al.*, 2015). At the same field site, a pine wood biochar produced using fast-pyrolysis with a particle size of 0.25 to 3 mm particle size was disk tilled in the fall of 2013 to a similar depth, and did not result in a similar loss of C after one season (Foster *et al.*, 2016). The smaller particle size and fall application with a winter snow cover may contribute to decreased susceptibility to erosion.

Other potential C losses may come from microbial decomposition or C transport through the soil profile. Biochar's recalcitrant aromatic structure prevents microbial mineralization over short timeframes (Lehmann, 2007; Spokas, 2010). When soils from this site were incubated with the same biochar under laboratory conditions, biochar did not increase soil respiration (Ramlow & Cotrufo, 2017). Similar to other field studies exploring biochar impacts on CO_2 fluxes (Liu *et al.*, 2016), automatic chamber-CRDS

CO₂ measurements confirmed that biochar did not significantly impact CO₂ fluxes (Fig. A4). Biochar's ability to increase hydraulic conductivity (Omondi *et al.*, 2016) may also result in the delivery of highly fragmented biochar particles deeper in the soil profile (Major *et al.*, 2010; Obia *et al.*, 2017). However, in this water limited system, such leaching is unlikely. No coarse biochar was recovered in the 10-30 cm depth and biochar amendments did not significantly increase soil C at this depth, indicating that biochar C was not fragmented and displaced lower in the soil profile after tillage events.

3.4.4.2. Biochar impacts on N₂O emissions

While biochar effects on cumulative N₂O emissions over the growing season were not significant, the trend of decreased cumulative N₂O emissions in biochar treatments (Fig 14) is consistent with a 11.5% N₂O emission reduction reported across biochar field studies in upland agricultural systems (Verhoeven *et al.*, 2017). Biochar's low N₂O emission reductions in this study relative to a lab incubation using the same soil (Ramlow & Cotrufo, 2018) may be due to drier field conditions that are less favorable to N₂O production, variable soil structure affecting water and gas transport, or more heterogenous biochar application in the field (Cayuela *et al.*, 2014; Verhoeven *et al.*, 2017). Applying best N management practices coupled with crop N uptake, which many lab incubations do not account for, may also significantly reduce the excess mineral N available for N₂O production, leading to lower biochar N₂O mitigation potentials in the field (Venterea *et al.*, 2012). Compared to the predicted emission factor of 0.83% of N fertilizer applied resulting in N₂O emissions, determined using a global N₂O emission factor regression (Shcherbak *et al.*, 2014), this site experienced lower N₂O emissions with an emission factor of 0.43% in the control plots. The relatively high CV for each treatment observed in this study is not uncommon in the N₂O literature with other studies with greater spatial replication reporting similar CVs (Turner *et al.*, 2016).

A variety of mechanisms for biochar-induced N₂O reductions in the field have been reported including; biochar increasing pH to enhance complete denitrification of N₂O to N₂ (Obia *et al.*, 2015; van Zwieten *et al.*, 2014), biochar improving aeration to reduce net denitrification (Saarnio *et al.*, 2013) and biochar reducing N₂O diffusion rates allowing for more complete denitrification (Harter *et al.*, 2016; Quin *et al.*, 2015). In these calcareous soils with a pH of 7.99 any biochar pH effect would be minimal, yet biochar plots still trended towards decreased N₂O emissions. Both biochar and control treatments resulted in lower WFPS across irrigation regimes (7 to 53% WFPS), within the range where nitrification would be the primary source of N₂O (Baggs & Bateman, 2005), and nitrification was evident by the decrease in NH₄⁺ coupled with accumulation of NO₃⁻ (Fig. 11). Thus biochar would not have improved soil aeration to decrease denitrification-derived N₂O emissions, which lab incubations have shown can be a factor at moderately anaerobic soil moisture regimes (Case *et al.*, 2012; Ramlow & Cotrufo, 2017). Biochar's N₂O sorption capacity (Cornelissen *et al.*, 2013; Quin *et al.*, 2015) may allow for N₂O entrapment in biochar pores allowing for the complete reduction of N₂O to N₂ during denitrification within anaerobic soil microsites (Harter *et al.*, 2016). If these physical explanations are the primary mechanism for biochar's N₂O reduction potential, the heterogeneous soil structure across field sites could help account for the wide spatial variability and lower biochar N₂O reduction in the field relative to lab incubations.

3.5. Conclusions

Despite improving soil water retention and maintaining greater soil moisture content throughout the growing season, woody biochar amendments did not improve maize biomass or grain yields in deficit irrigation treatments. The strong correlation between the average water stress coefficient and yield indicates that biochar's increased capacity to retain water did not alleviate crop water stress during critical growth stages. To achieve significant yield increases in deficit irrigation systems, biochar manufacturers could engineer biochars to maximize plant available water in soils and producers could adjust irrigation scheduling or target areas with low water holding capacity to best utilize biochar's

improved water retention. Biochar amendments had no significant impact on N cycling as evidenced by no changes in mineral N availability within the rooting zone or grain N uptake. In terms of environmental benefits, this study highlighted the mobility of coarse biochar C, which can be an important factor when monitoring *in situ* C sequestration. Biochar impacts on N₂O emissions were inconclusive, with trends toward decreased cumulative N₂O emissions across irrigation regimes similar to other field studies. Limited irrigation treatments also showed insignificant, but similar, potential for N₂O reduction and modest improvements in irrigation water-use efficiency. Overall, in this maize system, biochar demonstrated limited agronomic but some environmental benefits. This experiment underlined the importance of field trials to quantify the actual effects of biochar application to help managers weigh potential benefits.

4. PROMOTING REVEGETATION AND SOIL CARBON SEQUESTRATION ON DECOMMISSIONED FOREST ROADS IN COLORADO, USA: A COMPARATIVE ASSESSMENT OF ORGANIC SOIL AMENDMENTS³

4.1. Introduction

Forest lands in the United States contain a vast network of unpaved roads that increase sediment delivery to streams (Reid & Dunne, 1984), alter hillslope hydrology (Eastaugh *et al.*, 2008) and create habitat fragmentation (Robinson *et al.*, 2010; Trombulak & Frissell, 2001). Road construction and maintenance activities are primary sources of sediment to forest streams (Megahan & King, 2004), and sediment delivery rates from road surfaces can equal those from severely burned hillslopes (MacDonald & Larsen, 2009). One strategy to minimize the watershed effects of unpaved roads is to decommission underutilized roads and those located on sensitive soils, riparian and habitat areas (Madej, 2001; Switalski *et al.*, 2004). The US Forest Service has widely adopted this strategy, decommissioning 2,500 to 8,000 km of forest roads each year (Coghlan & Sowa, 1998; Forest Service, 2010). Road decommissioning includes a wide variety of treatments such as gating and blocking roads, decompacting and obliterating road prisms, recontouring hillslopes and revegetating road corridors (Bagley, 1998). Revegetation of decommissioned roads benefits watershed conditions and native plant diversity where it minimizes soil erosion, improves native plant cover and reduces or prevents invasion of non-native plants (Elseroad *et al.*, 2003; Swift, 1984; Switalski *et al.*, 2004). Intensive treatments, such as decompaction and addition of amendments, may simultaneously enhance revegetation and soil C sequestration. Organic soil amendments influence revegetation and C sequestration via numerous, interacting physical, chemical and biological processes (Fig. 15), that must be evaluated to increase understanding of treatment efficacy and inform sound management decisions.

³ Ramlow, M., Rhoades, C.C., Cotrufo, M.F. (2018). Promoting revegetation and soil carbon sequestration on Decommissioned forest roads Colorado, USA: A comparative assessment of organic soil amendments. *Forest Ecology and Management*, **247**, 230-241.

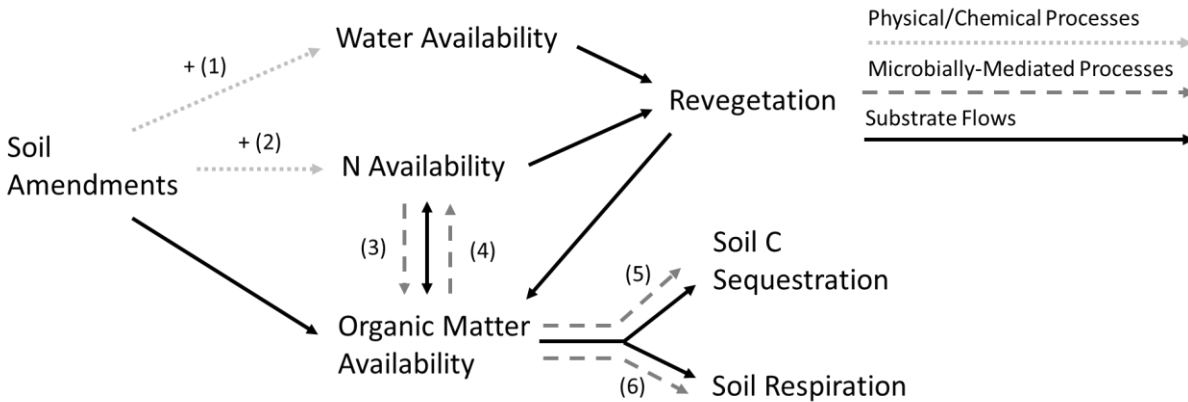


Fig. 15: Conceptual diagram depicting how organic soil amendments can impact revegetation and soil C sequestration through substrate flows of C, N and H₂O (black arrows), physical/chemical processes (light grey arrows) and microbially-mediated processes (grey arrows). Soil amendments can affect physical/chemical processes regulating soil water and N availability (with +/- indicating the direction of the effect) by increasing soil water holding capacity or decreasing evaporation (1) and increasing the soil exchange capacity to retain mineral N (2). Amendments can also impact soil microbial activity by directly affecting mineral N availability through gross N immobilization (3) or N mineralization (4), directly supplying C which can be microbially-processed and stabilized to mineral surfaces to sequester C (5) or respired (6), or indirectly influencing soil moisture or temperature.

Plant recovery on closed forest roads is often limited by compacted soils, reduced seed bank, low soil organic matter (SOM) stocks, poor soil moisture water retention and decreased nutrient cycling (Elseroad *et al.*, 2003). Low soil moisture can limit plant establishment, especially in arid and semi-arid ecosystems (Aronson *et al.*, 1993). The low SOM on forest roads, reduces soil water retention, especially in rocky and coarse-textured forest soils (Rawls *et al.*, 2003). Low SOM also results in limited substrates available to supply mineral N to plants through N mineralization (Booth *et al.*, 2005). Soil structure is also important for revegetation with numerous studies demonstrating that alleviating compaction through mechanical ripping or biological activity enhance revegetation efforts (Alban *et al.*, 1994; Ampoorter *et al.*, 2011; Greacen & Sands, 1980). Decommissioned roads are typically seeded to facilitate rapid plant establishment to reduce erosion and invasion by non-native plants and provide habitat and forage for wildlife (Grant *et al.*, 2011). However, after decompaction and seeding, SOM stocks may remain low relative to native soil (i.e., 30% lower (Viall *et al.*, 2014)), suggesting that organic

amendments that increase soil water, N and C content may more quickly or effectively meet revegetation objectives.

Soil amendments that persist over longer timespans (i.e. wood strand mulch or biochar), can improve soil water availability by increasing soil porosity, increasing the amount of water held at field capacity and decreasing soil evaporative losses. Mulching is commonly used to reduce surface erosion (Foltz, 2012; Sosa-Pérez & MacDonald, 2017), but may also benefit plant establishment by improving soil water retention (Benigno *et al.*, 2013). Woody mulches made from forest residues have been shown to increase soil water content in post-fire rehabilitation treatments while utilizing non-merchantable materials and reducing surface fuels (Rhoades *et al.* 2015 & 2017). Biochar, the product of biomass pyrolysis, may provide an alternative restoration treatment that can also be sourced from forest residues. Biochar has been shown to improve soil water retention by increasing soil porosity and surface area (Omondi *et al.*, 2016), with numerous studies in forest soil revealing increased soil water-holding capacity after biochar application (Li *et al.*, 2018).

Most forest ecosystems are N limited, and the low SOM content typical of decommissioned roads is likely to depress soil N availability and plant growth. Organic soil amendments can supply mineral N to enhance plant growth, but N in excess of plant demands can increase N losses to nearby waterways (Venner *et al.*, 2009) or encourage competition from invasive plants (Davis *et al.*, 2000). Organic fertilizer with low C:N ratios gradually release mineral N through mineralization. Compared to inorganic fertilizers, these organic amendments slowly deliver N over time. However, compared to recalcitrant organic amendments, the N supply from organic fertilizers is relatively short-lived. Recalcitrant organic amendments with high C:N ratios (e.g., wood strand mulch and biochar) are more likely to immobilize soil mineral N (Bulmer, 2000) and temporarily reduce plant available N before releasing mineral N via mineralization (Rhoades *et al.*, 2012 & 2017). Amendments can also affect soil chemical properties.

Biochar's high surface area and ion exchange capacity is known to increase soil N retention (Biederman & Harpole, 2013). Combining labile and recalcitrant organic amendments may provide water retention benefits and slow N release from high C:N material, but also ensure sufficient plant available N to support rapid revegetation of recently-decommissioned roads.

Organic soil amendments also contribute organic matter to fuel microbially-mediated processes and sequester soil C. As organic amendments decompose, a fraction of the C input is utilized by soil microbes to produce secondary compounds that can form associations with soil minerals and persist in soils for decades to centuries (Grandy & Neff, 2008). In contrast, biochar amendments add highly-recalcitrant condensed polyaromatic C compounds to soil that resist microbial processing (Cross & Sohi, 2011), retain their porous structure and sequester C in soils for centuries (Spokas, 2010; Wang *et al.*, 2016).

Organic fertilizers and mulches are commonly used to support revegetation of decommissioned forest roads, yet little is known about how their effects on chemical, physical and microbial soil processes may determine treatment efficacy. In this study, we examine organic fertilizer and wood strand mulch applications currently used to restore forest roads in Northern Colorado, as well as a woody biochar treatment, and combinations of the amendments. We expect soil amendments to have the greatest positive effect on revegetation and soil C sequestration of decommissioned roads when they reduce soil water, mineral N and SOM limitations (Fig. 15). We hypothesize:

- 1) Soil amendments, applied at rates commonly used in restoration practices, will impact revegetation and soil C sequestration on decommissioned forest roads through different processes:

Organic fertilizer can support revegetation by providing a short-term increase in N availability through N mineralization, but with no impact on soil moisture. Low C:N fertilizers will not significantly increase SOM content, thus will not sequester C.

Wood strand mulch can support revegetation primarily by increasing soil water content with mixed effects on mineral N; limiting N availability in the short-term due to its high C:N ratio leading to N immobilization, but supplying N through N mineralization in the long-term. Mulch can supply organic matter to support microbially-mediated process resulting in some soil C sequestration, but also increased soil respiration.

Woody biochar can support revegetation by increasing soil water content through increased porosity and increasing mineral N availability through enhanced soil ion exchange capacity. Biochar will sequester C in the particulate form and will not affect soil respiration or significantly increase the mineral soil C.

Combination treatments can support revegetation through synergistic effects of biochar and mulch improving soil moisture and the addition of fertilizer decreasing short-term N limitation in the mulch and biochar treatments. Fertilized biochar treatments are expected to retain the most fertilizer N in the short term. The combined biochar and mulch treatment will have the greatest soil C sequestration potential from biochar's recalcitrance and contributions of mulch C to the mineral soil fraction.

- 2) Soil amendments will facilitate sustained soil restoration if they support the physical, chemical or biological processes that improve water and/or N availability to plants. Amendments that only contribute substrates to the soil will only provide short-term benefits.

The results of this study can have important implications for understanding how a variety of organic soil amendments and their combinations applied at standard rates alter soil processes that influence initial revegetation and C sequestration on recently-decommissioned forest roads.

4.2. Materials and Methods

4.2.1. *Study Site and Experimental Design*

To evaluate how various organic soil amendments impact revegetation and soil C sequestration on decommissioned forest road, we selected four (50-80 m long) road sections on the Arapahoe-Roosevelt National Forest near Red Feather Lakes, CO. Within the study area, average temperature ranged from 3.7 to 5.6°C, with 429 to 491 mm rainfall (30-year normal, 1981-2010; PRISM Climate Group, 2017), and soils are characterized as Eutroboralfs, Argiborolls or Haploborolls (NRCS, 2017) with a gravelly to very gravelly loam texture (33-41% gravel, 27-30% sand, 26-31% silt, 4-12% clay). Roads were decompacted in October 2014 to a 30 cm depth using a three-tined mechanical ripper. Each road segment contained seven 3m x 5m plots with a 1m buffer between plots. Within each road segment we randomly assign each of the seven treatments (an unamended control, organic fertilizer, wood strand mulch, woody biochar and their pairwise combinations). Each plot contained two 1 m² squares reserved for plant cover and biomass sampling, and eight designated locations for destructive soil sampling >0.5 m from the plot edge. On Oct 16th, 2014, woody biochar, where applicable, was applied at a rate of 25 Mg ha⁻¹ (equivalent to a 2.1% by mass application rate) on the soil surface, and organic fertilizer, where applicable, was broadcast across the plot delivering 16 kg of N ha⁻¹. All plots were turned over to a 15 cm depth using hand tools to incorporate biochar, where applicable, and break up soil clods. Plots were then seeded with 1.5 g m⁻² of a native seed mix of grasses, forbs and shrubs and the seeds and fertilizer, where applicable, were covered with soil by tamping the soil surface with leaf rakes. Wood strand mulch, where applicable, was applied Oct 18th, 2014 at a rate of 12.3 Mg ha⁻¹ to achieve 50-70% coverage.

4.2.2. *Materials*

All the amendments used in this study are commercially available. The organic fertilizer, Biosol Forte[®], was produced from a fermented soy media used in penicillin production (Table 8). The woody biochar

was produced by Biochar Now (Berthoud, CO) from a beetle-killed lodgepole pine feedstock, and was analyzed by Hazen Research, Inc. (Golden, CO) in accordance with International Biochar Initiative protocols (Table 8). Wood-strand mulch was sourced from beetle-killed lodgepole pine feedstocks and supplied by Mountain Pine Manufacturing (Table 8).

Table 8: Organic amendment physical and chemical properties

Description	Organic Fertilizer	Wood-Strand Mulch	Biochar
Feedstock	Soybean and cottonseed meal	Beetle-killed lodgepole pine	Beetle-killed lodgepole pine
Production	Fermented media for fungal growth, dried	Biomass shredded, baled and air-dried	Slow pyrolysis, 550°C max temp
Size	2-4 mm granules	6-16 x 0.5 x 0.25 cm strands	Sieved to >3mm
Application Rate	16 kg N ha ⁻¹	12.3 Mg ha ⁻¹	25 Mg ha ⁻¹
Organic C (%)	35	52	86
H:C _{org} (molar ratio)	-	-	0.35
C:N (mass ratio)	5	556.0	478.8
pH	6.1	4.8	8.5

4.2.3. Cover and Biomass

Plant revegetation was evaluated using plant canopy cover and above- and belowground biomass. Cover was assessed in July of 2015, 2016 and 2017 by measuring plant canopy cover using a gridded point-intercept method in 1 m² sample quadrats, identifying plant species by functional groups; graminoids, forbs and shrubs. We clipped aboveground biomass on 0.5 m² sections of one of the quadrats in July of 2016 and 2017, dried samples at 60°C for 48 hour and separated samples into aforementioned plant functional groups. We sampled belowground biomass in the 0-15 cm and 15-30 cm soil depths from soil pit sampling described below (Section 2.7). Coarse root biomass was physically separated on a 4 mm sieve, rinsed in distilled water then dried at 110°C for 24 hours.

4.2.4. Soil Moisture

Soil moisture content was evaluated across treatments by sampling soil volumetric water content (VWC) 7-12 times throughout the growing season each year of the study using a hand-held time domain

reflectometry probe (CD 620, HydroSense Campbell Scientific, Logan, UT). Average VWC was composited from 5 measurements per plot taken in the 0-10 cm depth. Periodically (n=129), we collected soil samples in conjunction with VMC measurements and determined gravimetric water content (GWC) to develop a relation that allowed conversion of VMC measurements to GWC. Soils sampled for GWC analysis were collected from a 0-10 cm depth, transported to the lab in a cooler, and GWC was determined by oven drying a 15-20 g soil subsample at 110 °C for 24 hours. Soil moisture measured as VWC explained most of the variability in GWC ($R^2 = 0.89$) across the range of soil moisture encountered (1-20%) in our study. When calculating annual average GWC, only measurements from months sampled in all three years were included in the calculation.

4.2.5. Mineral Nitrogen Sampling

To determine soil mineral N availability, we used a combination of time-integrated ion exchange resin (IER) bag sampling and soil mineral N extracts at discrete points in time. In each plot, two IER bags were buried at a 10 cm depth in mineral soil and deployed for the winter (Oct to May) of 2014-2015, 2015-2016 and 2016-2017, and summer (May to Oct) of 2015, 2016 and 2017. Resin bags contained a 1:1 mixture of cation (Sybron Ionic C-249, Type 1 Strong Acid, Na⁺ form, Gel Type) and anion (Sybron Ionic ASB-1P Type 1, Strong Base OH⁻ form, Gel Type) exchange resin beads. IER bags were removed from the field and the recovered resins were extracted with 100 mL 2M KCl, shaken for one hour, filtered and frozen until analysis (Binkley & Matson, 1983). Time point samples for soil mineral N were extracted in October each year from the initial soils used for net mineralization assays (described below). Nitrate and ammonium concentrations of the extracts were measured by spectrophotometry using a flow injection analyzer (Lachat Company, Loveland, CO) in 2015 and 2016. In 2017 extracts were analyzed colorimetrically for nitrate and ammonium (Alpkem Flow Solution IV Automated wet chemistry system, O.I. Analytical, College Station, TX).

4.2.6. Carbon and Nitrogen Mineralization Assays and Soil pH

A 14-day aerobic mineralization assay was conducted each year to evaluate soil microbial respiration, potential N mineralization and potential nitrification, along with soil pH, modified from Stanford & Smith (1972) as described below. In October of 2014, 2015, 2016 and 2017, a soil sample was collected from each plot to a 10 cm depth using a bulb corer, and stored in a cooler during transport to the lab. After sieving to 2 mm, three soil subsamples were taken from each core: 1) a 20 g subsample for determining initial mineral N concentration; 2) a 20 g subsample for an aerobic C and N mineralization incubation; and 3) a 10 g subsample for soil pH. The incubated subsample was wetted to 60% field capacity and incubated for 14 days at 25°C in air-tight, quart-sized Mason jars with rubber septa for gas sampling. During the incubation, soils were periodically sampled for CO₂ concentration using an infrared gas analyzer (LI 6252, LI-COR, Lincoln, NE). Jar headspace was flushed and samples rewetted after seven days to prevent CO₂ from accumulating over 1%. Cumulative CO₂ was calculated by summing the changes in CO₂ concentration between sampling points over the 14-day incubation.

Initial and incubated soil subsamples were extracted with 2M KCl at a 5:1 ratio (extract:sample), shaken for one hour, filtered, and analyzed colorimetrically for ammonium and nitrate (Alpkem Flow Solution IV Automated wet chemistry system, O.I. Analytical, College Station, TX). Potential N transformations were calculated as follows:

$$\text{Potential N Mineralization} = (\text{NH}_4^+\text{-N} + \text{NO}_3^-\text{-N})_{\text{Final}} - (\text{NH}_4^+\text{-N} + \text{NO}_3^-\text{-N})_{\text{Initial}} / \text{Days} \quad (1)$$

$$\text{Potential Nitrification} = (\text{NO}_3^-\text{-N})_{\text{Final}} - (\text{NO}_3^-\text{-N})_{\text{Initial}} / \text{Days} \quad (2)$$

Soil pH was determined on a 1:1 (deionized water:sample) solution shaken for one hour and analyzed using a pH electrode and stirrer bar (Orion EA940 Expandable ionAnalyzer; Orion Research, Jacksonville, FL).

4.2.7. Soil Total Carbon and Nitrogen and Bulk Density

To assess treatment impacts on C and N stocks and bulk density immediately after application and over time, soils were sampled two weeks after incorporating the treatments in October 2014, after the first winter in June 2015 and two years later in August 2017. Soil samples were excavated from a 20 x 20 cm soil pit at designated soil sampling locations to a 0-15 and 15-30 cm depth and stored in a cooler during transport to the lab. To estimate bulk density, pit volume was estimated using the method of Boot *et al.* (2015), filling the excavated soil pit with sterilized millet seeds and measuring the millet volume. Field moist soils were weighed upon arrival to the lab and GWC determined by oven drying a 15-20 g soil subsample at 110 °C overnight. After air-drying, samples were sieved to the coarse (>2 mm) and soil (<2 mm) size fractions. Coarse fragments, including rocks, litter, roots, mulch and biochar particles, were physically separated to derive the proportional mass of the coarse fraction. Dry weights for coarse mulch and biochar particles were determined after oven drying at 110 °C overnight. The C and N content of coarse biochar and mulch particles was determined from their C and N concentrations (Table 8) and dry weight. For bulk soil total C and N measurements, oven-dried 2 mm sieved soils were pulverized and analyzed on a LECO True-Spec CN analyzer (Leco Corp., St. Joseph, MI, USA). Total mineral soil C stock was calculated using the hybrid bulk density approach of Throop *et al.* (2012), based on the mass of the fine earth fraction (<2 mm) and volume of the entire core.

4.2.8. Statistical Analyses

Treatment effects were analyzed on the following response variables: plant canopy cover, aboveground biomass, belowground biomass, soil bulk density, soil total C and N content, GWC, mineral N from IER and soil extracts, soil respiration, potential N mineralization and nitrification, and soil pH. All response variables were modeled using a mixed effect model (lme4 R package) with treatment and year as fixed effects and road segment blocks (and date for GWC or season for IER mineral N analysis) as a random effect. To account for repeated measures in the plant cover measurements, within plot variability was

treated as a random effect. Where model residuals were non-parametric, exponential or logarithmic transformations were applied to the response variables to achieve a normal distribution. Models were evaluated using Dunnett's test (multcomp R package) to determine significant treatment effects relative to the control. We examined overall fertilizer, mulch and biochar effects using one-way analysis of variance (stats R package) of the three treatments containing the relevant amendment relative to the comparable set of three treatments that did not receive the relevant amendment. To evaluate which soil factors had the greatest controls on revegetation, we used additive multiple linear regression models to evaluate the relationship between the measured soil properties, treatments and year to total plant cover, total plant aboveground biomass and belowground biomass. The best fit model was selected based on the Akaike information criterion (AIC) corrected for small sample sizes (MuMin R package) to determine the best soil predictors of plant response. All statistics were performed in R version 3.3.2 (R Core Team, 2016) with significance accepted at $p=0.10$.

4.3. Results

4.3.1. Cover and Biomass

Total plant canopy cover varied by year ($p<0.01$), where, across treatments, 2015 experienced the greatest total canopy cover averaging 43%, while the drier 2016 experienced much less cover at 24%, then cover rebounded to 37% in 2017. Fertilizer amended plots increased total plant cover by 21% ($p=0.08$) relative to unamended treatments, but mulch ($p=0.12$) and biochar amended plots did not significantly affect cover (Fig. 16a). However, considering the individual treatments relative to the control, the fertilized mulch (43%, $p=0.02$), fertilized (41%, $p=0.04$) and mulch (44%, $p=0.06$) treatments all significantly increased plant cover with no effect in any of the biochar treatments (Fig. 16d). Graminoids averaged 27% cover (77% of total plant cover), followed by forbs at 7% cover (20% of total plant cover) and shrubs with 1% cover (3% of total plant cover), across years and treatments. Average graminoid cover across treatments varied between years ($p<0.01$), while forb canopy cover steadily

increased from 6% to 8%, and shrub cover did not change over time (Fig. A7). Most of the response to treatments and annual changes were explained by changes in graminoid cover, with increased graminoid cover relative to the control in the mulch (81%, $p < 0.01$), fertilized (73%, $p < 0.01$), fertilized mulch (58%, $p = 0.02$), and mulched biochar (57%, $p = 0.06$) treatments, and no significant treatment response in forb or shrub canopy cover (Fig. A7).

Across treatments, average aboveground plant biomass increased from 2016 (9.2 g m^{-2}) to 2017 (12.9 g m^{-2} ; $p < 0.01$). While none of the effects were significant due to the high between site variability, aboveground biomass responded similarly to plant cover, where treatments receiving organic fertilizer and mulch tended to increase aboveground biomass relative to the unamended treatments, while biochar tended to slightly reduce plant biomass (Fig. 16b). Relative to the unamended plots, mulch (78%, $p = 0.02$) and fertilizer (67%, $p = 0.09$) amendments significantly increased root biomass, while biochar amendments had no significant effect (Fig. 16c).

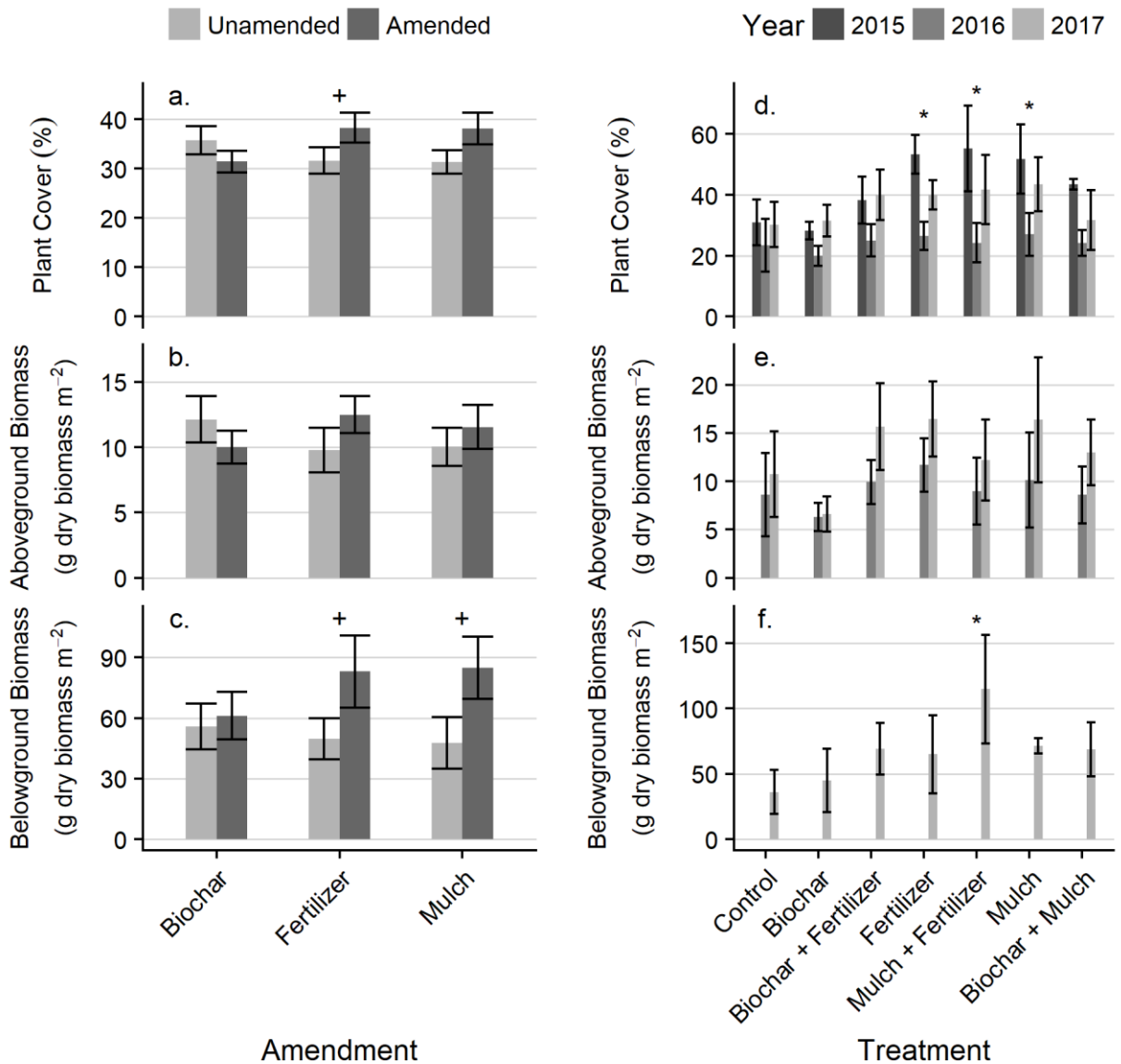


Fig. 16: Mean plant cover, aboveground biomass and belowground biomass for the amendments across years (Fig. 16a, 16b, 16c) and for each of the individual treatments by year (Fig. 16d, 16e, 16f). Amendments represent the three-year mean value of the 3 treatments containing the amendment vs the respective 3 unamended treatments. Error bars display one standard error, with significance effects across the three years denoted by + relative to the unamended plots and * relative to the control treatment.

4.3.2. Soil Moisture

Across treatments, 2015 experienced higher average annual soil moisture (7.3% GWC, $p < 0.01$) than 2016 (5.5% GWC) and 2017 (5.7% GWC). Annual soil moisture patterns reflected precipitation inputs, where 2015 received 567 mm, 24% greater than the 30-year normal (456 mm), whereas 2016 received

less at 426 mm and 2017 received 535 mm (PRISM Climate Group, 2017). Over the growing season, soil moisture content tended to decrease, reaching relatively dry values <5% GWC by July except after rain events (data not shown). Relative to the unamended plots, biochar (26%, $p<0.01$) and fertilizer amendments (10%, $p<0.01$) increased average GWC, while mulch had no significant effect (Fig 17a). Over the three growing seasons among the individual treatments relative to the control, the mulched biochar treatment had the greatest increase in GWC (44%, $p<0.01$) followed by the fertilized biochar treatment (27%, $p<0.01$; Fig. 17b). The mulch only (-17%, $p<0.01$), fertilized mulch (-26%, $p<0.01$) and biochar only (-14%, $p=0.09$) treatments all decreased average GWC relative to the control (Fig. 17b). Such treatment effects remained consistent across soil water contents (Fig. 18).

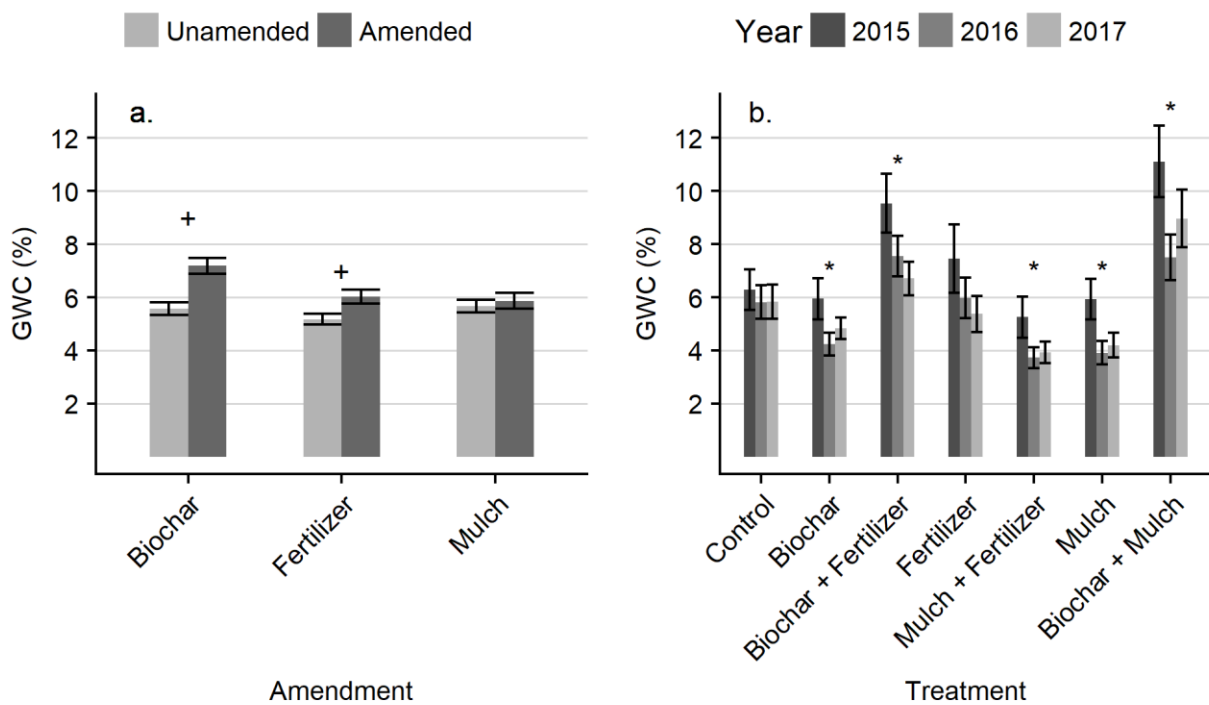


Fig. 17: Gravimetric water content (GWC) averaged over the growing season for the amendments across years (Fig. 17a) and for each of the individual treatments by year (Fig. 17b). Amendments represent the mean value of the 3 treatments containing the amendment vs the respective 3 unamended treatments. Error bars display one standard error, with significance effects across the three years denoted by + relative to the unamended plots and * relative to the control treatment.

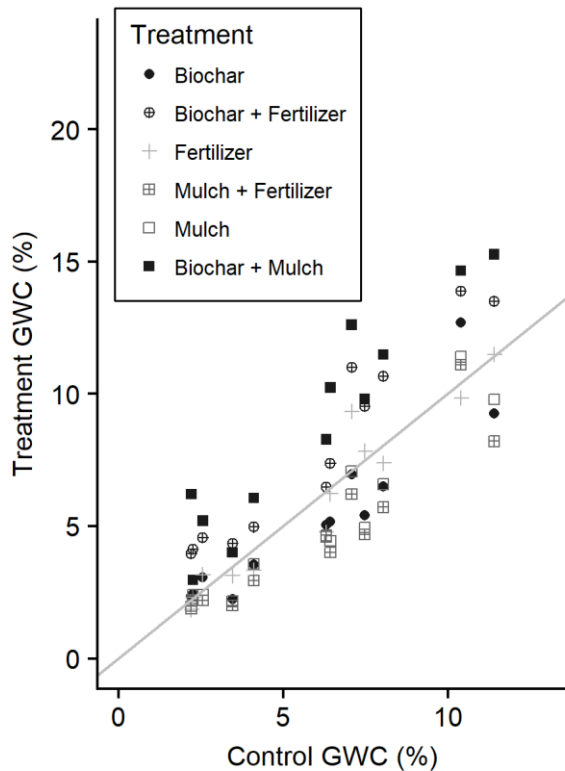


Fig. 18: Gravimetric water content (GWC) of the treatments relative to the GWC of the control plots sampled on the same date. The light gray line displays the 1:1 line.

4.3.3. Mineral Nitrogen Availability

After organic fertilizer application, the fall 2014 soil extracts in the fertilized treatments contained twelve times the mineral N than the unfertilized treatments (Fig. 19b), equivalent to 22.8% of the N added as organic fertilizer. Mineral N availability remained elevated in the fertilized treatments with a 425% increase ($p < 0.01$) relative to the unfertilized treatments in the first winter IERs (Fig. 19c) and an 81% increase ($p = 0.07$) in the 2015 summer IER (Fig. 19a). After the first year, mineral N measurements showed no fertilization effect, whether measured by IER or soil extracts.

IER tended to recover more mineral N as nitrate (NO_3^- -N) than ammonium (NH_4^+ -N) with a greater NO_3^- -N proportion in the winter months (70% NO_3^- -N) than the summer months (50% NO_3^- -N, $p < 0.01$) and an increasing NO_3^- -N proportion over time ($p < 0.01$) from 49% NO_3^- -N in 2015 to 72% NO_3^- -N in 2015 (data not shown). Soil extracts contained much greater total mineral N than IER extracts (Fig. 19) and revealed

a greater contribution from NH_4^+ -N at an average 32% NO_3^- -N. Similar to IER, soil extracts also showed an increasing proportion of NO_3^- -N over time ($p < 0.01$) increasing from 16% NO_3^- -N in 2014 to 44% NO_3^- -N in 2017 (data not shown).

Among the fertilized treatments, the fertilized biochar treatment contained the highest mineral N content relative to the fertilizer only treatments in fall 2014 soil extracts (229%, $p = 0.03$; Fig. 19e). Even after the initial mineral N pulse in year one, the fertilized biochar treatment continued to contain 30% more mineral N in soil extracts than the fertilizer only treatments ($p = 0.09$, Fig. 19e). The fertilized mulch treatments had no effect on mineral N from soil extracts or IER relative to the fertilizer only treatments (Fig. 19). There was no impact of biochar, mulch or their combination on mineral N from IER or soil extracts in unfertilized treatments relative to the control.

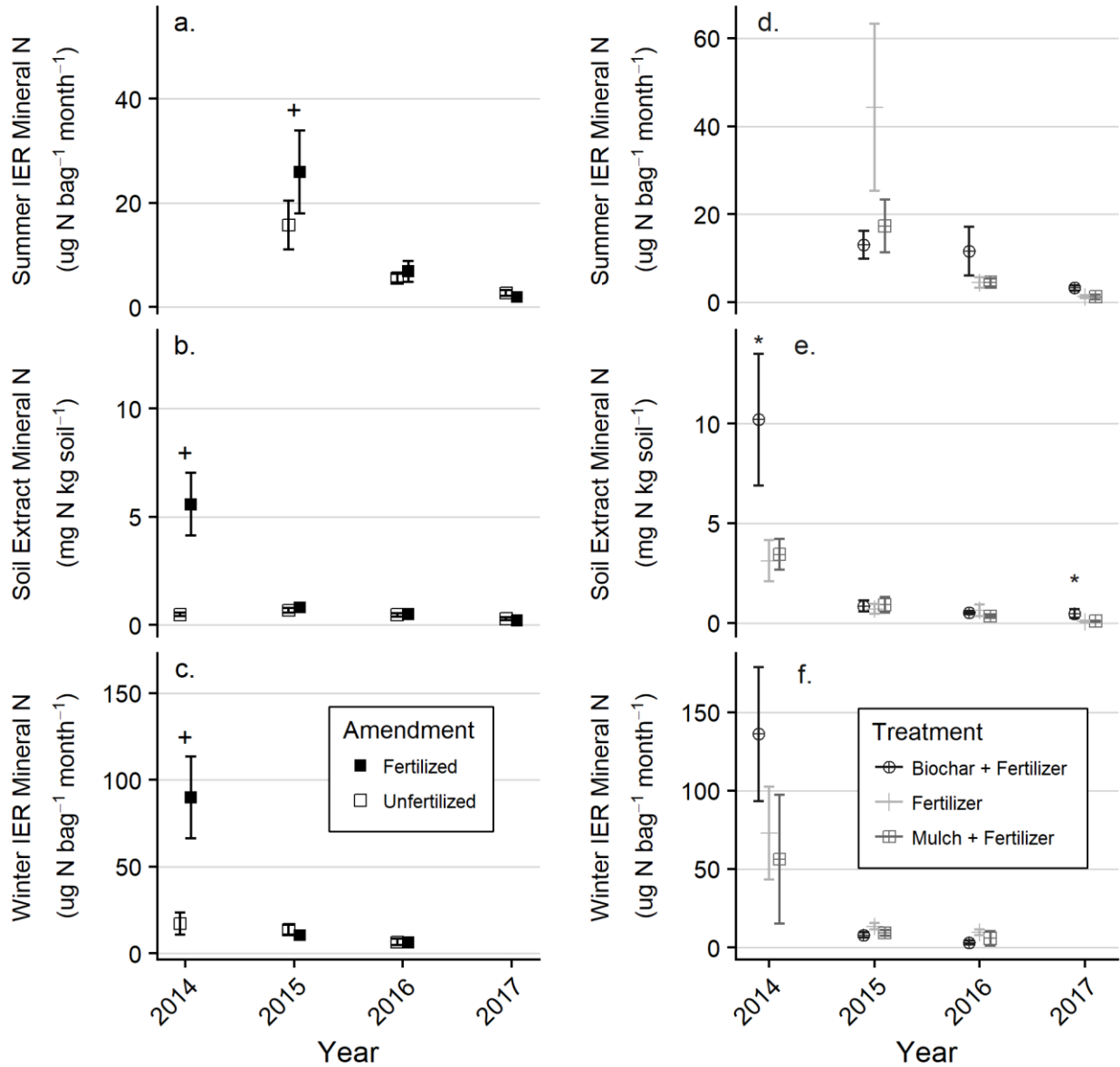


Fig. 19: Mean mineral N from soil extracts in the fall of each year (Fig. 19b, 19e) or ion exchange resin (IER) bags deployed in the winter (Fig. 19c, 19f) or summer (Fig. 19a, 19d) of each year for fertilized vs unfertilized amendments (Fig. 19a, 19b, 19c) or each of the fertilized treatments (Fig. 19d, 19e, 19f). Individual unfertilized treatments did not have a significant effect on mineral N availability relative to the unfertilized control. Error bars display one standard error, with significant effects denoted by + relative to the unamended plots and * relative to the fertilizer only treatment.

4.3.4. Carbon and Nitrogen Mineralization Assays and Soil pH

Several of the fertilized treatments in the fall of 2014 had negative potential N mineralization estimates due to the high initial mineral N content, which was likely lost over the 14-day aerobic incubation to

immobilization or N volatilization, yet soil respiration measurements indicated mineralization did occur. Removing these negative potential N mineralization estimates, the fertilizer amended plots showed increased potential N mineralization in 2014 (250%, $p < 0.01$) and 2016 (67%, $p = 0.02$), but did not significantly differ from the unamended plots in 2015 and 2017 (Fig. 20f). Similarly, fertilizer amended plots increased potential nitrification across years ($p = 0.06$) with interactions by year. In 2014 fertilizers increased nitrification by 241% ($p < 0.01$; Fig. 20g), but in later years shifted to having no effect to decreasing potential nitrification in 2017 (-57%, $p = 0.01$). Fertilization did not impact soil respiration (Fig. 6e) or pH (Fig. 20h).

Mulch amendments increased soil respiration relative to un-mulched plots across years to an increasing degree, from 14.2% in 2014 to 57.9% in 2017 ($p < 0.01$; Fig. 20i). While mulch tended to increase N cycling across years, such effect was not significant across years for potential N mineralization (Fig. 20j) or nitrification (Fig. 20k). Mulch decreased soil pH relative to un-mulched plots across years ($p = 0.01$) and by 0.3 in 2017 ($p = 0.03$; Fig. 20l).

Despite the large C additions, biochar amendments did not impact soil respiration or potential N mineralization relative to unamended plots, but decreased potential nitrification by 44% ($p = 0.01$; Fig. 20c) and increased soil pH across years ($p = 0.01$), with a 0.2 pH increase in 2014 ($p = 0.08$; Fig. 20d).

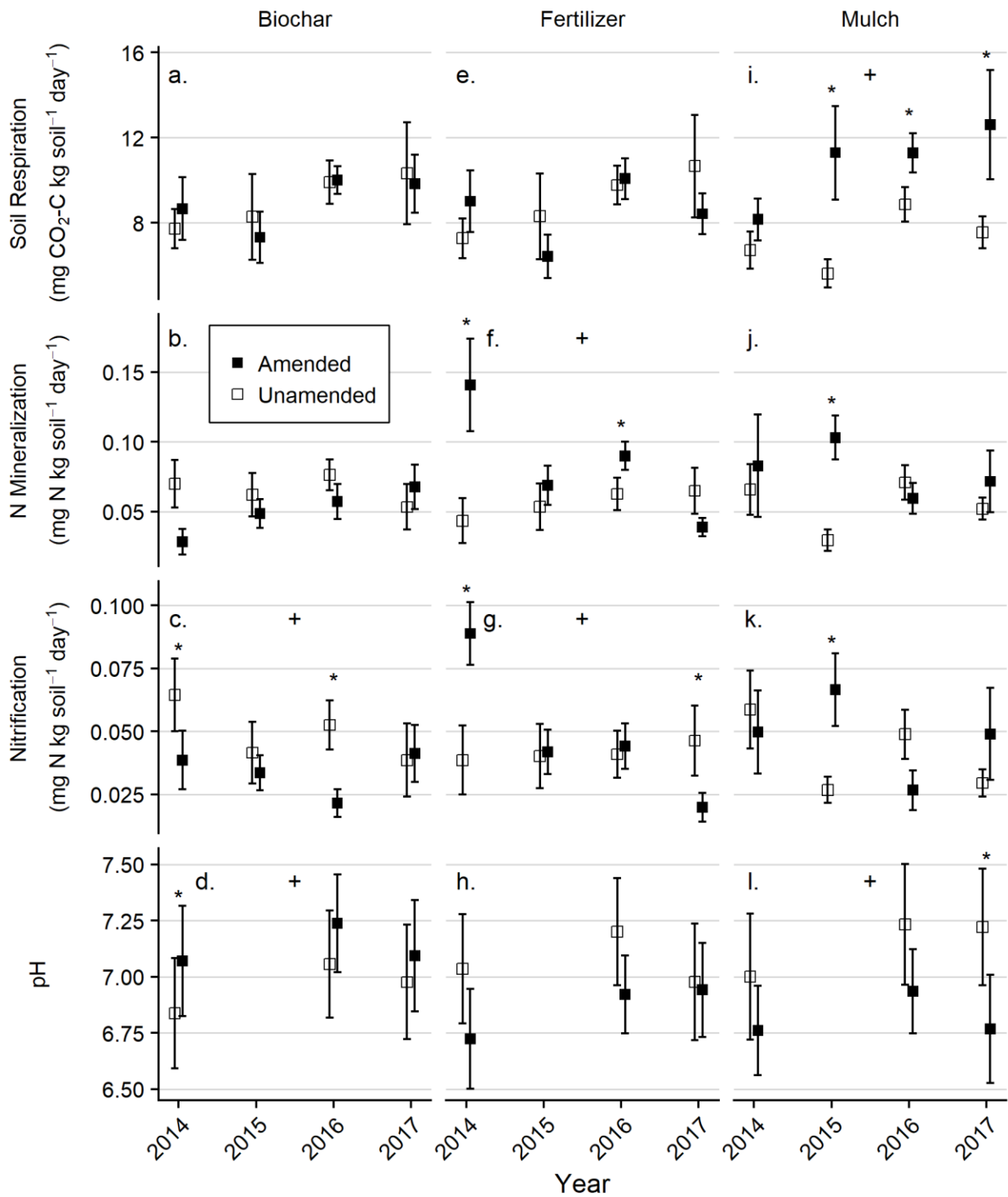


Fig. 20: Result of annual 14-day aerobic mineralization assays including cumulative soil respiration (Fig. 20a, 20e, 20i) potential N mineralization (Fig. 20b, 20f, 20j), potential nitrification (Fig. 20c, 20g, 20k) and pH (Fig. 20d, 20h, 20l) for the three amendments across all years sampled. Amendments represent the mean value of the 3

treatments containing the amendment vs the respective 3 unamended treatments. Error bars display one standard error, with significant effects by + across all years and * for individual years.

4.3.5. Soil Total Carbon and Nitrogen and Bulk Density

Total C, including the mineral soil C, mulch C and biochar C, showed high variance due to site differences in coarse fragments and mineral soil C content. Recovery of coarse biochar and mulch particles was variable and comprised the majority of the total C within treatments. After three field seasons, 23.1 ± 7.1 Mg C ha⁻¹ was recovered in coarse biochar particles, which was within the variability of the initial application rates. In mulched treatments, 5.6 ± 1.1 Mg C ha⁻¹ was recovered in coarse mulch particles indicating a loss of residual mulch C.

Mineral soil C averaged 7.5 ± 1.0 kg C ha⁻¹ and 9.7 ± 2.4 kg C ha⁻¹ in the 0-15 cm and 15-30 cm control treatments, with low soil C concentration ranging from 0.24% to 0.93% C. Mineral soil C did not change over the three-year study. Relative to unamended treatments, mulch amendments increased soil C by 3.6 kg C ha⁻¹ ($p=0.05$; Fig. 21a) and 5.2 kg C ha⁻¹ ($p=0.02$) for the 0-15 cm and 15-30 cm depths. In total this comprised 1% of the apparent loss in residual mulch C. Organic fertilizers and biochar amendments did not affect mineral soil C stocks at either depth. Total soil N did not change by depth, over time or by any of the amendments (Fig. 21b) or treatments (Fig. 21e). Over the three-year study, pit bulk density decreased from 1.61 to 1.14 g cm⁻³ in the 0-15 cm depth ($p<0.01$) but remained at 1.77 g cm⁻³ at the 15-30 cm depth. At the 0-15 cm depth, pit bulk density decreased due to biochar (14%, $p=0.05$) and mulch (17%, $p=0.01$) amendments (Fig. 21c). Among the individual treatment relative to the control, the fertilized biochar treatment experienced an 18% decrease in pit bulk density ($p=0.04$, Fig. 21f).

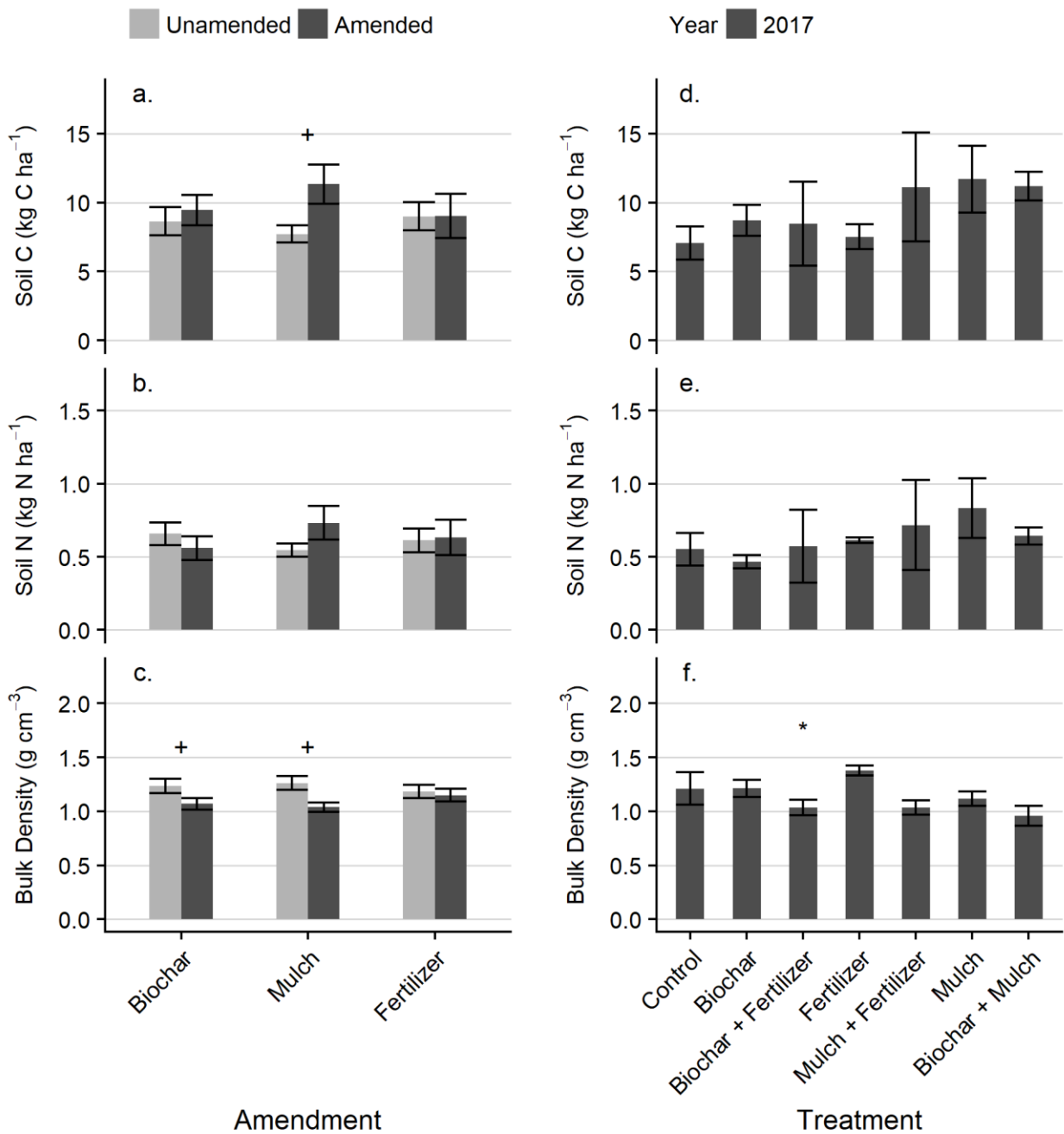


Fig. 21: Mineral soil C and N and bulk density measured at the 0-15 cm depth in the fall of 2017 for the amendments (Fig. 21a, 21b, 21c) and each of the individual treatments (Fig. 21d, 21e, 21f). Amendments represent the mean value of the 3 treatments containing the amendment vs the respective 3 unamended treatments. Error bars display one standard error, with significance effects denoted by + relative to the unamended plots and * relative to the control treatment.

4.3.6. Soil Factors and Processes Influencing Revegetation

Indicators of soil microbial activity (soil respiration, potential N mineralization and potential nitrification), soil C and N content and soil mineral N availability emerged as the best predictors of revegetation. Using all data available, total plant cover was best explained by a linear model containing year ($p < 0.01$), potential nitrification ($p < 0.01$), treatment ($p = 0.01$), and soil respiration ($p = 0.10$; $R^2 = 0.51$; Table 9). Summer IER mineral N was another important factor included in related models. In 2015 and 2017 where soil C and N content measurements were available, these properties emerged as the best predictors of plant cover ($R^2 = 0.62$, both $p < 0.01$) along with treatment, IER mineral N sampled during the summer months and potential nitrification (all $p < 0.01$).

Table 9: Statistical table of revegetation model selection using additive multiple linear regression models of soil variables to predict the given revegetation metric. Soil carbon (C) and nitrogen (N) emerged as a strong predictor but data was only available for 2015 and 2017. Thus, sample size (n) of the data modeled is provided. Model degrees of freedom (df), coefficient of determination (R^2), and Akaike information criterion (AIC) were used to assess model fit, where the best fit model (bold text) is represented by a Δ AIC score of zero. Predictor variables include year (Yr), treatment (Trt); soil respiration (CO_2), potential nitrification (Nit), potential N mineralization (NMin), pH (pH) and soil mineral N extracted from soil (NEx) from aerobic mineralization assay conducted in the fall of each year; summer ion exchange resin mineral N extracts (S.IER); mean gravimetric water content (GWC) for each year; and soil carbon C and N content from the 0-15 cm mineral soil depth.

Revegetation Metric	Soil C & N	n	Model	df	R^2	AIC	Δ AIC
Total Plant Cover	Yes	52	S.IER + N + Nit + C + Trt	12	0.62	160.0	0
			Nit + N + C + Trt	11	0.60	160.3	0.36
			C + Nit + N + S.IER	6	0.51	161.0	0.99
	No	79	Yr + Nit + Trt + CO_2	12	0.51	258.8	0
			Yr + Nit + Trt + S.IER + CO_2	13	0.52	259.1	0.32
			Yr + Nit + Trt + S.IER	12	0.50	259.5	0.68
Total Aboveground Biomass	Yes	28	N + NEx + NMin + Trt	11	0.65	82.3	0
			N + NEx + Nit + Trt	11	0.65	82.4	0.12
			N + Nit + Trt + BD	11	0.65	82.6	0.34
	No	55	Nit + CO_2 + Yr + Trt	11	0.58	147.8	0
			Nit + CO_2 + Yr + Trt + GWC	12	0.59	148.0	0.18
			Nit + CO_2 + Yr + Trt + S.IER	12	0.58	148.9	1.13
Total Belowground Biomass	Yes	27	pH	3	0.35	134.6	0
			pH + S.IER	4	0.38	135.5	0.85
			pH + GWC	4	0.38	135.5	0.93

Total aboveground biomass was best predicted by potential nitrification ($p < 0.01$), soil respiration ($p < 0.01$), year ($p = 0.02$) and treatment ($p = 0.06$; $R^2 = 0.58$; Table 9). When only looking at 2017 data where soil C and N content were available, N availability parameters including soil N content ($p < 0.01$), mineral N extracted from soil ($p = 0.02$), potential N mineralization ($p = 0.04$) and treatment ($p = 0.12$) best predicted aboveground biomass ($R^2 = 0.65$; Table 9). Root biomass was best explained by soil pH ($p < 0.01$, $R^2 = 0.35$; Table 9), with IER mineral N sampled during the summer months and GWC also contributing in related models. Single factor regressions between the best soil predictors of total plant cover (Fig. A8) and total aboveground biomass (Fig. A9) are provided for reference.

4.4. Discussion

4.4.1. *Soil Amendments' Impact on Revegetation*

4.4.1.1. *Organic Fertilizer*

The organic fertilizer used in this study increased total plant cover, comprised primarily of graminoids, the first year of the study. The same organic fertilizer, applied at a higher rate, increased total plant cover along roadways in Mesa Verde National Park, in southwestern Colorado throughout a four year study (Paschke *et al.*, 2000). The predominant effect of the fertilization we measured on graminoids agreed with a recent meta-analysis showing N additions are positively correlated to grass biomass in grassland ecosystems with neutral or negative effects on forb biomass (You *et al.*, 2017). This may be due to grasses' increased height and cover outcompeting forbs for light, or branched root architecture that can better access soil mineral N (You *et al.*, 2017). In our study, increased graminoid cover in fertilized plots resulted in greater root biomass three years after treatment, a factor critical for reducing sediment movement from road surfaces (Brooks *et al.*, 2011). Organic fertilizers can also improve soil nutrient cycling by increasing N mineralization over time, with different amendments ranging from rapid N mineralization (fertilizers) to induced N immobilization (mulches) (Lashermes *et al.*, 2010). The organic fertilizer applied in our study mineralized rapidly as evidenced by a 250% increase in potential N

mineralization during laboratory mineralization assays from soils treated with organic fertilizers. Nearly a quarter of the N applied in the organic fertilizer was recovered within soil mineral N extracts within one month of application. Incubations of other commercial organic fertilizers reveal similar results with the majority of N mineralization occurring within the first month of application (Baldi & Toselli, 2014). Such improvements in potential N mineralization and nitrification and the resulting impacts on soil mineral N availability were no longer evident in later years of this study, indicating that a one-time fertilization did not sustain microbially-mediated nutrient cycling within these treatments. While the organic fertilizer used in this study did not support sustained mineral N provisioning in soils through gradual N mineralization, it may allow for direct mobilization of the initial mineral N pulse into root biomass.

4.4.1.2. *Wood Strand Mulch*

Wood strand mulch increased graminoid cover the first year after application, but our results are not explained by mulch effects on soil moisture or mineral N availability. The effect of mulch application on plant recovery varies among studies based on mulch type, application rate and site conditions. For example, neither wood shred nor wood strand mulches (applied at ~50% cover) increased plant cover compared to untreated roads in the Northern Rockies (Foltz, 2012). On decommissioned roads near our study sites, the same wood strand mulch type (applied at a lower 6.2 Mg ha^{-1}) and organic N fertilizer treatment (21 kg N ha^{-1}) combination used in this study also increased basal plant cover (Sosa Pérez & MacDonald, 2017). In contrast to most studies of organic mulches (Benigno *et al.*, 2013; Goldin & Hutchinson, 2014; Rhoades *et al.*, 2012 & 2015; Roberts, *et al.*, 2005), we found no effect on soil moisture content beneath wood strand mulch, with some individual treatments showing a decrease in GWC relative to the control (Fig. 17). The effects of wood mulch on soil moisture increases with application rate and depth (Rhoades *et al.* 2012) and the 12.5 Mg ha^{-1} rate of this study is lower than most wood mulch studies. Mulch effects on soil moisture have also been shown to vary with seasonal

soil moisture, with the greatest mulch effect under moderately moist conditions (Rhoades *et al.* 2012 & 2017). In this study, we found no evidence of increased soil moisture beneath mulch, even during relatively moist early-season conditions (Fig. 18). However, wood strand mulch increased total plant cover and thus soil water demand relative to the unamended control. Overall, the low wood strand mulch application rate would limit the potential effects of mulch on evaporative losses while the increased density and plant water use would have depleted soil moisture, especially during the drier years of this study. These possible plant feedbacks impacting mulch's ability to increase soil moisture contents, highlights the importance of considering aboveground-belowground linkages in restoration treatments (Kardol & Wardle, 2010).

The low wood strand mulch application rate did not increase soil moisture when applied alone, but when combined with biochar's capacity to retain soil moisture a synergistic effect led to the highest soil moisture contents (Fig. 17). Similar to the current study, application of mulch in combination with biochar is known to increase soil moisture content in degraded forest soils (Rhoades *et al.*, 2017). However, on the severely-burned hillslopes of that study, both mulch added alone at 3-times the rate of the current study and biochar added at a comparable rate to this study increased soil moisture compared to untreated soils. Such differences in mulch treatment effects may relate to low water holding capacity of these coarse-textured soil and the extremely low soil organic matter of our decommissioned roads (0.6% C) compared to the burned forest soils (1.7% C) (Saxton & Rawls, 2006). With the addition of biochar, the poor water retention of the road soil improved allowing for a synergistic effect with mulch's ability to decrease evaporative losses leading to improved soil moisture. Mulches can also regulate soil N availability in restoration treatments, providing long-term N supply through gradual N mineralization but also short-term immobilization of excess soil mineral N to discourage competition from invasive plants (Perry *et al.*, 2010; Vasquez *et al.*, 2008). In this short-term

study mulch had no significant impact on soil mineral N availability. Other studies have reported wood mulch increasing soil mineral N where it is used for erosion control on semi-arid lands (Bai *et al.*, 2014), in poplar plantations (Fang *et al.*, 2011) and in coniferous forest fuel reduction treatments (Rhoades *et al.*, 2012). Changes in mulching effects on mineral N over time were observed in forest fuels reduction treatments where soil mineral N availability was not impacted initially, but increased after three years (Miller & Seastedt, 2009). In this study, the mineralization assays provided no clear trends of mulch immobilizing or supplying mineral N with variable potential N mineralization and nitrification results across years (Fig. 20). Over time, N mineralization of the mulch may supply some N to decommissioned road soils (Rhoades *et al.*, 2012) but the limited amount of N supplied from mulch over time is not likely to provide a significant source of N to support early revegetation efforts (Laiho & Prescott, 2004).

4.4.1.3. Biochar

Despite indications of improved mineral N and water availability in biochar treatments, biochar did not improve revegetation efforts and in some years performed worse than the control (Fig. 16). This may indicate that mineral N retained on biochar particles was not readily accessible to plants and the increased water retention failed to alleviate plant water stress. Biochar's porous structure with high surface area allows for increased water retention through both its internal macroporosity and alteration of pore structure between soil particles (Liu *et al.*, 2017). This increased porosity not only resulted in biochar increasing GWC but was also apparent through the decrease in bulk density in the fertilized biochar treatments. However, there was evidence that N limitation had a stronger control on plant establishment than water limitation, as the mulched biochar treatment, which had the greatest improvements in water retention, experienced less revegetation than the fertilized treatment. The fertilized biochar treatment contained some of the highest mineral N availability as measured by both IER and soil extracts in the first year (Fig. 19), with this increased N availability sustained throughout the study for the soil extracts, although the magnitude of this effect was much smaller in

later years. Woody biochar's high surface area with diverse functional groups increases the ion-exchange capacity of soils allowing for improved N retention (Gai *et al.*, 2014). Woody biochar amendments to boreal forest soils showed a similar effect increasing NH_4^+ availability in soil but with no significant impact on vegetation (Gundale *et al.*, 2016). Despite indications of improved N availability, neither plant cover nor biomass was enhanced by biochar suggesting that either this mineral N is not readily available to plants or not sufficient to overcome N limitation and significantly improve revegetation efforts.

4.4.2. Importance of Biological Soil Processes for Revegetation

While the fertilized treatments only provided a short-lived provisioning of N to soils, biochar, mulch and the combination treatments showed potential to restore soil physical, chemical and biological processes to improve revegetation. Restoration treatments that integrate improvements in soil physical, chemical and biological properties provide the best opportunities to achieve sustained restoration of critical soil processes like nutrient cycling and C regulation (Heneghan *et al.*, 2008). Such benefits were evident when considering mulch's ability to enhance plant cover and biomass. In these low SOM soils, mulch provided a sustained source of labile C to support microbial community structure and function resulting in improved plant nutrient uptake (Bai *et al.*, 2014; Huang *et al.*, 2008). This was evident in the mulch treatments which significantly increased soil respiration relative to unmulched treatments each year (Fig. 20). Indicators of improved microbial activity, such as soil respiration, potential N mineralization and potential nitrification, were also consistently the best predictors of both plant cover and biomass (Table 9). When soil C and N content data were available, these factors also emerged as the best predictors of plant cover and biomass (Table 9), highlighting the importance of improving SOM content to continually supply nutrients to meet plant demand. In the restoration of semi-arid shrublands, improved SOM content was correlated with improved microbial activity and nutrient cycling, with different organic amendments influencing the microbial community composition (Bastida *et al.*, 2015).

Biochar also improved soil mineral N availability over the study, but likely by retaining mineral N on biochar surfaces via physical entrapment or ion exchange processes as opposed to increasing microbial N cycling. Similarly, improving physical properties to increase soil water content only emerged as an important predictor of revegetation in some models (Table 9). The greater revegetation response in the mulch treatments which supported microbial activity compared to no revegetation effect in the biochar treatments which improved soil chemical and physical properties, highlights the importance of promoting soil microbial communities in the restoration of decommissioned forest roads.

4.4.3. Soil Amendments' Impact on Carbon Sequestration

4.4.3.1. Wood Strand Mulch

Wood strand mulch's ability to promote microbial activity not only supported revegetation efforts, but also provided broader environmental benefits through soil C sequestration. Mulch increased both soil C content and soil respiration, and recovery of mulch particles was decreased relative to initial application rates, indicating decomposition of residual mulch particles. In these soils with low C content, microbial processing of mulch C not only stimulated microbial activity and N mineralization, but the microbial byproducts may also contribute to SOM formation. Such microbially-processed C can become adsorbed to the silt and clay particles to help alleviate the C saturation deficit, the proportion of soil C relative to the maximum absorption on silt and clay particles (Grandy & Neff, 2008; Hassink, 1997). However, these rocky, loam soils with 4-12% clay content would have limited capacity for such matrix stabilization and eventually would reach C saturation (Stewart *et al.*, 2007). In this study the increased soil C was roughly 1% of the apparent loss of residual mulch C. Therefore results indicate that mulch can stimulate microbial activity in these SOM depleted soils, but the total C sequestration potential will likely be limited by the capacity of the silt and clay fraction to retain such microbially-processed C (Six *et al.*, 2002). The remaining mulch C will likely be respired as CO₂ within a decadal timescale (Laiho & Prescott, 2004).

4.4.3.2. Biochar

Recovery of biochar particles was within the variation of the initial application rates and primarily consisted of the original coarse particle size fraction. Physical fragmentation of biochar can also be an important process that determines the longevity and effectiveness of biochar as a soil amendment (Spokas *et al.*, 2014), but did not appear to be a significant factor in this system. The lack of a significant increase in the mineral soil C content and no effect on soil respiration indicates that in these forest soils biochar was neither highly fragmented nor contributed labile C to soils to prime C mineralization. This confirms biochar's ability to contribute to long term soil C sequestration primarily through its inherent recalcitrance (Spokas, 2010; Wang *et al.*, 2016), rather than actively contributing to SOM formation through the progressive decomposition of the organic matter and stabilization of the smaller biopolymers within aggregates or on mineral surfaces (Lehmann & Kleber, 2015). However, over time mineral stabilization of biochar C may play an important role, as pyrogenic C has been found to be mineral associated in soil historically amended with charcoal (Glaser *et al.*, 2000) or in native grassland soil (Brodowski *et al.*, 2006). In contrast to the mechanisms for soil C sequestration in the mulch treatments, biochar particles show evidence of biochemical protection allowing for long-term C accumulation above C saturation controlled by matrix stabilization (Lehmann *et al.*, 2006; Lorenz & Lal, 2014).

4.4.4. Management Implications

This short-term field study provides insights into the soil processes and properties affected by organic amendments that influence initial revegetation and C sequestration on decommissioned forest roads. Both organic fertilizer and wood strand mulch increased plant cover and root biomass, where the organic fertilizer increased soil N availability, and mulch increased soil C and microbial activity. Conversely, biochar had no effect on revegetation though it increased mineral N and soil moisture. When combined with organic fertilizer, the biochar treatment sustained higher mineral N availability

throughout the three-year study, though surprisingly it had no effect on plant cover. Both the wood strand mulch and biochar applications increased C, though biochar alone and in combinations showed the greatest potential for C sequestration. The wood strand mulch application was the only treatment that enhanced both revegetation and C sequestration objectives on these decommissioned roads. Across all amendments, we found that microbially-mediated soil processes (i.e., C and N mineralization) were good general predictors of road revegetation; this highlights the importance of soil ecological knowledge to optimize restoration activities (Heneghan *et al.* 2008). Longer-term monitoring of these treatments and well-replicated evaluation of different application rates and combinations are needed to better understand the soil processes that regulate soil recovery and to optimize treatment design for revegetation and C sequestration on gravelly, coarse-texture, low SOM forest roads.

5. ESTIMATING BIOCHAR'S CARBON SEQUESTRATION POTENTIAL AND ITS MAJOR CONTROLS

5.1. Introduction

With international commitments to climate change mitigation falling short of the targets necessary to stabilize our climate system (Rogelj *et al.*, 2015), there is a clear need for the adoption of negative emission strategies (Fuss *et al.*, 2014). The land use sector provides ample opportunities to sequester C while achieving other co-benefits, with international policies underway to implement practices for reforestation, avoided forest conversion and natural forest management (Griscom *et al.*, 2017). While policies have advanced within the forestry sector, opportunities for soil C sequestration have faced greater barriers to implementation. The use of biochar soil amendment has great potential for soil C sequestration with conservative global estimates predicting biochar could deliver 1.0 to 1.8 Pg CO₂-eq year⁻¹ of GHG emission reductions (Paustian *et al.*, 2016; Woolf *et al.*, 2010). However, uncertainties around biochar's long-term stability and effects on crops yield have prevented economic or policy incentives from supporting widespread adoption of such practices (Bach *et al.*, 2016). Quantifying the uncertainties in biochar's C sequestration potential over time can help build confidence for policymakers in advancing biochar as a strategy for climate change mitigation.

Due to biochar's unique C sequestration potential, with an initial C debit from pyrolysis, it is important to understand the full C sequestration profile over the lifetime of a biochar project. GHG emission reductions are typically evaluated based on 100-year time horizons, however some are calling for policymakers to evaluate both the short-term and long-term accounting of GHG emission reductions (Ocko *et al.*, 2017). Standard C accounting practices assess the GHG mitigation potential of an intervention by comparing the predicted emissions or removals of applying that practice to those of a standard or theoretical baseline scenario (Whitman *et al.*, 2014). Such emission reductions are typically converted to CO₂ equivalent using 100-year global warming potentials for comparability. Ex-ante

predictions of biochar's C sequestration potential thus require estimates for both the stability of pyrolyzed feedstocks over time under a biochar scenario and the decay profile for the same feedstocks if left to naturally decompose under a baseline scenario (Lehmann *et al.*, 2006). Over time, biochar's C sequestration potential can be estimated by considering the difference between this baseline scenario and the biochar scenario. With biomass losses from pyrolysis to the gaseous and liquid fraction on the order of 60 to 90% of the feedstock (Neves *et al.*, 2011), the solid biochar remaining results in an initial C debit relative to the baseline. As the feedstocks in the baseline scenario decompose, biochar's C sequestration potential will increase rapidly in the short term as the biochar C remains stable while the feedstock C mineralizes. In the medium- to long-term we expect biochar's C sequestration profile to slowly decrease as the biochar is decomposed. In general, we expect that in the short- to medium-term biochar's C sequestration profile is largely controlled by the feedstock decay rate and resulting soil organic matter stabilization in the baseline scenario, while the long-term dynamics are controlled by biochar stability in the biochar scenario.

In the absence of pyrolysis many sustainably sourced biochar feedstocks, including woody debris, agricultural residues, or manure would be left to naturally decompose as litter. Feedstock or litter decay in the baseline scenario can vary on the order of years to decades (Laiho & Prescott, 2004; Zhang *et al.*, 2018). The decomposition rates, k , will vary depending on the litter quality, environmental conditions and soils where litter is deposited (Smith *et al.* 1979). Litter quality, largely defined by the chemical composition of the litter, can have a large control on decomposition based on the energetic and nutrient requirements by the microbes decomposing various plant components. The lignocellulose index, a ratio of the lignin content to the lignin + holocellulose has emerged as a strong predictor due to the exoenzymes necessary to breakdown lignin (Moorhead *et al.*, 2013). Plant N content also plays a major role in litter decay, where with litter with low C:N are more readily consumed to meet microbial demands for N (Taylor *et al.*, 1989). As these compounds are broken down by microbial communities,

litter chemistry impacts the microbial substrate use efficiency (i.e., the proportion of compounds assimilated *versus* mineralized) exerting an important control on the carbon remaining in microbial products, while the soil mineral matrix will also influence the ability of such products to be stabilized and persist within soils (Cotrufo *et al.*, 2013). Emerging process-based models of litter decomposition dynamics can represent such mechanisms and improve predictions of the decay dynamics based on litter quality (Campbell *et al.*, 2016).

Only a small fraction of the original litter and its decomposition products will become stabilized in soil affecting the medium to long-term decomposition dynamics. Contemporary understanding of organic matter decomposition can be represented as a continuum of organic polymers progressively breaking down in smaller molecule weight structures to complete mineralization, with soil mineral surfaces and physical protection in aggregates offering protection from decomposition, thus decreasing turnover rates (Lehmann & Kleber, 2015). Much of the organic matter that persists in soils can be found in the fraction stabilized to mineral surfaces (Grandy & Neff, 2008). Over time soils reach an equilibrium level of soil organic C based on C inputs relative to C losses. Empirical models indicate that the equilibrium level of soil organic C becomes saturated with respect to C inputs (Stewart *et al.*, 2007). Soil texture exerts an important control on soil C saturation with soils eventually losing capacity to retain more C as the silt and clay fraction becomes saturated with soil organic matter (Mayes *et al.*, 2012; Six *et al.*, 2002). The C saturation deficit, or the current amount of C adhering to soil silt and clay fraction compared to the maximum capacity of that fraction, can serve as an important indicator of soil's additional C sequestration capacity (Barré *et al.*, 2017). Soil mineralogy can also control the ability to stabilize organic matter to mineral surfaces with increased retention of organic matter on 2:1 clays. The amphoteric nature of iron oxides can also lead to enhanced dissolved organic C retention based on soil pH (Jardine *et al.*, 1989). Such dynamics for the stabilization of decomposition product are beginning to

be explicitly represented in process-based soil organic matter models (Campbell & Paustian, 2015; see also Abramoff *et al.*, 2017; Ahrens *et al.*, 2015; Malamoud *et al.*, 2009; Robertson *et al.*, *in review*).

Under a biochar scenario, decomposition of biochar is much slower at the century timescales (Gurwick *et al.*, 2013; Singh *et al.*, 2012; Spokas, 2010; Wang *et al.*, 2016). The condensed aromatic C structure of biochar is far more resistant to microbial decomposition than the unpyrolyzed feedstock (Wiedemeier *et al.*, 2015). Biochar produced from biomass pyrolysis can generally be characterized by two pools; 1) a small labile component consisting of aliphatic structures that resisted transformation during pyrolysis and non-condensed aromatic compounds, and 2) a large recalcitrant component consisting of more highly condensed polycyclic aromatic C sheets (Bird *et al.*, 2015; Lian & Xing, 2017). The pyrolysis temperature, heating time and feedstock quality will impact both the fraction that can be classified within the labile vs recalcitrant component, and the decomposition rates of those pools (Fang *et al.*, 2015; Singh *et al.*, 2012; Spokas, 2010).

The capacity of the soil to retain biochar may also play an important role in biochar stabilization, particularly at the centuries to millennial timescale. Biochar can be viewed as an artificially produced model compound for naturally occurring pyrogenic organic matter (Py-OM). By considering Py-OM dynamics within soils we can better understand and model biochar stability in soils. Studies find that in the short-term the majority of the Py-OM remains in the particulate fraction as pyrogenic particulate organic matter (Py-POM) (Singh *et al.*, 2012; Soong & Cotrufo, 2015). However, in century-old wildfire soils and anthropogenic Terra Preta soils, much of the Py-OM is found within the mineral fraction as pyrogenic mineral-associated organic matter (Py-MAOM) (Brodowski *et al.*, 2006; Glaser *et al.*, 2001). Over time, as biochar fractionates and weathers in soils, its surfaces oxidize, increasing its polarity and thus solubility, allowing it to become incorporated into the pyrogenic dissolved organic matter (Py-DOM) fraction of soils (Bostick *et al.*, 2018; Mia *et al.*, 2016). With increased oxidation, biochar's

exchange capacity also improves, thus Py-DOM may more readily interact with mineral surfaces via adsorption or complexing with metals (Knicker, 2011; Mia *et al.*, 2016). This may indicate a similar stabilization pathway for Py-DOM as plant-derived organic matter based on soil matrix stability, further lengthening biochar's mean residence time in soils. However, this chemically distinct Py-DOM fraction with more oxidized functional groups and a less condensed aromatic structure may also make it more susceptible to mineralization (Bostick *et al.*, 2018). Such dynamics highlight the importance of understanding the transformation of biochar through different functional Py-OM pools to represent differences in biochar decomposition rates and mobility over time (Spokas *et al.*, 2014).

Process-based soil biogeochemical models can be applied to represent these various controls on feedstock and biochar decomposition. To our knowledge, the only existing soil biogeochemical model exploring biochar dynamics in soil is the biochar model within the Agricultural Production Systems sIMulator (APSIM) software (Archontoulis *et al.*, 2016). While the APSIM biochar model is parameterized to simulate biochar impacts on agricultural soils, here we developed a new mechanistic model to trace biochar decomposition as it moves through different functional Py-OM pools. In this modeling framework we simulate feedstock decomposition and stabilization within soils in both the baseline (i.e., unpyrolyzed biomass) and biochar scenario to estimate the extent of biochar C sequestration over time. Using this model, we explore model sensitivities and uncertainty ranges and estimate biochar's C sequestration potential for four scenarios:

- Woody debris applied to forest soils,
- Cereal crop residues applied to cropland soils,
- Grass residues applied to grassland soils, and
- Grass residues applied to reclaimed soils

Such analysis is intended to inform both policy and future biochar research on the current uncertainties in estimating biochar's C sequestration potential.

5.2. Materials and Methods

To assess the C sequestration potential of various biochar feedstocks and applications, we created the Pyrogenic Organic Matter module of the Microbial Efficiency and Matrix Stabilization model (MEMS-PyOM) to simulate biochar's C sequestration potential over time. The MEMS-PyOM module is structured on the MEMS v1.0 model, a process-based model designed to simulate empirical C pools allowing for a mechanistic representation of soil C cycling (Robertson et al, *in review*).

A key assumption of the approach we used to estimate the C sequestration potential of biochar soil amendments is that the biochar feedstock is sustainably sourced, and otherwise would have been left in a natural system to decompose. Lifecycle assessments of biochar GHG emissions have established that biochar feedstocks must not endanger food security or conservation efforts to ensure biochar production does not displace GHG emissions elsewhere (Woolf *et al.*, 2010). We conservatively assume natural decomposition of the feedstocks and no additional methane or nitrous oxide emissions from alternative baseline scenarios involving waste management. The model also assumes pyrolysis facilities contain sufficient emission capture systems to ensure complete combustion or recovery of gaseous pyrolysis products to prevent detrimental environmental effects (Mezzerette & Girard, 1991).

5.2.1. Model Structure and Assumptions

This model runs two simulations to estimate biochar's C sequestration potential over time: (1) a baseline scenario simulating decay of the unpyrolyzed residue, and (2) a biochar scenario, simulating the fate of the same residue after pyrolysis. In the baseline scenario, after initializing soil C pools to site conditions, the decay of the organic matter feedstock is simulated using a single input added to the standard C pools and parameterization of the MEMS v1.0 model. A description of the MEMS v1.0 structure,

assumptions and parameterization can be found in Robertson *et al.* (*in review*) and the MEMS User manual. In the biochar scenario, the feedstock is first pyrolyzed then the decay of the resulting biochar applied to soils is simulated using additional pools to represent the decay and stabilization of the biochar, hereafter named pyrogenic organic matter (Py-OM) for the sake of the model designed to simulate also natural Py-OM, within soil. Applying the MEMS v1.0 model architecture, we track C using pools for Py-POM, pyrogenic-dissolved organic matter Py-DOM and pyrogenic-mineral associated organic matter Py-MAOM. The general structure of the MEMS-PyOM module is represented in Fig. 22 with the mathematical representation detailed in Table 10.

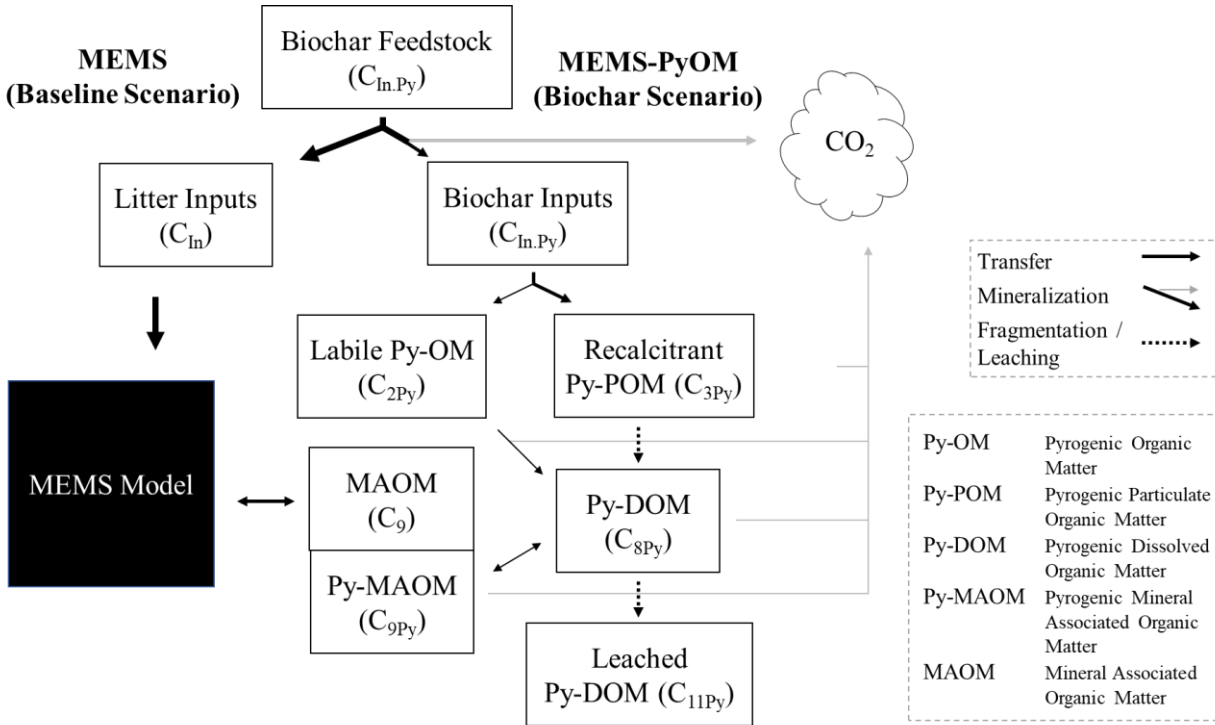


Fig. 22: Microbial Efficiency and Matrix Stabilization Pyrogenic Organic Matter (MEMS-PyOM) module structure.

For each simulation the parameter ρ is used to pass feedstock inputs to the two scenarios; the baseline scenario where the feedstock decays using the MEMS v1.0 model ($\rho = 0$), and the biochar scenario where the feedstock is first pyrolyzed then decays using the MEMS-PyOM module ($\rho = 1$). Parameter estimates for the biochar scenario of the MEMS-PyOM module are provided in Table 11. In the biochar

scenario, C losses from pyrolysis are accounted for using the ratio of biochar C to feedstock C (r_{Py}), to determine the biochar C remaining after pyrolysis. The parameter estimate for r_{Py} were based on the pyrolysis yield model of Neves *et al.* (2011), assuming a biochar C content of 0.88, feedstock C content of 0.50 and pyrolysis temperatures of 550°C with a distribution ranging from 400°C to 1,000°C. When applied to soils, biochar C is portioned into a labile Py-OM (C_{2Py}) and recalcitrant Py-POM (C_{3Py}) pool using the recalcitrant fraction of biochar (f_{3Py}). We applied a similar, yet simplified, model structure as the MEMS model, assuming that the decay of recalcitrant Py-OM results in the complete mineralization to pyrogenically-derived CO₂ (C_{7Py}) and does not generate Py-DOM (C_{8Py}) through microbial processing. However, the biochar scenario does include an abiotic fractionation pathway to form Py-DOM based on the fragmentation rate of Py-POM to Py-DOM (l_{3Py}), developed using data from Bostick *et al.* (2018). It is worth noting that in this model Py-DOM is considered as any fraction of PyOM transportable in water either dissolved or suspended. The MEMS-PyOM module applies a rate modifier to the decay of labile Py-OM ($\mu_{k,Py}$) and estimates the Py-DOM generated from the decay of labile Py-OM (λ_{Py}) assuming the same parameter values as those from the decay of recalcitrant litter (e.g., lignin and lignin encrusted celluloses) used in the MEMS model (μ_k and λ_3).

Table 10: First order differential equations used to simulate dynamics of pyrogenic C pools, eq. 3-8. Additional equations for allocating pyrogenic carbon inputs (eq. 9-12) and relating pyrogenic parameters to those of the MEMS model (eq. 13-16).

Pyrogenic C Pool	Equation
C_{2Py} Labile Py-POC	$\frac{dC_{2Py}}{dt} = C_{In.2Py} - (C_{2Py} * \mu_{k,Py} * k_{2Py}) \quad (3)$
C_{3Py} Recalcitrant Py-POC	$\frac{dC_{3Py}}{dt} = C_{In.3Py} - (C_{3Py} * k_{3Py}) - (C_{3Py} * l_{3Py}) \quad (4)$
C_{7Py} Pyrogenically-derived CO ₂ -C	$\frac{dC_{7Py}}{dt} = C_{In.7Py} + (C_{2Py} * \mu_{k,Py} * k_{2Py} * (1 - \lambda_{Py})) + (C_{3Py} * k_{3Py}) + (C_{8Py} * k_{8Py}) + (C_{9Py} * k_{9Py}) \quad (5)$

$$\begin{aligned} C_{8Py} \\ \text{Py-DOC} \end{aligned} \quad \frac{dC_{8Py}}{dt} = (C_{2Py} * \mu_{k.Py} * k_{2Py} * \lambda_{py}) + (C_{3Py} * l_{3Py}) - (C_{8Py} * k_{8Py}) - \left(C_{8Py} * \frac{Q_{max} * \left(\frac{K_{lm.Py} * C_{8Py}}{1 + K_{lm.Py} * C_{8Py}} \right) - C_{9Py}}{Q_{max}} \right) - (C_{8Py} * l_{8Py}) \quad (6)$$

$$\begin{aligned} C_{9Py} \\ \text{Py-MAOC} \end{aligned} \quad \frac{dC_{9Py}}{dt} = \left(C_{8Py} * \frac{Q_{max} * \left(\frac{K_{lm.Py} * C_{8Py}}{1 + K_{lm.Py} * C_{8Py}} \right) - C_{9Py}}{Q_{max}} \right) - (C_{9Py} * k_{9Py}) \quad (7)$$

$$\begin{aligned} C_{11Py} \\ \text{Leached Py-DOC} \end{aligned} \quad \frac{dC_{11Py}}{dt} = (C_{8Py} * l_{8Py}) \quad (8)$$

Initial conditions (In) for pyrogenic C pools are calculated as:

$$C_{In} = C_{In.Py} * (1 - \rho) \quad (9)$$

$$C_{In.2Py} = C_{In.Py} * \rho * r_{Py} * (1 - f_{3Py}) \quad (10)$$

$$C_{In.3Py} = C_{In.Py} * \rho * r_{Py} * f_{3Py} \quad (11)$$

$$C_{In.7Py} = C_{In.Py} * \rho * (1 - r_{Py}) \quad (12)$$

Other derived parameters include:

$$\mu_{k.Py} = \mu_k * r_{\mu k.Py} \quad (13)$$

$$\lambda_{py} = \lambda_3 * r_{\lambda.Py} \quad (14)$$

$$K_{lm.Py} = K_{lm} * r_{Klm.Py} \quad (15)$$

$$l_{8Py} = DOC_{lch} * r_{l.Py} \quad (16)$$

* See the MEMS v1.0 model (Robertson *et al.*, *in review*) for the derivation and parameter values of Q_{max} , μ_k , λ_3 , K_{lm} and DOC_{lch}

The MEMS-PyOM module uses the decay rates for labile C (k_{2Py}) and recalcitrant C estimated by the most recent meta-analysis of biochar stability in soil, applying a double first-order exponential decay model (Wang *et al.*, 2016). The decay rate of recalcitrant Py-OM is applied as the parameter value for the decay rate of the Py-POM (k_{3Py}), Py-DOM (k_{8Py}) and Py-MAOM (k_{9Py}) (Table 11). However, when

sampling the potential distribution of Py-POM parameter values to assess model sensitivity, these decay rates are assigned different distributions, as described below.

Table 11: MEMS-PyOM module parameter values and distributions.

MEMS-PyOM Base Parameters					
Parameter	Definition	Unit	Value (Range)	Equation	Source
f_{3Py}	Recalcitrant fraction of pyrogenic inputs	0-1 scaling	0.97 (0.88-0.99)	10, 11	See Table 13
k_{2Py}	Maximum decay rate of labile Py-OM (C_{2Py})	day ⁻¹	$9.26 \cdot 10^{-3} \text{ day}^{-1}$ ($3.29 \cdot 10^{-3} - 1.52 \cdot 10^{-2}$)	3, 5, 6	(Wang <i>et al.</i> , 2016)
k_{3Py}	Maximum decay rate of recalcitrant Py-OM (C_{3Py})	day ⁻¹	$4.93 \cdot 10^{-6} \text{ day}^{-1}$ ($4.53 \cdot 10^{-6} - 7.56 \cdot 10^{-6}$)	4, 5	See Table 13
k_{8Py}	Maximum decay rate of Py-DOM (C_{9Py})	day ⁻¹	$4.93 \cdot 10^{-6} \text{ day}^{-1}$ ($4.53 \cdot 10^{-6} - 9.87 \cdot 10^{-6}$)	5, 6	Same as k_{3Py} but distribution is up to 50% faster
k_{9Py}	Maximum decay rate of Py-MAOM (C_{9Py})	day ⁻¹	$4.93 \cdot 10^{-6} \text{ day}^{-1}$ ($3.29 \cdot 10^{-6} - 7.56 \cdot 10^{-6}$)	5, 7	Same as k_{3Py} but distribution is up to 50% slower
$r_{\mu_k.Py}$	Ratio of the rate modifier labile Py-OM decay ($\mu_{k.Py}$) to that of labile litter decay (μ_k)	ratio	1 (0.9-1.1)	13	Assumes MEMS μ_k value derived from (Campbell <i>et al.</i> , 2016) $\pm 10\%$
$r_{\lambda.Py}$	Ratio of the DOM generated from labile Py-OM decay (λ_{Py}) to that of recalcitrant litter decay (λ_3)	ratio	1 (0.9-1.1)	14	Assumes MEMS λ_3 value derived from (Campbell <i>et al.</i> , 2016) $\pm 10\%$
$r_{K_{lm}.Py}$	Ratio of the binding affinity for Py-DOC sorption to mineral surfaces ($K_{lm.Py}$) to the binding affinity for DOC sorption to mineral surfaces (K_{lm})	ratio	1 (0.9-1.1)	15	Assumes MEMS K_{lm} value derived from (Mayes <i>et al.</i> , 2012) $\pm 10\%$
$r_{l.Py}$	Ratio of the maximum specific rate of Py-DOC leached (l_{8Py}) to that of DOC leached (DOC_{lch})	ratio	0.106 (0.099-0.113)	16	(Jaffé <i>et al.</i> , 2013)

MEMS-PyOM Scenario-Specific Variables

Variable	Definition	Unit	Value (Range)	Equation	Source
$C_{In.Py}$	C input of biochar feedstock	g C m ⁻²	100 g m ⁻²	8, 10, 11, 12	
ρ	Fraction of biochar feedstock undergoing pyrolysis	0-1 scaling	1 (pyrolysis scenario) 0 (baseline scenario)	9, 10, 11, 12	
r_{Py}	Solid fraction of biochar feedstock C remaining after pyrolysis	0-1 scaling	0.187 (0.057-0.284)	10, 11, 12	(Neves <i>et al.</i> , 2011)
l_{3Py}	Fragmentation rate of Py-POM to Py-DOM	0-1 scaling	0.0001 day ⁻¹ (0-0.003)	6, 8	(Bostick <i>et al.</i> , 2018)

In the MEMS-PyOM module, Py-DOM (C_{8Py}) is subject to mineralization to pyrogenically-derived CO₂ (C_{7Py}), net sorption-desorption to mineral surfaces Py-MAOM (C_{9Py}) or lost as leached Py-DOC (C_{11Py}). The sorption dynamics for Py-DOC are modeled using the same approach as the MEMS model, applying a Langmuir sorption isotherm to estimate net sorption-desorption of organic matter to mineral surfaces (Abramoff *et al.* 2017; Mayes *et al.*, 2012; Robertson *et al.*, *in review*). The MEMS-PyOM module uses the Six *et al.* (2002) parameterization for determining the maximum sorption capacity of soil organic matter to soil mineral surfaces Q_{max} (Robertson *et al.*, *in review*), which is controlled by the sand content. Due to lack of literature estimates, we assume the binding affinity of Py-DOC sorption to mineral surfaces ($K_{Im.Py}$) is similar to that of DOC, which is modeled using soil pH as proxy for mineralogy (Mayes *et al.*, 2012; Abramoff *et al.* 2017; Robertson *et al.*, *in review*). The MEMS v1.0 model does not simulate water flow, thus the rate of Py-DOC leaching (l_{8Py}) is estimated relative to the leaching of DOC applied in the MEMS model (Trumbore *et al.*, 1992) and finding of Jaffé *et al.* (2013) that soluble charcoal accounts for 10% of the global riverine flux of DOC.

5.2.2. Model Simulations

Using the base parameterization in Table 11 and Table 12 we ran the MEMS PyOM-module to simulate a 100-year time horizon. To estimate the C sequestration potential of a simulation the estimates of the C

in the feedstock and soil organic matter fractions of the baseline scenario (i.e., unpyrolyzed feedstock) were subtracted from the biochar and Py-OM fractions of the biochar scenario at each timestep. This value was then divided by the initial biochar C to express it on a percentage basis of C remaining to provide a metric independent of biochar rate. To compare across different potential feedstocks and uses, we developed the four different biochar scenarios listed above. Values controlling the feedstock decay in the baseline scenario and stabilization of both the feedstock and biochar within soils are provided in Table 12 with a detailed description of the datasets provided below.

Table 12: Site-specific driving variables for the MEMS model with general values and distribution provided for the base run and distributions specific to the four biochar application scenarios simulated. See text for references for values and distributions.

MEMS Application-Specific Variables							
Variable	Definition	Unit	Base Run	Forest	Agriculture	Grassland	Reclaimed
<i>NPP</i>	Annual net primary production for the site	g C m ⁻² yr ⁻¹	525 (411-639)	577 (437-717)	533 (433-633)	241 (216-266)	25 (0-50)
<i>f_{iigi}</i>	Fraction of inputs allocated to recalcitrant feedstock C (C ₃)	0-1 scalar	0.21 (0.05-0.37)	0.30 (0.08-0.52)	0.06 (0.04-0.08)	0.15 (0.03-0.27)	0.15 (0.03-0.27)
<i>LitN</i>	N content of the feedstock inputs	% N	1.15 (0.23-2.07)	0.50 (0.29-0.71)	0.91 (0.74-1.08)	1.36 (1.20-1.52)	1.36 (1.20-1.52)
<i>sand</i>	Sand content of the soil layer simulated	% sand	44 (33.5-54.5)	39 (30.5-47.5)	40 (29-51)	47 (34-60)	55 (45-65)
<i>pH</i>	pH of the soil layer simulated	pH	6.2 (5.2-7.2)	5.5 (4.9-6.1)	6.5 (6.0-7.0)	6.9 (6.0-7.8)	6.9 (6.0-7.8)

5.2.3. Evaluating Model Sensitivities and Uncertainty

Given concerns with the integrity of biochar C sequestration estimates, we assessed both model sensitivity and uncertainty. A one-at-a-time sensitivity analysis was applied using the base parameterization given in the Table 11 and Table 12. Sensitivity was assessed along the probable range of parameter values with the biochar C sequestration potential given for years 10 and 100. We performed an uncertainty analysis to assess how variability in the inputs is propagated through the

model to affect variability in the outputs (Smith & Smith, 2007). Within the given distribution, we used Latin hypercube sampling to obtain parameter estimates for 100 simulation runs, then determined the 95% confidence interval on the estimates for biochar's 100-year C sequestration potential. Model simulations and statistical analyses were performed in R version 3.3.1 (R Core Team, 2016). Descriptions for how the parameter and variable distributions were derived are provided below.

5.2.3.1. *Baseline Scenario – Feedstock Decomposition and Stabilization in Soil*

To explore the sensitivity of biochar applications to different litter chemistry and soil types, distributions for parameters and variables controlling the feedstock decay in the baseline scenario and stabilization of both the feedstock and biochar within soils (Table 12) were obtained from the literature. Net primary productivity (NPP) and soil variables in forests and grasslands were derived from the Ecosystem Model-Data Intercomparison, Class A dataset (Olson *et al.*, 2013), while cropland values were derived from United States Department of Agriculture, National Agricultural Statistic Service data for the Central US (Prince *et al.*, 2013). Values for litter chemistry were assessed using the TRY Plant Trait Database (Kattge & Boenisch, 2018). The values and ranges for the reclaimed land scenario were derived assuming similar conditions as for grassland but with higher sand content in soil, due to erosion, and minimal net primary productivity.

5.2.3.2. *Biochar Scenario – Biochar Decomposition*

To explore model sensitivity to biochar decomposition parameters, we ... For all scenarios we assumed a feedstock input of $100 \text{ g C m}^{-2} (C_{in.Py})$, a 18.7% biochar C yield from pyrolysis (r_{py}) and a 1×10^{-4} fragmentation rate for Py-POM to Py-DOM. We estimated biochar decomposition using the two-pool exponential decay models of Fang *et al.* (2015), Singh *et al.* (2012) and Wang *et al.* (2016) to develop probable ranges for k_{2Py} and k_{3Py} across biochar types. Eq. 17 represents a two-pool exponential decay

model applying parameter notation from the MEMS-PyOM module. This can be rearranged to solve for the C remaining at time t, or for the case of this analysis, after 100 years (C_{R100} ; eq. 18).

$$C_t = C_0(f_{3Py}e^{-k_{3Py}t} + (1 - f_{3Py})e^{-k_{2Py}t}) \quad (17)$$

$$C_{R100} = \frac{C_{100}}{C_0} = f_{3Py}e^{-100k_{3Py}} + (1 - f_{3Py})e^{-100k_{2Py}} \quad (18)$$

$$k_{3Py} = -\frac{\ln\left(\frac{C_{R100} - (1 - f_{3Py})e^{-100k_{2Py}}}{f_{3Py}}\right)}{100} \quad (19)$$

$$f_{3Py} = \frac{C_{R100} - e^{-100k_{2Py}}}{e^{-100k_{3Py}} - e^{-100k_{2Py}}} \quad (20)$$

Rearranging eq. 18 we calculated equivalent parameter values for f_{3Py} (eq. 19) and k_{3Py} (eq. 20) using the C_{R100} estimates from the study's original parameterization and fixing the other parameter values to those from the Wang *et al.* (2016) meta-analysis (Table 13). We used these values to set the distribution for biochar decay rates. The value for k_{2Py} was sampled from a normal distribution based on Wang *et al.* (2016) uncertainty values, as k_{2Py} values from this study were equivalent to that of labile litter used in the MEMS model.

Table 6: Derivation of the Py-OM decay parameters.

MEMS-PyOM Decay Parameters						
Study	k_{2Py}	f_{3Py}	k_{3Py}	C_{R100}	Equivalent f_{3Py} value	Equivalent k_{3Py} value
Wang <i>et al.</i> , 2016	$9.26 \cdot 10^{-3} \text{ day}^{-1}$ (108 day MRT)	0.97	$4.93 \cdot 10^{-6} \text{ day}^{-1}$ (555 yr MRT)	81.0%	-	-
Fang <i>et al.</i> , 2015	$2.86 \cdot 10^{-2} \text{ day}^{-1}$ (35 day MRT)	0.996	$5.25 \cdot 10^{-6} \text{ day}^{-1}$ (521 yr MRT)	82.2%	0.984	$4.53 \cdot 10^{-6} \text{ day}^{-1}$ (605 yr MRT)
Singh <i>et al.</i> , 2012	$9.15 \cdot 10^{-4} \text{ day}^{-1}$ (1,093 day MRT)	0.83	$3.29 \cdot 10^{-6} \text{ day}^{-1}$ (833 yr MRT)	73.6%	0.88	$7.56 \cdot 10^{-6} \text{ day}^{-1}$ (362 yr MRT)

5.2.3.3. Biochar Scenario – Biochar Stabilization in Soils

Because of the lack of parameter estimates from the literature, the estimates for the decay of Py-DOM (k_{8Py}) and Py-MAOM (k_{9Py}) were set to the same value as that of Py-POM (k_{3Py}). Py-DOM may experience faster decay relative to Py-POM due to increased fragmentation and oxidation of surface functional group. We tested the sensitivity by simulating 3 distributions for decay rate for Py-DOM (k_{8Py}): 1) applying the same uniform distribution as k_{3Py} (no oxidation effect), 2) a normal distribution centered on upper range for k_{3Py} (minor oxidation effect), and 3) a uniform distribution from the base k_{3Py} value to a 50% increase in the decay rate (strong oxidative effect). Py-MAOM may experience slower decay relative to Py-POM due to increased physical protection (Knicker *et al.*, 2011). Potential stabilization of Py-OM to mineral surfaces was assessed on the decay rate of Py-MAOM (k_{9Py}) by: 1) applying the same uniform distribution as k_{3Py} (no stabilization), 2) a normal distribution centered on lower bound (minor stabilization effect), and 3) a uniform distribution from the base k_{3Py} value to a 50% decrease in the decay rate (strong stabilization effect).

5.3. Results

Model results using the base parameterization reveal that after 100 years 59% (51%, 66%) of the biochar C added will be sequestered in soils relative to the baseline scenario (Fig. 23). In the short-term, as litter decays in the baseline scenario, biochar's C sequestration profile quickly rises reaching upwards of 73% after 40 years. The model estimates that biochar takes 5.5 years (2, 13.5) to pay off the carbon debit from pyrolysis. The model also estimates that by 100 years 19.6% (13.8%, 28.2%) of the original biochar C is lost through leaching of Py-DOM. This leaching of Py-DOM is not included in the soil C sequestration estimates, but assuming a similar decay rate for Py-DOM total C sequestration potential could reach up to 79% (72%, 84%) (Fig. A10).

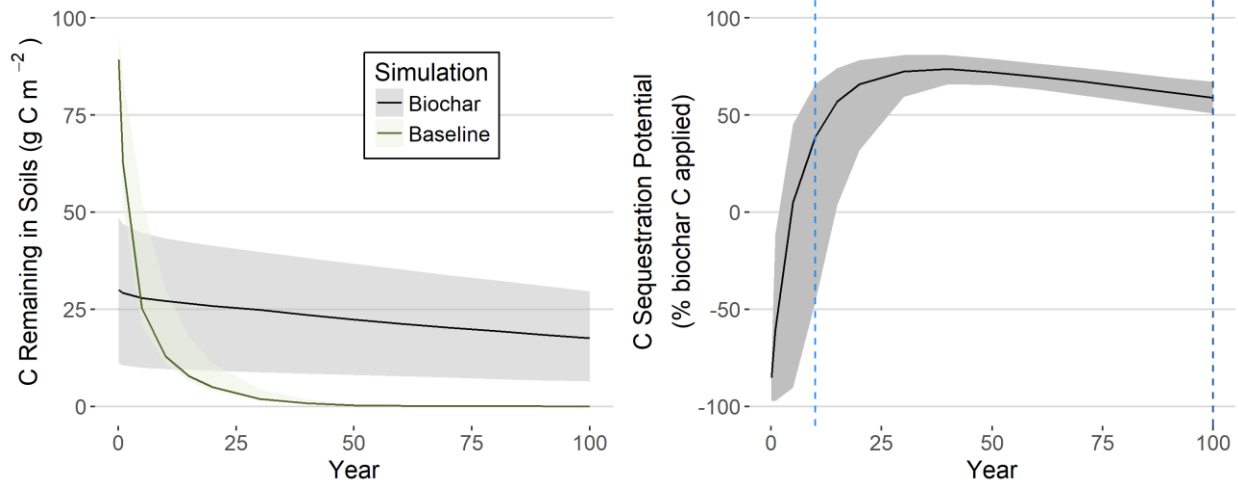


Fig. 23: 100-year MEMS-PyOM model run for the base scenario displaying the carbon remaining in soils for the biochar and baseline simulations in the base scenario (left panel) and resulting biochar C sequestration potential (biochar scenario – baseline scenario; right panel) over time. Shaded area displays the 95% confidence interval.

The 100-year C sequestration potential in the four different biochar application scenarios resulted in similar values ranging from 51.5% in the reclaimed scenario up to 63.5% for forest applications (Fig. 24). In the forest application biochar did not repay the initial pyrolysis debit until 7.2 years, however in other scenarios this happened much more quickly from 3.6 to 3.9 years (data not shown).

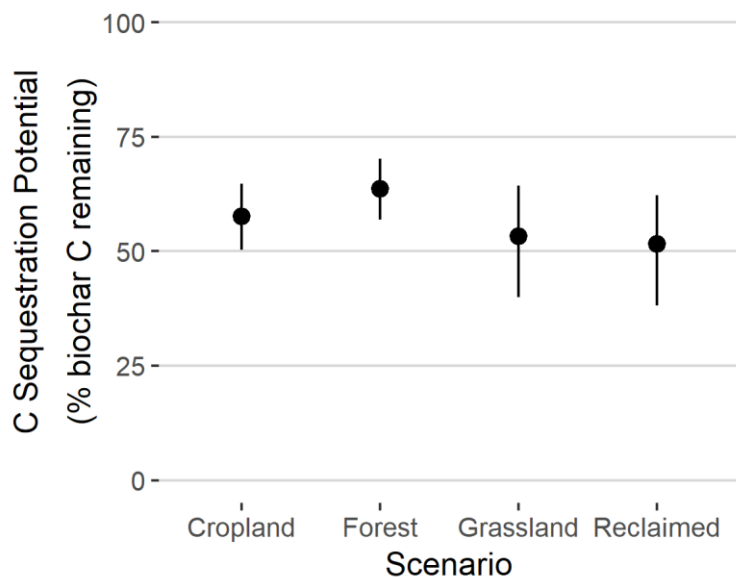


Fig. 24: 100-year biochar C sequestration potential for the four scenarios. Error bars display the 95% confidence intervals.

5.3.1. Baseline Scenario – Sensitivity to Feedstock Decomposition and Stabilization in Soil

Feedstock variables had minimal effects on biochar's 100-year C sequestration potential (Fig. 25).

Biochar feedstocks with low N content resulted in slower decomposition in the baseline scenario, delaying biochar's C sequestration benefits, but had little effect on biochar's long-term C sequestration.

Soil variables primarily affected both feedstock and biochar stabilization to soil minerals with impacts on biochar's 100-year C sequestration potential. The amount of C previously stabilized to mineral surfaces upon biochar application, the C saturation deficit, had minimal effect on biochar's long-term C sequestration potential. Finer soils within increased capacity for retaining C led to increased stabilization of both MAOM and Py-MAOM. This increased biochar's C sequestration potential due to the longer residence times of Py-MAOM. Soil pH, a proxy for soil mineralogy which affects the binding affinity of organic matter, experienced the greatest C sequestration potential at lower values, reflecting increased capacity of iron oxides to retain SOM (Fig. 25).

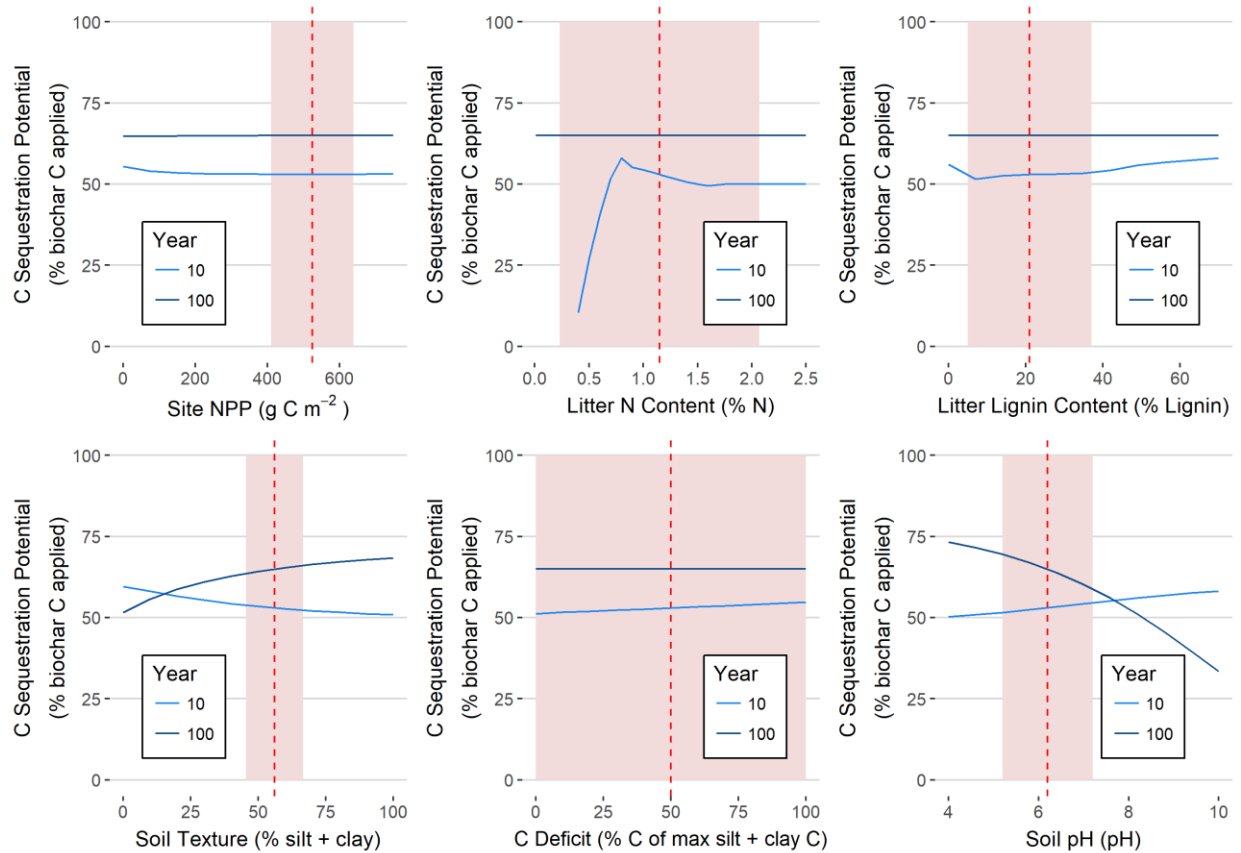


Fig. 25: Sensitivity of MEMS-PyOM module estimates for biochar’s 10- (light blue) and 100- (dark blue) year C sequestration potential (expressed as a percentage of the biochar applied) to litter chemistry and soil variables. Variables included are the net primary productivity (NPP) for the site, feedstock N content, feedstock lignin content, soil texture, C saturation deficit (expressed as the percentage of the initial mineral associated organic matter pool from the equilibrium sorption capacity) and soil pH. Dashed red lines display the fixed values when assessing sensitivity of other variable, while the shaded area displays the sampling distribution for model runs derived from literature values.

5.3.2. Biochar Scenario – Sensitivity to Biochar Decay

The pyrolysis yield (r_{Py}), recalcitrant fraction of Py-OM (f_{3Py}), Py-POM decay rate (k_{3Py}) and Py-MAOM decay rate (k_{9Py}) had the greatest controls over biochar’s C sequestration potential. The pyrolysis yield had very little impact on the 100-year sequestration potential but significantly impacted the time it takes for the biochar scenario to start sequestering carbon relative to the baseline (Fig. 26). Biochar yields of <10% required over 12 years to repay the carbon debt associated with CO₂ losses from pyrolysis.

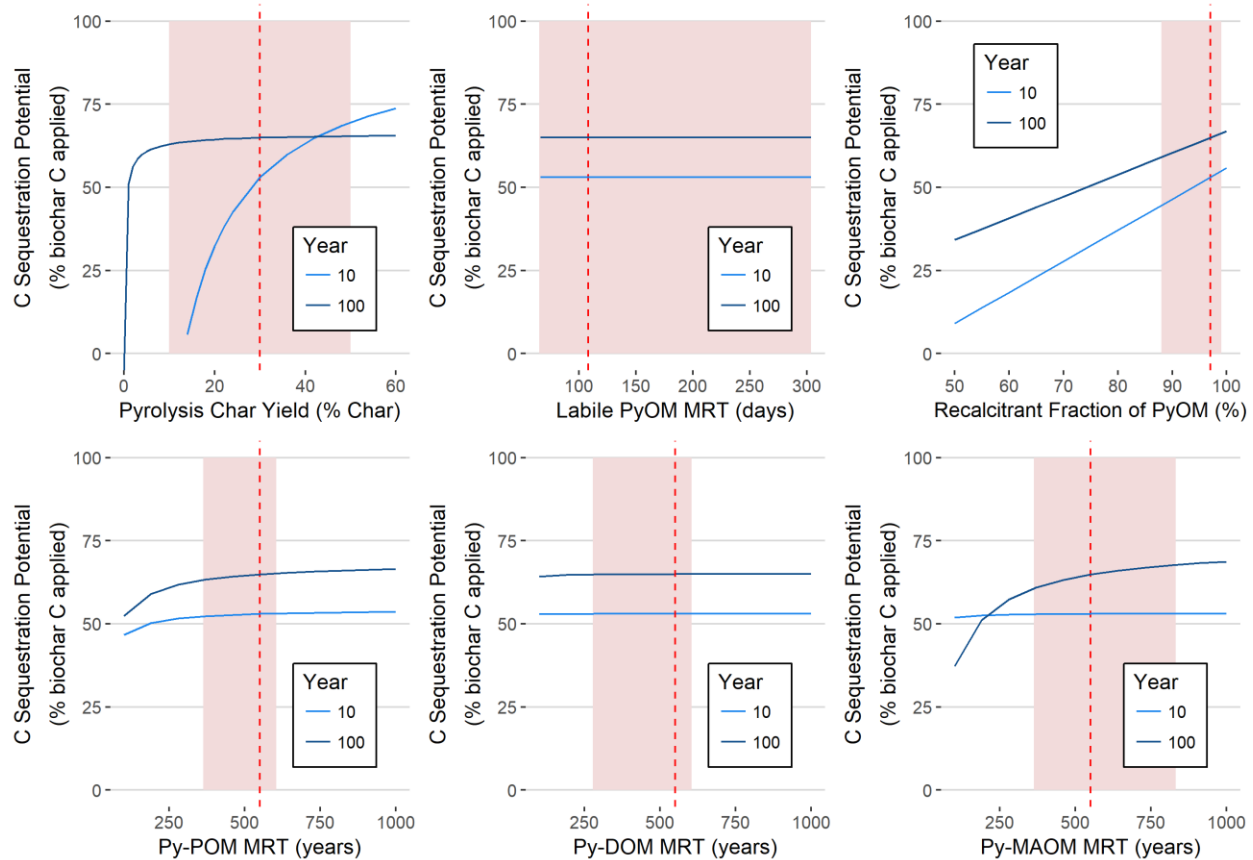


Fig. 9: Sensitivity of the MEMS-PyOM module estimates for biochar’s 10- (light blue) and 100- (dark blue) year C sequestration potential (expressed as a percentage of the biochar applied) to biochar decay parameters. Parameters include the decay rates for the labile pyrogenic organic matter (Py-OM) pyrogenic-particulate organic matter (Py-POM), pyrogenic dissolved organic matter (Py-DOM) and pyrogenic-mineral associated organic matter (Py-MAOM) fractions, the biochar yield from pyrolysis (r_{Py}) and the recalcitrant fraction of Py-OM (f_{3Py}). For the decay parameters the x axis represents the mean residence time (MRT) or $1/k$. Dashed red lines display the fixed values when assessing sensitivity of other variable, while the shaded area displays the sampling distribution for model runs derived from literature values.

The fraction of biochar going into the recalcitrant fraction has the greatest influence on biochar’s 100-year C sequestration potential (Fig. 26). However, within the distribution sampled for this analysis (Table 11), the 100-year C sequestration potential never dropped below 59% of the biochar C applied. The decay rates for Py-POM and Py-MAOM also have an important control on biochar’s C sequestration potential but to a lesser extent. Even when considering mean residence time of less than 250 years, the model still estimates that >50% of the C will remain sequestered after 100 years (Fig. 26). If using a

parameter estimate with longer Py-POM and Py-MAOM mean residence times the model estimates that up to 66% and 69% of the original biochar C applied will remain sequestered in soils.

5.3.3. *Biochar Scenario – Biochar Stabilization in Soils*

In the biochar scenario 98.5% of all biochar inputs remaining in soil after 100 years are within the Py-MAOM fraction. Assuming no stabilization of Py-MAOM or increase in Py-DOM mineralization, these fractions follow the same dynamics as Py-POM. When assuming only a minor stabilization and oxidation effect as in the base scenario, biochar's 100-year C sequestration potential increases slightly. This increase is largely because Py-DOM decay has very little control on biochar's 100-year C sequestration potential relative to Py-MAOM decay (Fig. 26). Assuming a strong stabilization and oxidation effect (up to a 50% that of Py-POM), biochar's median 100-year C sequestration potential increases by 6%.

5.4. Discussion

Model simulations show that despite variability in parameter estimates, uncertainties in biochar's 100-year C sequestration potential can be quantified and biochar does deliver GHG benefits even when considering shorter mean residence times. Litter chemistry, as it affects decay in the baseline scenario, did not impact the 100-year carbon sequestration potential but can extend the time it takes biochar to repay its C debt from pyrolysis. This resulted in the woody debris biochar scenario having the longest C debt due to the lower N content of woody feedstocks. The soil capacity to retain organic matter, as represented in the model by soil texture and pH, impacts the long-term stability of both SOM and PyOM alike (Knicker, 2011). This explains why the reclaimed and grassland biochar scenarios with coarser texture and high pH resulted in the lowest C sequestration potential at 100 years, due to their low capacity to retain OM. Modeling such mechanisms can be important to understand risks when quantifying biochar C sequestration potential for GHG mitigation programs. However, the similar ranges of C sequestration potentials between biochar applications despite the various distributions for litter

quality and soil variables emphasizes the relatively limited controls that the baseline scenario has on biochar's 100-year C sequestration potential.

The greatest control on the MEMS PyOM model is the fraction of biochar that is recalcitrant *versus* labile. Two-pool models for biochar decay have a clear advantage over single-pool models as they can more accurately represent empirical biochar pools: resistant unpyrolysed aliphatic compounds *versus* highly condensed aromatic C sheets (Bird *et al.*, 2015). Linking a mathematical two-pool model to functional biochar pools as opposed to kinetic pools, allows for a more realistic modeling approach (Elliott *et al.*, 1996). The applicability of a two-pool decay model has also been demonstrated by the decreasing decay rates over time in longer-term biochar stability studies (Kuzyakov *et al.*, 2014).

Isolating functionally distinct labile and recalcitrant biochar pools and Py-OM pools within soils can also pose significantly challenges. Measurement proxies such as the O:C ratio, oxidation techniques, and the % fixed C from a proximate analysis can help assess biochar stability (Crombie *et al.*, 2013; Spokas, 2010). Given the limited number of studies applying isotope labeling techniques to trace biochar in soil distinguishing different decay rates for groups or developing regressions to predict decay rates often results in insignificant or variable effects (Singh *et al.*, 2012; Wang *et al.*, 2016). General woody biochars tend to have slower decay rates along with biochars produced at high pyrolysis temperatures and applied to finer soils (Wang *et al.*, 2016). Refining methods to identify measurement proxies that can accurately represent functional biochar pools and identify trends between biochar types can significantly improve such modeling efforts.

This mechanistic model simulation of functional Py-OM pools also highlighted the important role of Py-DOM leaching and stabilization as Py-MAOM. There is much evidence for the delivery of land-derived Py-DOM to waterways (Jaffé *et al.*, 2013), yet Py-DOM losses are often overlooked when estimating biochar decay (Spokas *et al.*, 2014). While leached Py-DOM concentrations were not included in the

estimates for soil C sequestration, it is likely that such C will also have longer mean residence times depending on the deposition environment. When we added the concentration of leached Py-DOM to estimates of biochar's soil C sequestration, it reached 79%, within the typical ranges assumed in the literature (Paustian *et al.*, 2016; Woolf *et al.*, 2010). Retention of oxidized Py-OM within the soil mineral fraction has strong empirical support from Py-OM soil fractionation studies (Brodowski *et al.*, 2006; Qayyum *et al.*, 2014; Glaser *et al.*, 2000; Herath *et al.*, 2014; Singh & Cowie, 2014), and a global Py-OM inventory indicates that the greatest concentrations of Py-OM are found in high clay content soils (Reisser *et al.*, 2016). Additional research is necessary to better understand these dynamics driving the stabilization of Py-OM to mineral surfaces, as results from this study indicate potential biochar fragmentation and leaching can significantly affect biochar sequestration potential. Additional improvements to the MEMS-PyOM module include simulation of water flow dynamics to better predict Py-DOM leaching and further exploration of the interactions between Py-OM and native SOM.

5.5. Conclusions

This study reveals that even when considering some of the faster biochar decay rates reflected in the literature, greater than 50% of the biochar C applied is likely to be sequestered in soils after 100 years. While economic obstacles must still be overcome, uncertainties in biochar C sequestration potential can be quantified and should not be viewed as a barrier to including incentives for biochar amendments into climate change mitigation programs. The MEMS-PyOM module can serve as a basis for determining the permanence of biochar C in GHG mitigation programs, and help direct future research to further decrease uncertainties in the soil C sequestration benefits biochar can provide.

6. CONCLUSION

There have been many claims regarding biochar's ability to enhance productivity and reduce GHG impacts. These studies revealed that biochar had mixed results in achieving such benefits. Biochar's ability to increase soil moisture was evident in both field studies (Ramlow *et al.*, *in review*; Ramlow *et al.*, *in press*). Despite increased soil moisture in the deficit irrigation field trials and forest road restoration study, neither application resulted in increased productivity from application of this woody biochar. Biochar improved water retention but this increased capacity had limited effects when precipitation or irrigation inputs were low. During these dry periods water content still dropped below critical thresholds resulting in plant water stress. In irrigated systems such effects may be mitigated by scheduling the irrigation water application with shorter time intervals to account for biochar's increased water holding capacity. However, in natural systems that experience longer periods without precipitation, biochar's increased capacity for water retention is likely to have little effect in alleviating plant water stress.

The woody biochar we used in our studies showed minimal capacity to impact bulk soil mineral N availability, particularly to an extent that would benefit plant growth. Lab incubations demonstrated that biochar did not significantly alter mineral N concentration even as they were transformed via microbial processing. Individual biochar particles also did not show evidence of preferentially retaining NH_4^+ or NO_3^- . Biochar did increase the soil's ability to retain mineral N over time, but the magnitude of the increase was small and did not result in increased plant biomass or cover. In laboratory incubations, the lack of a biochar impact on mineral N availability, despite significant N_2O emission reductions in the fertilized incubations, indicated that biochar impacts on N substrate availability could not explain biochar's impact on N_2O .

Biochar's ability to reduce N_2O was significantly impacted by soil moisture regime. In the laboratory incubation, I found that under moderately anaerobic conditions (roughly 80% WFPS) biochar ability to

reduce N₂O emissions was significantly improved. This may be due to increased aeration partially inhibiting denitrification. The incubation also revealed that in fertilized treatments biochar could achieve annual N₂O emissions reductions that are equivalent to its C sequestration benefit annualized over 100 years. Under field conditions biochar didn't significantly reduce N₂O emissions, however in this semi-arid climate total emissions were lower than global estimates.

To assess biochar's potential C sequestration benefits we developed the MEMS-PyOM module to simulate biochar decay against decay of the biochar feedstock. This model estimated that after 100 years 59% of the initial biochar added will remain, with up to 79% if including leached biochar fragments. Biochar's 100-year C sequestration potential was most sensitive to biochar decay parameters with some additional controls based on the soil's ability to stabilize organic matter. The simulations also highlighted the importance of potential biochar fragmentation and leaching over time. Of the applications considered, this research illustrated that within the US Interior West woody biochar is best suited for sequestering C in soils. This underscores the importance of assessing biochar's purported benefits to discover and refine the beneficial applications biochar can actually achieve.

REFERENCES

- Abel, S., Peters, A., Trinks, S., Schonsky, H., Facklam, M., & Wessolek, G. (2013). Impact of biochar and hydrochar addition on water retention and water repellency of sandy soil. *Geoderma*, 202–203, 183–191. <http://doi.org/10.1016/j.geoderma.2013.03.003>
- Abramoff, R., Xu, X., Hartman, M., O'Brien, S., Feng, W., Davidson, E., Finzi, A., Moorhead, D., Schimel, J., Torn, M., Mayes, M.A. (2018). The Millennial model: in search of measurable pools and transformations for modeling soil carbon in the new century. *Biogeochemistry*, 137, 51–71. <https://doi.org/10.1007/s10533-017-0409-7>
- Adams, M.A. (2013). Mega-fires, tipping points and ecosystem services: Managing forests and woodlands in an uncertain future. *Forest Ecology and Management*, 294, 250–261. <http://doi.org/10.1016/j.foreco.2012.11.039>
- Ahrens, B., Braakhekke, M.C., Guggenberger, G., Schrumpf, M., Reichstein, M. (2015). Contribution of sorptin, DOC transport and microbial interactions to the 14C age of a soil organic carbon profile: Insights from a calibrated process model. *Soil Biology and Biochemistry*, 88, 390–402.
- Alban, D.H., Host, G.E., Elioff, J.D., Shadis, D. (1994). Soil and vegetation response to soil compactation and forest floor removal after aspen harvesting. *U.S. Dept. of Agriculture, Forest Service, North Central Forest Experiment Station*, 1–8.
- Ali, S., Rizwan, M., Qayyum, M.F., Ok, Y.S., Ibrahim, M., Riaz, M., Shahzad, A.N. (2017). Biochar soil amendment on alleviation of drought and salt stress in plants: a critical review. *Environmental Science and Pollution Research*, 24(14), 12700–12712. <http://doi.org/10.1007/s11356-017-8904-x>
- Allen, R.G., Pereira, L.S., Raes, D., Smith, M., Ab, W. (1998). Crop evapotranspiration - Guidelines for computing crop water requirements - FAO Irrigation and drainage paper 56, 1–15.
- Ampoorter, E., De Schrijver, A., De Frenne, P., Hermy, M., Verheyen, K. (2011). Experimental assessment of ecological restoration options for compacted forest soils. *Ecological Engineering*, 37(11), 1734–1746. <http://doi.org/10.1016/j.ecoleng.2011.07.007>
- Andrenelli, M.C., Maienza, A., Genesio, L., Miglietta, F., Pellegrini, S., Vaccari, F.P., & Vignozzi, N. (2016). Field application of pelletized biochar: Short term effect on the hydrological properties of a silty clay loam soil. *Agricultural Water Management*, 163, 190–196. <http://doi.org/10.1016/j.agwat.2015.09.017>
- Angst, T.E., Six, J., Reay, D.S., Sohi, S.P. (2014). Impact of pine chip biochar on trace greenhouse gas emissions and soil nutrient dynamics in an annual ryegrass system in California. *Agriculture, Ecosystems and Environment*, 191, 17–26. <http://doi.org/10.1016/j.agee.2014.03.009>
- Archontoulis, S.V., Huber, I., Miguez, F.E., Thorburn, P.J., Rogovska, N., Laird, D.A. (2016). A model for mechanistic and system assessments of biochar effects on soils and crops and trade-offs. *GCB Bioenergy*, 8(6), 1028–1045. <http://doi.org/10.1111/gcbb.12314>
- Aronson, J., Floret, C., Le Floc'h, E., Ovalle, C., Pontanier, R. (1993). Restoration and rehabilitation of degraded ecosystems in arid and semi-arid lands. I. A View from the South. *Restoration Ecology*, 1(1), 8–17. <http://doi.org/10.1111/j.1526-100X.1993.tb00004.x>
- Asbjornsen, H., Shepherd, G., Helmers, M., Mora, G. (2008). Seasonal patterns in depth of water uptake

- under contrasting annual and perennial systems in the Corn Belt Region of the Midwestern U.S., 69–92. <http://doi.org/10.1007/s11104-008-9607-3>
- Asseng, S., Turner, N.C., Keating, B.A. (2001). Analysis of water- and nitrogen-use efficiency of wheat in a Mediterranean climate. *Plant and Soil*, 233(1), 127–143.
- Atkinson, C.J., Fitzgerald, J.D., Hips, N.A. (2010). Potential mechanisms for achieving agricultural benefits from biochar application to temperate soils: A review. *Plant and Soil*, 337(1–2), 1–18. <http://doi.org/10.1007/s11104-010-0464-5>
- Augustenborg C.A., Hepp S., Kammann C. (2012) Biochar and earthworm effects on soil nitrous oxide and carbon dioxide emissions. *Journal of Environmental Quality*, 41, 1203–1209.
- Aulakh, M.S., Malhi, S.S. (2005). Interactions of nitrogen with other nutrients and water: Effect on crop yield and quality, nutrient use efficiency, carbon sequestration, and environmental pollution. *Advances in Agronomy*, 86, 341–409. [http://doi.org/10.1016/S0065-2113\(05\)86007-9](http://doi.org/10.1016/S0065-2113(05)86007-9)
- Bach, M., Wilske, B., Breuer, L. (2016). Current economic obstacles to biochar use in agriculture and climate change mitigation. *Carbon Management*, 7(3–4), 183–190. <http://doi.org/10.1080/17583004.2016.1213608>
- Baggs, E.J., Bateman, E.M. (2005). Contributions of nitrification and denitrification to N₂O emissions from soils at different water-filled pore space. *Biology and Fertility of Soils*, 41, 379–388. <http://doi.org/10.1007/s00374-005-0858-3>
- Bagley, E.M. (1998). *A citizen's guide to wildland road removal*. University of Montana.
- Bai, S.H., Blumfield, T.J., Reverchon, F. (2014). The impact of mulch type on soil organic carbon and nitrogen pools in a sloping site. *Biology and Fertility of Soils*, 50(1), 37–44. <http://doi.org/10.1007/s00374-013-0829-z>
- Baldi, E., Toselli, M. (2014). Mineralization dynamics of different commercial organic fertilizers from agro-industry organic waste recycling: An incubation experiment. *Plant, Soil and Environment*, 60(3), 93–99.
- Barakat, M., Cheviron, B., Angulo-Jaramillo, R. (2016). Influence of the irrigation technique and strategies on the nitrogen cycle and budget: A review. *Agricultural Water Management*, 178, 225–238. <http://doi.org/10.1016/j.agwat.2016.09.027>
- Barré, P., Angers, D.A., Basile-doelsch, I., Bispo, A., Cécillon, L., Chevallier, T., Pellerin, S. (2017). Ideas and perspectives: Can we use the soil carbon saturation deficit to quantitatively assess the soil carbon storage potential, or should we explore other strategies?, *Biogeosciences Discuss*, 1–12. <https://doi.org/10.5194/bg-2017-395>
- Basso, A.S., Miguez, F.E., Laird, D.A., Horton, R., Westgate, M. (2013). Assessing potential of biochar for increasing water-holding capacity of sandy soils. *GCB Bioenergy*, 5(2), 132–143. <http://doi.org/10.1111/gcbb.12026>
- Bastida, F., Selevsek, N., Torres, I.F., Hernández, T., García, C. (2015). Soil restoration with organic amendments: Linking cellular functionality and ecosystem processes. *Scientific Reports*, 5, 1–12. <http://doi.org/10.1038/srep15550>
- Bedard, C., Knowles, R. (1989). Physiology, biochemistry, and specific inhibitors of CH₄, NH₄⁺, and CO

- oxidation by methanotrophs and nitrifiers. *Microbiologic Reviews*, 53(1), 68–84.
- Benigno, S.M., Dixon, K.W., Stevens, J.C. (2013). Increasing soil water retention with native-sourced mulch improves seedling establishment in postmine Mediterranean sandy soils. *Restoration Ecology*, 21(5), 617–626. <http://doi.org/10.1111/j.1526-100X.2012.00926.x>
- Biederman, L.A., Stanley Harpole, W. (2013). Biochar and its effects on plant productivity and nutrient cycling: A meta-analysis. *GCB Bioenergy*, 5(2), 202–214. <http://doi.org/10.1111/gcbb.12037>
- Binkley, D. (1984). Ion exchange resin bags: Factors affecting estimates of nitrogen availability. *Soil Sci. Soc. Am. J.*, 48, 1181–1184.
- Binkley, D., Matson, P. (1983). Ion exchange resin bag method for assessing forest soil nitrogen availability. *Soil Sci. Soc. Am. J.*, 47(47), 1050–1052.
- Bird, M.I., Wynn, J.G., Saiz, G., Wurster, C.M., McBeath, A. (2015). The pyrogenic carbon cycle. *Annual Review of Earth and Planetary Sciences*, 43(1), 273–298. <http://doi.org/10.1146/annurev-earth-060614-105038>
- Blagodatsky, S., Smith, P. (2012). Soil physics meets soil biology: Towards better mechanistic prediction of greenhouse gas emissions from soil. *Soil Biology and Biochemistry*, 47, 78–92. <http://doi.org/10.1016/j.soilbio.2011.12.015>
- Boot, C.M., Haddix, M., Paustian, K., Cotrufo, M.F. (2015). Distribution of black carbon in ponderosa pine forest floor and soils following the High Park wildfire. *Biogeosciences*, 12(10), 3029–3039. <http://doi.org/10.5194/bg-12-3029-2015>
- Booth, M.S., Stark, J.M., Rastetter, E. (2005). Controls on nitrogen cycling in terrestrial ecosystems: A synthetic analysis of literature data. *Ecological Monographs*, 72(2), 139–157.
- Bostick, K.W., Zimmerman, A.R., Wozniak, A.S., Mitra, S. (2018). Production and composition of pyrogenic dissolved organic matter from a logical series of laboratory-generated chars, *Frontiers in Earth Science*, 6(43), 1–14. <http://doi.org/10.3389/feart.2018.00043>
- Bouwman, A.F. (1996). Direct emission of nitrous oxide from agricultural soils. *Nutrient Cycling in Agroecosystems*, 46, 53–70.
- Box, G.E.P., Cox, D.R. (1964). An analysis of transformations. *Journal of the Royal Statistical Society*, 211–252. <http://doi.org/10.2307/2287791>
- Brantley, K.E., Savin, M.C., Brye, K.R., Longer, D.E. (2015). Pine woodchip biochar impact on soil nutrient concentrations and corn yield in a silt loam in the mid-southern U.S., *Agriculture*, 5, 30–47. <http://doi.org/10.3390/agriculture5010030>
- Brassard, P., Godbout, S.E., Raghavan, V. (2016). Soil biochar amendment as a climate change mitigation tool: Key parameters and mechanisms involved. *Journal of Environmental Management*, 181, 484–497. <http://doi.org/10.1016/j.jenvman.2016.06.063>
- Brewer, C.E., Schmidt-rohr, K., Satrio, J.A., Brown, R.C. (2009). Characterization of biochar from fast pyrolysis and gasification systems, *Environmental Progress & Sustainable Energy*, 28(3). <http://doi.org/10.1002/ep>
- Brodowski, S., John, B., Flessa, H., Amelung, W. (2006). Aggregate-occluded black carbon in soil. *European Journal of Soil Science*, 57(4), 539–546. <http://doi.org/10.1111/j.1365-2389.2006.00807.x>

- Brooks, R., McFarland, A., Schnepf, C. (2011). Grass seeding forest roads, skid trails, and landings in the inland northwest. *Pacific Northwest Extension Publication*, (PNW 628), 1–8.
- Bruun, E.W., Petersen, C.T., Hansen, E., Holm, J.K., Hauggaard-Nielsen, H. (2014). Biochar amendment to coarse sandy subsoil improves root growth and increases water retention. *Soil Use and Management*, 30(March), 109–118. <http://doi.org/10.1111/sum.12102>
- Bulmer, C. (2000). Reclamation of forest soils with excavator tillage and organic amendments. *Forest Ecology and Management*, 133, 157–163. [http://doi.org/10.1016/S0378-1127\(99\)00306-0](http://doi.org/10.1016/S0378-1127(99)00306-0)
- Butterbach-Bahl, K., Baggs, E.M., Dannenmann, M., Kiese, R., Zechmeister-Boltenstern, S. (2013). Nitrous oxide emissions from soils: how well do we understand the processes and their controls? *Philosophical Transactions of the Royal Society of London. Series B, Biological Sciences*, 368(1621), 20130122. <http://doi.org/10.1098/rstb.2013.0122>
- Campbell, E.E., Parton, W.J., Soong, J.L., Paustian, K., Hobbs, N.T., Cotrufo, M.F. (2016). Using litter chemistry controls on microbial processes to partition litter carbon fluxes with the Litter Decomposition and Leaching (LIDEL) model. *Soil Biology and Biochemistry*, 100, 160–174. <http://doi.org/10.1016/j.soilbio.2016.06.007>
- Campbell, E.E., Paustian, K. (2015). Current developments in soil organic matter modeling and the expansion of model applications: A review. *Environmental Research Letters*, 10(12), 123004. <http://doi.org/10.1088/1748-9326/10/12/123004>
- Case, S.D.C., McNamara, N.P., Reay, D.S., Whitaker, J. (2012). The effect of biochar addition on N₂O and CO₂ emissions from a sandy loam soil- The role of soil aeration. *Soil Biology and Biochemistry*, 51, 125–134. <http://doi.org/10.1016/j.soilbio.2012.03.017>
- Cayuela, M.L., Jeffery, S., van Zwieten, L. (2015). The molar H:C_{org} ratio of biochar is a key factor in mitigating N₂O emissions from soil. *Agriculture, Ecosystems & Environment*, 202, 135–138. <http://doi.org/10.1016/j.agee.2014.12.015>
- Cayuela, M.L., van Zwieten, L., Singh, B.P., Jeffery, S., Roig, A., Sánchez-monedero, M.A. (2014). Biochar's role in mitigating soil nitrous oxide emissions: A review and meta-analysis. *Agriculture, Ecosystems and Environment*, 191, 5–16. <http://doi.org/10.1016/j.agee.2013.10.009>
- Cayuela, M.L., Sánchez-Monedero, M.A., Roig, A., Hanley, K., Enders, A., Lehmann, J. (2013). Biochar and denitrification in soils: when, how much and why does biochar reduce N₂O emissions? *Scientific Reports*, 3, 1–7. <http://doi.org/10.1038/srep01732>
- Clough, T.J., Condon, L.M., Kamman, C., Müller, C. (2013). A review of biochar and soil nitrogen dynamics. *Agronomy*, 3, 275–293. <http://doi.org/10.3390/agronomy3020275>
- Coglan, G., Sowa, R. (1998). *National Forest Road System and Use*. Washington, DC.
- Colorado Agricultural Meteorological nETwork (CoAgMET), Colorado Climate Center. Colorado State University. Retrieved from <https://coagmet.colostate.edu/>. Accessed 12/28/2017.
- Cornelissen, G., Rutherford, D.W., Arp, H.P.H., Dörsch, P., Kelly, C.N., Rostad, C.E. (2013). Sorption of pure N₂O to biochars and other organic and inorganic materials under anhydrous conditions. *Environmental Science & Technology*, 47(14), 7704–7712. <http://doi.org/10.1021/es400676q>
- Cotrufo, M.F., Wallenstein, M.D., Boot, C.M., Denef, K., Paul, E. (2013). The Microbial Efficiency-Matrix

- Stabilization (MEMS) framework integrates plant litter decomposition with soil organic matter stabilization: Do labile plant inputs form stable soil organic matter? *Global Change Biology*, 19(4), 988–995. <http://doi.org/10.1111/gcb.12113>
- Crombie, K., Mašek, O., Sohi, S. P., Brownsort, P., & Cross, A. (2013). The effect of pyrolysis conditions on biochar stability as determined by three methods. *GCB Bioenergy*, 5(2), 122–131. <http://doi.org/10.1111/gcbb.12030>
- Cross, A., Sohi, S. P. (2011). The priming potential of biochar products in relation to labile carbon contents and soil organic matter status. *Soil Biology and Biochemistry*, 43(10), 2127–2134. <http://doi.org/10.1016/j.soilbio.2011.06.016>
- Cui, X., Hao, H., Zhang, C., He, Z., Yang, X. (2016). Capacity and mechanisms of ammonium and cadmium sorption on different wetland-plant derived biochars. *Science of the Total Environment*, 539(January 2016), 566–575. <http://doi.org/10.1016/j.scitotenv.2015.09.022>
- Dan, T., Zhong-Yi, Q., Mang-Mang, G., Bo, L., Yi-Jia, L. (2015). Experimental study of influence of biochar on different texture soil hydraulic characteristic parameters and moisture holding properties. *Polish Journal of Environmental Studies*, 24(3), 1435–1442.
- Davis, M.A., Grime, J.P., Thompson, K. (2000). Fluctuating resources in plant communities: A general theory of invasibility. *Journal of Ecology*, 88(3), 528–534. <http://doi.org/10.1046/j.1365-2745.2000.00473.x>
- de Melo Carvalho, M.T., de Holanda Nunes Maia, A., Madari, B.E., Bastiaans, L., Van Oort, P.A.J., Heinemann, A.B., Meinke, H. (2014). Biochar increases plant-available water in a sandy loam soil under an aerobic rice crop system. *Solid Earth*, 5(2), 939–952. <http://doi.org/10.5194/se-5-939-2014>
- Downie A., Crosky A., Munroe O. (2009) Chapter 2: physical properties of biochar. In: *Biochar for Environmental Management: Science and Technology* (eds Lehmann J., Joseph S.), pp. 183–205. Earthscan, London.
- Eastaugh, C.S., Rustomji, P.K., Hairsine, P.B. (2008). Quantifying the altered hydrologic connectivity of forest roads resulting from decommissioning and relocation. *Hydrological Processes*, 22, 2438–2448. <http://doi.org/10.1002/hyp>
- Elliott, E.T., Paustian, K., Frey, S.D. (1996). Modeling the measurable or measuring the modelable: A hierarchical approach to isolating meaningful soil organic matter fractions. In *Evaluation of Soil Organic Matter Models* (p. 161). Fort Collins, CO: Springer-Verlag Berlin Heidelberg.
- Elseroad, A.C., Fulé, P.Z., Covington, W.W. (2003). Forest road revegetation: Effects of seeding and soil amendments. *Ecological Restoration*. <http://doi.org/10.3368/er.21.3.180>
- Enders, A., Hanley, K., Whitman, T., Joseph, S., Lehmann, J. (2012). Characterization of biochars to evaluate recalcitrance and agronomic performance. *Bioresource Technology*, 114, 644–653. <http://doi.org/10.1016/j.biortech.2012.03.022>
- Fang, S., Xie, B., Liu, D., Liu, J. (2011). Effects of mulching materials on nitrogen mineralization, nitrogen availability and poplar growth on degraded agricultural soil. *New Forests*, 41(2), 147–162. <http://doi.org/10.1007/s11056-010-9217-9>
- Fang, Y., Singh, B., Pal, B. (2015). Effect of temperature on biochar priming effects and its stability in

- soils. *Soil Biology and Biochemistry*, 80, 136–145. <http://doi.org/10.1016/j.soilbio.2014.10.006>
- Feng, Y., Xu, Y., Yu, Y., Xie, Z., Lin, X. (2012). Mechanisms of biochar decreasing methane emission from Chinese paddy soils. *Soil Biology and Biochemistry*, 46, 80–88. <http://doi.org/10.1016/j.soilbio.2011.11.016>
- Field, J.L., Keske, C.M.H., Birch, G.L. (2013). Distributed biochar and bioenergy coproduction : a regionally specific case study of environmental benefits and economic impacts. *Global Change Biology Bioenergy*, 5, 177–191. <http://doi.org/10.1111/gcbb.12032>
- Foltz, R.B. (2012). A comparison of three erosion control mulches on decommissioned forest road corridors in the northern Rocky Mountains, United States. *Journal of Soil and Water Conservation*, 67(6), 536–544. <http://doi.org/10.2489/jswc.67.6.536>
- Forest Service. (2010). *Legacy roads and trails accomplishment report*. Washington, DC: USDA Forest Service, Pacific Northwest Region
- Foster, E.J., Hansen, N., Wallenstein, M., Cotrufo, M.F. (2016). Biochar and manure amendments impact soil nutrients and microbial enzymatic activities in a semi-arid irrigated maize cropping system. *Agriculture, Ecosystems and Environment*, 233, 404–414. <http://doi.org/10.1016/j.agee.2016.09.029>
- Fuss, S., Canadell, J.G., Peters, G.P., Tavoni, M., Andrew, R. M., Ciais, P., Yamagata, Y. (2014). Betting on negative emissions. *Nature Climate Change*, 4(10), 850–853. <http://doi.org/10.1038/nclimate2392>
- Gai, X., Wang, H., Liu, J., Zhai, L., Liu, S., Ren, T., Liu, H. (2014). Effects of feedstock and pyrolysis temperature on biochar adsorption of ammonium and nitrate. *PLoS ONE*, 9(12), 1–20. <http://doi.org/10.1371/journal.pone.0113888>
- Geerts, S., Raes, D. (2009). Deficit irrigation as an on-farm strategy to maximize crop water productivity in dry areas. *Agricultural Water Management*, 96, 1275–1284. <http://doi.org/10.1016/j.agwat.2009.04.009>
- Glaser, B., Balashov, E., Haumaier, L., Guggenberger, G., Zech, W. (2000). Black carbon in density fractions of anthropogenic soils of the Brazilian Amazon region. *Organic Geochemistry*, 31(7–8), 669–678. [http://doi.org/10.1016/S0146-6380\(00\)00044-9](http://doi.org/10.1016/S0146-6380(00)00044-9)
- Glaser, B., Haumaier, L., Guggenberger, G., Zech, W. (2001). The “Terra Preta” phenomenon: a model for sustainable agriculture in the humid tropics. *Naturwissenschaften*, 88, 37–41. <http://doi.org/10.1007/s001140000193>
- Goldin, S.R., Hutchinson, M.F. (2014). Coarse woody debris reduces the rate of moisture loss from surface soils of cleared temperate Australian woodlands. *Soil Research*, 52(7), 637–644. <http://doi.org/10.1071/SR13337>
- Gonzalez-Dugo, V., Durand, J.-L., Gastal, F. (2010). Water deficit and nitrogen nutrition of crops. A review. *Agronomy for Sustainable Development*, 30(3), 529–544. <http://doi.org/10.1051/agro/2009059>
- Grandy, A.S., Neff, J.C. (2008). Molecular C dynamics downstream: The biochemical decomposition sequence and its impact on soil organic matter structure and function. *Science of the Total Environment*, 404, 519–529. <http://doi.org/10.1016/j.scitotenv.2007.11.013>

- Grant, A.S., Nelson, C.R., Switalski, T.A., Rinehart, S.M. (2011). Restoration of native plant communities after road decommissioning in the Rocky Mountains: Effect of seed-mix composition on vegetative establishment. *Restoration Ecology*, 19(201), 160–169. <http://doi.org/10.1111/j.1526-100X.2010.00736.x>
- Gray, M., Johnson, M.G., Dragila, M.I., Kleber, M. (2014). Water uptake in biochars: The roles of porosity and hydrophobicity. *Biomass and Bioenergy*, 61, 196–205. <http://doi.org/10.1016/j.biombioe.2013.12.010>
- Greacen, E.L., Sands, R. (1980). Compaction of forest soils. A review. *Australian Journal of Soil Research*, 18(2), 163–189. <http://doi.org/10.1111/j.1574-6941.2006.00175.x>
- Griscom, B.W., Adams, J., Ellis, P.W., Houghton, R.A., Lomax, G., Miteva, D.A., Fargione, J. (2017). Natural climate solutions. *Proceedings of the National Academy of Sciences*, 114(44), 11645–11650. <http://doi.org/10.1073/pnas.1710465114>
- Güereña, D., Lehmann, J., Hanley, K., Enders, A., Hyland, C., Riha, S. (2013). Nitrogen dynamics following field application of biochar in a temperate North American maize-based production system. *Plant and Soil*, 365, 239–254. <http://doi.org/10.1007/s11104-012-1383-4>
- Gundale, M.J., Nilsson, M.C., Pluchon, N., Wardle, D.A. (2016). The effect of biochar management on soil and plant community properties in a boreal forest. *GCB Bioenergy*, 8(4), 777–789. <http://doi.org/10.1111/gcbb.12274>
- Gurwick, N.P., Moore, L.A., Kelly, C., Elias, P. (2013). A systematic review of biochar research, with a focus on its stability in situ and its promise as a climate mitigation strategy. *PLoS ONE*, 8(9), 1–9. <http://doi.org/10.1371/journal.pone.0075932>
- Haider, G., Koyro, H.W., Azam, F., Steffens, D., Muller, C., Kammann, C. (2014). Biochar but not humic acid product amendment affected maize yields via improving plant-soil moisture relations. *Plant and Soil*, 395(1–2), 141–157. <http://doi.org/10.1007/s11104-014-2294-3>
- Haider, G., Steffens, D., Moser, G., Müller, C., Kammann, C.I. (2017). Biochar reduced nitrate leaching and improved soil moisture content without yield improvements in a four-year field study. *Agriculture, Ecosystems and Environment*, 237, 80–94. <http://doi.org/10.1016/j.agee.2016.12.019>
- Hardie, M., Clothier, B., Bound, S., Oliver, G., Close, D. (2014). Does biochar influence soil physical properties and soil water availability? *Plant and Soil*, 376, 347–361. <http://doi.org/10.1007/s11104-013-1980-x>
- Harter, J., Weigold, P., El-Hadidi, M., Huson, D.H., Kappler, A., Behrens, S. (2016). Soil biochar amendment shapes the composition of N₂O-reducing microbial communities. *Science of the Total Environment*, 562, 379–390. <http://doi.org/10.1016/j.scitotenv.2016.03.220>
- Hassink, J. (1997). The capacity of soils to preserve organic C and N by their association with silt and clay particles. *Soil Science Society of America Journal*, 61, 131–139.
- He L., Zhao X., Wang S. (2016). The effects of rice-straw biochar addition on nitrification activity and nitrous oxide emissions in two Oxisols. *Soil and Tillage Research*, 164, 52–62.
- Heneghan, L., Miller, S.P., Baer, S., Callahan, M.A., Montgomery, J., Pavao-Zuckerman, M., Richardson, S. (2008). Integrating soil ecological knowledge into restoration management. *Restoration Ecology*, 16(4), 608–617. <http://doi.org/10.1111/j.1526-100X.2008.00477.x>

- Herath, H.M.S.K., Camps-Arbestain, M., Hedley, M., Van Hale, R., Kaal, J. (2014). Fate of biochar in chemically- and physically-defined soil organic carbon pools. *Organic Geochemistry*, 73, 35–46. <http://doi.org/10.1016/j.orggeochem.2014.05.001>
- Hicke, J.A., Johnson, M.C., Hayes, J.L., Preisler, H.K. (2012). Effects of bark beetle-caused tree mortality on wildfire. *Forest Ecology and Management*, 271, 81–90. <http://doi.org/10.1016/j.foreco.2012.02.005>
- Huang, Z., Xu, Z., Chen, C. (2008). Effect of mulching on labile soil organic matter pools, microbial community functional diversity and nitrogen transformations in two hardwood plantations of subtropical Australia. *Applied Soil Ecology*, 40(2), 229–239. <http://doi.org/10.1016/j.apsoil.2008.04.009>
- Hudson, B.D. (1994). Soil organic matter and available water capacity. *Journal of Soil and Water Cons.*, 49(April), 189–194.
- Jaffé, R., Ding, Y., Niggemann, J., Vähätalo, A. V., Stubbins, A., Spencer, R. G. M., Dittmar, T. (2013). Global charcoal mobilization from soils via dissolution and riverine transport to the oceans, *Science*, 340, 345–348.
- Jardine, P.M., Weber, N.L., McCarthy, J.F. (1989). Mechanisms of dissolved organic carbon adsorption on soil. *Soil Science Society of America Journal*, 53, 1378–1385.
- Jeffery, S., Verheijen, F.G.A., Kammann, C., Abalos, D. (2016). Biochar effects on methane emissions from soils: A meta-analysis. *Soil Biology and Biochemistry*, 101, 251–258. <http://doi.org/10.1016/j.soilbio.2016.07.021>
- Jiang, X., Haddix, M.L., Cotrufo, M.F. (2016). Interactions between biochar and soil organic carbon decomposition: Effects of nitrogen and low molecular weight carbon compound addition. *Soil Biology and Biochemistry*, 100, 92–101. <http://doi.org/10.1016/j.soilbio.2016.05.020>
- Kang, Y., Khan, S., Ma, X. (2009). Climate change impacts on crop yield, crop water productivity and food security- A review. *Progress in Natural Science*, 19(12), 1665–1674. <http://doi.org/10.1016/j.pnsc.2009.08.001>
- Kangoma, E., Blango, M.M., Rashid-noah, A.B., Sherman-kamara, J., Moiwo, J.P., Kamara, A. (2017). Potential of biochar-amended soil to enhance crop productivity under deficit irrigation. *Irrigation and Drainage*, 614, 600–614. <http://doi.org/10.1002/ird.2138>
- Kardol, P., Wardle, D.A. (2010). How understanding aboveground-belowground linkages can assist restoration ecology. *Trends in Ecology and Evolution*, 25(11), 670–679. <http://doi.org/10.1016/j.tree.2010.09.001>
- Karhu, K., Mattila, T., Bergström, I., Regina, K. (2011). Biochar addition to agricultural soil increased CH₄ uptake and water holding capacity- Results from a short-term pilot field study. *Agriculture, Ecosystems and Environment*, 140(1–2), 309–313. <http://doi.org/10.1016/j.agee.2010.12.005>
- Kattge, J., Boenisch, G. (2018). TRY Plant Trait Database: Data set. Available on-line [<https://www.try-db.org>] from the Max Planck Institute for Biogeochemistry, Jena, Germany.
- Kloss, S., Zehetner, F., Dellantonio, A., Hamid, R., Ottner, F., Liedtke, V., Soja, G. (2012). Characterization of slow pyrolysis biochars: Effects of feedstocks and pyrolysis temperature on biochar properties.

- Journal of Environmental Quality*, 41, 990–1000. <http://doi.org/10.2134/jeq2011.0070>
- Knicker, H. (2011). Pyrogenic organic matter in soil: Its origin and occurrence, its chemistry and survival in soil environments. *Quaternary International*, 243(2), 251–263. <http://doi.org/10.1016/j.quaint.2011.02.037>
- Kuzyakov, Y., Bogomolova, I., Glaser, B. (2014). Biochar stability in soil: Decomposition during eight years and transformation as assessed by compound-specific 14C analysis. *Soil Biology and Biochemistry*, 70, 229–236. <http://doi.org/10.1016/j.soilbio.2013.12.021>
- Laiho, R., Prescott, C.E. (2004). Decay and nutrient dynamics of coarse woody debris in northern coniferous forests: A synthesis. *Canadian Journal of Forest Research*, 34(4), 763–777. <http://doi.org/10.1139/x03-241>
- Lashermes, G., Nicolardot, B., Parnaudeau, V., Thuriès, L., Chaussod, R., Guillotin, M. L., Houot, S. (2010). Typology of exogenous organic matters based on chemical and biochemical composition to predict potential nitrogen mineralization. *Bioresource Technology*, 101(1), 157–164. <http://doi.org/10.1016/j.biortech.2009.08.025>
- Lehmann, J. (2007). Bio-energy in the black. *Frontiers in Ecology and the Environment*, 5(7), 381–387. [http://doi.org/10.1890/1540-9295\(2007\)5\[381:BITB\]2.0.CO;2](http://doi.org/10.1890/1540-9295(2007)5[381:BITB]2.0.CO;2)
- Lehmann, J., Gaunt, J., Rondon, M. (2006). Bio-char sequestration in terrestrial ecosystems- A review. *Mitigation and Adaptation Strategies for Global Change*, 11(2), 403–427. <http://doi.org/10.1007/s11027-005-9006-5>
- Lehmann, J., Kleber, M. (2015). Perspective The contentious nature of soil organic matter. *Nature*, 1–9. <http://doi.org/10.1038/nature16069>
- Li, Y., Hu, S., Chen, J., Müller, K., Li, Y., Fu, W., Wang, H. (2018). Effects of biochar application in forest ecosystems on soil properties and greenhouse gas emissions: A review. *Journal of Soils and Sediments*, 18, 546–563.
- Lian, F., Xing, B. (2017). Black carbon (biochar) in water/soil environments: Molecular structure, sorption, stability, and potential risk. *Environmental Science & Technology*, 51, 13517–13532. <http://doi.org/10.1021/acs.est.7b02528>
- Linn, D.M., Doran, J.W. (1984). Effect of water-filled pore space on carbon dioxide and nitrous oxide production in tilled and nontilled soils. *Soil Science Society of America Journal*, 48, 1267–1272. <http://doi.org/10.2136/sssaj1984.03615995004800060013x>
- Liu, S., Zhang, Y., Zong, Y., Hu, Z. (2016). Response of soil carbon dioxide fluxes, soil organic carbon and microbial biomass carbon to biochar amendment: A meta-analysis. *Global Change Biology Bioenergy*, 8, 392–406. <http://doi.org/10.1111/gcbb.12265>
- Liu, Z., Dugan, B., Masiello, C.A., Gonnermann, H.M. (2017). Biochar particle size, shape, and porosity act together to influence soil water properties. *PLoS ONE* 12(6), 1–20.
- Lorenz, K., Lal, R. (2014). Biochar application to soil for climate change mitigation by soil organic carbon sequestration. *Journal of Plant Nutrition and Soil Science*, 177(5), 651–670. <http://doi.org/10.1002/jpln.201400058>

- Lu W., Ding W., Zhang J. (2014). Biochar suppressed the decomposition of organic carbon in a cultivated sandy loam soil: A negative priming effect. *Soil Biology and Biochemistry*, 76, 12–21.
- MacDonald, L.H., Larsen, I.J. (2009). Runoff and erosion from wildfires and roads: Effects and mitigation, ch 9. *Land Restoration to Combat Desertification: Innovative Approaches, Quality Control and Project Evaluation*, (Dissmeyer 2000), 145–167.
- Madej, M.A. (2001). Erosion and sediment delivery following removal of forest roads. *Earth Surface Processes and Landforms*, 26(2), 175–190. [http://doi.org/10.1002/1096-9837\(200102\)26:2<175::AID-ESP174>3.0.CO;2-N](http://doi.org/10.1002/1096-9837(200102)26:2<175::AID-ESP174>3.0.CO;2-N)
- Major, J., Lehmann, J., Rondon, M., Goodale, C. (2010). Fate of soil-applied black carbon: Downward migration, leaching and soil respiration. *Global Change Biology*, 16(4), 1366–1379. <http://doi.org/10.1111/j.1365-2486.2009.02044.x>
- Malamoud K., McBratney A.B., Minasny B., Field D.J. (2009). Modelling how carbon affects soil structure. *Geoderma*, 149, 19-26.
- Mandal, S., Sarkar, B., Bolan, N., Novak, J., Ok, Y.S., van Zwieten, L., Naidu, R. (2016). Designing advanced biochar products for maximizing greenhouse gas mitigation potential. *Critical Reviews in Environmental Science and Technology*, 46(17), 1367–1401. <http://doi.org/10.1080/10643389.2016.1239975>
- Mayes, M.A., Brandt, C.C., Phillips, J.R., Jardine, P.M. (2012). Relation between soil order and sorption of dissolved organic carbon in temperate subsoils. *Soil Science Society of America Journal*, 76, 1027–1037. <http://doi.org/10.2136/sssaj>
- Megahan, W.F., King, J. G., Megahan, W. F., & King, J. G. (2004). Erosion, sedimentation, and cumulative effects in the Northern Rocky Mountains. *Ice, George G.; Stednick, John D., Eds. A Century of Forest and Wildland Watershed Lessons*, 201–222.
- Mezerette C., Girard P. (1991). Environmental aspects of gaseous emissions from wood carbonisation and pyrolysis processes. In: Bridgwater A.V., Grassi G. (eds.) *Biomass Pyrolysis Liquids Upgrading and Utilization*. Springer, Dordrecht
- Mia S., Dijkstra F.A., Singh B. (2016) Long-term aging of biochar: A molecular understanding with agricultural and environmental implications. *Advances in Agronomy*, 141, 1-51.
- Miller, E.M., Seastedt, T.R. (2009). Impacts of woodchip amendments and soil nutrient availability on patterns of understory vegetation establishment following thinning of a ponderosa pine forest. *Forest Ecology and Management*, 258(3), 263–272.
- Moorhead, D.L., Lashermes, G., Sinsabaugh, R.L., Weintraub, M.N. (2013). Calculating co-metabolic costs of lignin decay and their impacts on carbon use efficiency. *Soil Biology and Biochemistry*, 66, 17–19. <http://doi.org/10.1016/j.soilbio.2013.06.016>
- Mosier, A.R., Duxbury, J.M., Freney, J.R., Heinemeyer, O., Minami, K., Johnson, D.E. (1998). Mitigating agricultural emissions of methane. *Climatic Change*, 40, 39–80.
- Mukherjee, A., Lal, R., Zimmerman, A.R. (2014). Effects of biochar and other amendments on the physical properties and greenhouse gas emissions of an artificially degraded soil. *Science of the Total Environment*, 487(1), 26–36. <http://doi.org/10.1016/j.scitotenv.2014.03.141>

- Myhre, G., Shindell, D., Breon, F.M. (2013) Anthropogenic and natural radiative forcing, in: Stocker, T.F., Qin, D., Plattner, G.K., *et al.* (Eds.) *Climate Change 2013: The Physical Science Basis. Contribution of Working Group I to the Fifth Assessment Report of the Intergovernmental Panel on Climate Change*. Cambridge University Press, Cambridge, UK and New York, NY, USA.
- Natural Resources Conservation Service (NRCS), USDA. Web soil survey. Retrieved from <https://websoilsurvey.sc.egov.usda.gov/>. Accessed 12/28/2017.
- Neves, D., Thunman, H., Matos, A., Tarelho, L., Gómez-Barea, A. (2011). Characterization and prediction of biomass pyrolysis products. *Progress in Energy and Combustion Science*, 37(5), 611–630. <http://doi.org/10.1016/j.pecs.2011.01.001>
- Nguyen, T.T.N., Xu, C.Y., Tahmasbian, I., Che, R., Xu, Z., Zhou, X., Bai, S.H. (2017). Effects of biochar on soil available inorganic nitrogen: A review and meta-analysis. *Geoderma*, 288, 79–96. <http://doi.org/10.1016/j.geoderma.2016.11.004>
- Noss, R.F., Franklin, J.F., Baker, W.L., Schoennagel, T., Moyle, B., Noss, R.F., Moyle, P.B. (2006). Managing fire-prone forests in the western United States. *Frontiers in Ecology and the Environment*, 4(9), 481–487.
- Obia, A., Børresen, T., Martinsen, V., Cornelissen, G., Mulder, J. (2017). Vertical and lateral transport of biochar in light-textured tropical soils. *Soil and Tillage Research*, 165, 34–40. <http://doi.org/10.1016/j.still.2016.07.016>
- Obia, A., Cornelissen, G., Mulder, J., Dörsch, P. (2015). Effect of soil pH increase by biochar on NO, N₂O and N₂ production during denitrification in acid soils. *PLoS ONE*, 10(9), 1–19. <http://doi.org/10.5061/dryad.m8q78>
- Ocko, I.B., Hamburg, S.P., Jacob, D.J., Keith, D.W., Keohane, N.O., Oppenheimer, M., Pacala, S.W. (2017). Unmask temporal trade-offs in climate policy debates. *Science*, 356(6337), 492–493.
- Olson, R.J., Scurlock, J.M.O., Prince, S.D., Zheng, D.L., Johnson, K.R. (eds.). (2013). NPP Multi-Biome: NPP and Driver Data for Ecosystem Model-Data Intercomparison, R2. Data set. Available on-line [<http://daac.ornl.gov>] from Oak Ridge National Laboratory Distributed Active Archive Center, Oak Ridge, Tennessee, USA. doi:10.3334/ORNLDAAC/615
- Omondi, M.O., Xia, X., Nahayo, A., Liu, X., Korai, P.K., Pan, G. (2016). Quantification of biochar effects on soil hydrological properties using meta-analysis of literature data. *Geoderma*, 274, 28–34. <http://doi.org/10.1016/j.geoderma.2016.03.029>
- Pansu M., Gautheyrou J. (2006) Handbook of soil analysis – Mineralogical, organic and inorganic methods. Springer-Verlag, Berlin.
- Paris, O., Zollfrank, C., Zickler, G.A. (2005). Decomposition and carbonisation of wood biopolymers - A microstructural study of softwood pyrolysis. *Carbon*, 43(1), 53–66. <http://doi.org/10.1016/j.carbon.2004.08.034>
- Parkin, T.B., Venterea, R.T. (2010). Chamber-based trace gas flux measurements. *USDA-ARS GRACEnet Project Protocols*, 1–39.
- Paschke, M.W., Deleo, C., Redente, E.F. (2000). Revegetation of roadcut slopes in Mesa Verde National Park, U.S.A. *Restoration Ecology*, 8(3), 276–282.
- Paustian, K., Lehmann, J., Ogle, S., Reay, D., Robertson, G.P. (2016). Climate-smart soils. *Nature*, 1, 49–

57. <http://doi.org/10.1038/nature17174>

Payero, J.O., Tarkalson, D.D., Irmak, S., Davison, D., Petersen, J.L. (2009). Effect of timing of a deficit-irrigation allocation on corn evapotranspiration, yield, water use efficiency and dry mass. *Agricultural Water Management*, 96, 1387–1397. <http://doi.org/10.1016/j.agwat.2009.03.022>

Perry, L.G., Redente, E.F., Perry, L.G., Blumenthal, D.M., Paschke, M.W., Redente, E.F. (2010). Immobilizing nitrogen to control plant invasion Immobilizing nitrogen to control plant invasion, *Oecologia*, 163, 13-24. <http://doi.org/10.1007/s00442-010-1580-x>

Pfister, M. Saha, S. (2017) Effects of biochar and fertilizer management on sunflower (*Helianthus annuus* L.) feedstock and soil properties. *Archives of Agronomy and Soil Science*, 63(5), 651-662.

Pignatello, J.J., Kwon, S., Lu, Y. (2006). Effect of natural organic substances on the surface and adsorptive properties of environmental black carbon (char): Attenuation of surface activity by humic and fulvic acids. *Environmental Science and Technology*, 40, 7757–7763.

Powlson, D.S., Goulding, K.W.T., Willison, T.W., Webster, C.P., Hutsch, B.W. (1997). The effect of agriculture on methane oxidation in soil. *Nutrient Cycling in Agroecosystems*, 49, 59–70. <http://doi.org/10.1098/rsta.1995.0036>

Preston, C.M., Schmidt, M.W.I. (2006). Black (pyrogenic) carbon: a synthesis of current knowledge and uncertainties with special consideration of boreal regions. *Biogeosciences*, 3(4), 397–420. <http://doi.org/10.5194/bg-3-397-2006>

Prince, S.D., Haskett, J., Steininger, M., Strand, H., Wright, R. (2013). NPP Cropland: Gridded Data for the Central USA, 1982-1996, R1. Data set. Available on-line [<http://daac.ornl.gov>] from the Oak Ridge National Laboratory Distributed Active Archive Center, Oak Ridge, Tennessee, USAdoi:10.3334/ORNLDAAC/612

Qayyum, M.F., Steffens, D., Reisenauer, H.P., Schubert, S. (2014). Biochars influence differential distribution and chemical composition of soil organic matter. *Plant Soil Environment*, 60(8), 337–343.

Quin, P., Joseph, S., Husson, O., Donne, S., Mitchell, D., Munroe, P., van Zwieten, L. (2015). Lowering N₂O emissions from soils using eucalypt biochar: The importance of redox reactions. *Sci Rep*, 5, 16773. <http://doi.org/10.1038/srep16773>

R Core Team (2016) R: A Language and Environment for Statistical Computing. R Foundation for Statistical Computing, Vienna, Austria.

Ramlow, M., Cotrufo, M.F. (2017). Woody biochar's greenhouse gas mitigation potential across fertilized and unfertilized agricultural soils and soil moisture regimes. *GCB Bioenergy*, 1–15. <http://doi.org/10.1111/gcbb.12474>

Ramlow, M., Foster, E.J., del Grosso, S. Cotrufo, M.F. *in review*. The limited benefits of biochar in limited irrigaiton maize. *Agriculture Ecosystems and the Environment*.

Ramlow, M., Rhoades, C.C., Cotrufo, M.F. *in press*. Promoting revegetation and soil carbon sequestration on decommissioned forest roads Colorado, USA: A comparative assessment of organic soil amendments. *Forest Ecology and Management*.

Rawls, W.J., Pachepsky, Y.A., Ritchie, J.C., Sobecki, T.M., Bloodworth, H. (2003). Effect of soil organic carbon on soil water retention. *Geoderma*, 116(1–2), 61–76. <http://doi.org/10.1016/S0016->

- Reid, L.M., Dunne, T. (1984). Sediment production from forest road surfaces. *Water Resources Research*, 20(11), 1753–1761.
- Reisser, M., Purves, R.S., Schmidt, M.W.I., Abiven, S. (2016). Pyrogenic carbon in soils : A literature-based inventory and a global estimation of its content in soil organic carbon and stocks. *Frontiers in Earth Science*, 4(80), 1–14. <http://doi.org/10.3389/feart.2016.00080>
- Rhoades, C.C., Battaglia, M.A., Rocca, M.E., Ryan, M.G. (2012). Short- and medium-term effects of fuel reduction mulch treatments on soil nitrogen availability in Colorado conifer forests. *Forest Ecology and Management*, 276, 231–238. <http://doi.org/10.1016/j.foreco.2012.03.028>
- Rhoades, C.C., Fornwalt, P.J., Paschke, M.W., Shanklin, A., Jonas, J.L. (2015). Recovery of small pile burn scars in conifer forests of the Colorado Front Range. *Forest Ecology and Management*, 347, 180–187. <http://doi.org/10.1016/j.foreco.2015.03.026>
- Rhoades, C.C., Minatre, K.L., Pierson, D.N., Fegell, T.S., Cotrufo, M.F., Kelly, E.F. (2017). Examining the potential of forest residue-based amendments for post-wildfire rehabilitation in Colorado, USA. *Scientifica*, 2017. <http://doi.org/10.1155/2017/4758316>
- Roberts K.G., Gloy B.A., Joseph S. *et al.* (2010). Life cycle assessment of biochar systems: Estimating the energetic, economic, and climate change potential. *Environmental Science and Technology*, 44, 827–833.
- Roberts, S.D., Harrington, C.A., Terry, T.A. (2005). Harvest residue and competing vegetation affect soil moisture, soil temperature, N availability, and Douglas-fir seedling growth. *Forest Ecology and Management*, 205(1–3), 333–350. <http://doi.org/10.1016/j.foreco.2004.10.036>
- Robertson, A.D., Ogle, S., Wallenstein, M.D., Lugato, E., Paustian, K., Cotrufo, M.F. *in review*. Unifying soil organic matter formation and persistence frameworks: the MEMS model. *Biogeosciences*.
- Robinson, C., Duinker, P.N., Beazley, K.F. (2010). A conceptual framework for understanding, assessing, and mitigating ecological effects of forest roads. *Environmental Reviews*, 18, 61–86. <http://doi.org/10.1139/A10-002>
- Rogelj, J., Elzen, M. Den, Höhne, N., Fransen, T., Fekete, H., Winkler, H., Sha, F. (2015). Paris Agreement climate proposals need a boost to keep warming well below 2 °C. *Nature*, 534, 631–639. <http://doi.org/10.1038/nature18307>
- Rogovska, N., Laird, D., Cruse, R., Fleming, P., Parkin, T., Meek, D. (2011). Impact of biochar on manure carbon stabilization and greenhouse gas emissions. *Soil Science Society of America Journal*, 75(3), 871–879. <http://doi.org/10.2136/sssaj2010.0270>
- Ronsse, F., Van Hecke, S., Dickinson, D., Prins, W. (2013). Production and characterization of slow pyrolysis biochar: Influence of feedstock type and pyrolysis conditions. *Global Change Biology Bioenergy*, 5, 104–115. <http://doi.org/10.1111/gcbb.12018>
- Saarnio, S., Heimonen, K., Kettunen, R. (2013). Biochar addition indirectly affects N₂O emissions via soil moisture and plant N uptake. *Soil Biology and Biochemistry*, 58, 99–106. <http://doi.org/10.1016/j.soilbio.2012.10.035>
- Sadasivam, B.Y., Reddy, K.R. (2014). Quantifying the effects of moisture content on transport and adsorption of methane through biochar in landfills. *Geotechnical Special Publication*, (241), 191–

- Sánchez-García, M., Roig, A., Sánchez-Monedero, M.A., Cayuela, M.L. (2014). Biochar increases soil N₂O emissions produced by nitrification-mediated pathways. *Frontiers in Environmental Science*, 2(25), 1–10. <http://doi.org/10.3389/fenvs.2014.00025>
- Saxton, K.E., Rawls, W.J. (2006). Soil water characteristic estimates by texture and organic matter for hydrologic solutions. *Soil Science Society of America Journal*, 70(5), 1569. <http://doi.org/10.2136/sssaj2005.0117>
- Scheer, C., Grace, P.R., Rowlings, D.W., Kimber, S., van Zwieten, L. (2011). Effect of biochar amendment on the soil-atmosphere exchange of greenhouse gases from an intensive subtropical pasture in northern New South Wales, Australia. *Plant and Soil*, 345(1), 47–58. <http://doi.org/10.1007/s11104-011-0759-1>
- Sharma, L.K., Bali, S.K. (2018). A review of methods to improve nitrogen use efficiency in agriculture. *Sustainability*, 10(51), 1–23. <http://doi.org/10.3390/su10010051>
- Sherrod L.A., Dunn G., Peterson G.A. (2002) Inorganic carbon analysis by modified pressure-calimeter method. *Soil Science Society of America Journal*, 66, 299–305.
- Shcherbak, I., Millar, N., Robertson, G.P. (2014). Global metaanalysis of the nonlinear response of soil nitrous oxide (N₂O) emissions to fertilizer nitrogen. *Proceedings of the National Academy of Sciences*, 111(25), 9199–9204. <http://doi.org/10.1073/pnas.1322434111>
- Silva, F.C., Borrego, C., Keizer, J.J., Amorim, J.H., Verheijen, F.G.A. (2015). Effects of moisture content on wind erosion thresholds of biochar. *Atmospheric Environment*, 123, 121–128. <http://doi.org/10.1016/j.atmosenv.2015.10.070>
- Singh, B.P., Cowie, A.L. (2014). Long-term influence of biochar on native organic carbon mineralisation in a low-carbon clayey soil. *Scientific Reports*, 4, 3687. <http://doi.org/10.1038/srep03687>
- Singh, B.P., Cowie, A.L., Smernik, R.J. (2012). Biochar carbon stability in a clayey soil as a function of feedstock and pyrolysis temperature. *Environmental Science and Technology*, 46(21), 11770–11778. <http://doi.org/10.1021/es302545b>
- Singh, N., Abiven, S., Torn, M.S., Schmidt, M.W.I. (2012). Fire-derived organic carbon in soil turns over on a centennial scale, 2847–2857. <http://doi.org/10.5194/bg-9-2847-2012>
- Six, J., Conant, R.T., Paul, E.A., Paustian, K. (2002). Stabilization mechanisms of soil organic matter: Implications for C-saturation of soils. *Plant and Soil*, 241(2), 155–176.
- Smith, P., Bustamante, M. (2014). *Agriculture, Forestry and Other Land Use (AFOLU). Climate Change 2014: Mitigation of Climate Change*. Cambridge, United Kingdom: Cambridge University Press.
- Smith, P. (2016). Soil carbon sequestration and biochar as negative emission technologies. *Global Change Biology*, 22(3), 1315–1324. <http://doi.org/10.1111/gcb.13178>
- Smith, M.J., Heal, O.W., Anderson, J.M. (1979). *Decomposition in Terrestrial Ecosystems*. Berkeley, CA: University of California Press.
- Smith, J., Smith, P. (2009). *Environmental Modeling: An Introduction*. Oxford, United Kingdom CA: Oxford University Press.

- Sohi, S. P., Krull, E., Lopez-Capel, E., Bol, R. (2010). A review of biochar and its use and function in soil. *Advances in Agronomy*, 105, 47–82. [http://doi.org/10.1016/S0065-2113\(10\)05002-9](http://doi.org/10.1016/S0065-2113(10)05002-9)
- Soinne, H., Hovi, J., Tammeorg, P., Turtola, E. (2014). Effect of biochar on phosphorus sorption and clay soil aggregate stability. *Geoderma*, 219–220, 162–167. <http://doi.org/10.1016/j.geoderma.2013.12.022>
- Soong, J.L., Cotrufo, M.F. (2015). Annual burning of a tallgrass prairie inhibits C and N cycling in soil, increasing recalcitrant pyrogenic organic matter storage while reducing N availability. *Global Change Biology*, 21, 2321–2333. <http://doi.org/10.1111/gcb.12832>
- Sosa-Pérez, G., MacDonald, L.H. (2017). Reductions in road sediment production and road-stream connectivity from two decommissioning treatments. *Forest Ecology and Management*, 398, 116–129. <http://doi.org/10.1016/j.foreco.2017.04.031>
- Spokas, K.A., Novak, J.M., Masiello, C.A., Johnson, M.G., Colosky, E.C., Ippolito, J.A., Trigo, C. (2014). Physical disintegration of biochar: An overlooked process. *Environmental Science and Technology Letters*, 1(8), 326–332. <http://doi.org/10.1021/ez500199t>
- Spokas, K.A. (2010). Review of the stability of biochar in soils: predictability of O:C molar ratios. *Carbon Management*, 1(2), 289–303. <http://doi.org/10.4155/cmt.10.32>
- Spokas, K.A., Reicosky, D.C. (2009). Impacts of sixteen different biochars on soil greenhouse gas production. *Annals of Environmental Science*, 3(612), 179–193.
- Stanford, G., Smith, S.J. (1972). Nitrogen mineralization potentials of soils. *Soil Science Society of America Journal*, 36(3), 465–472. <http://doi.org/10.2136/sssaj1972.03615995003600030049x>
- Stewart, C.E., Zheng, J., Botte, J., Cotrufo, M.F. (2013). Co-generated fast pyrolysis biochar mitigates greenhouse gas emissions and increases carbon sequestration in temperate soils. *GCB Bioenergy*, 5(2), 153–164. <http://doi.org/10.1111/gcbb.12001>
- Stewart, C.E., Paustian, K., Conant, R.T., Plante, A.F., Six, J. (2007). Soil carbon saturation: Concept, evidence and evaluation. *Biogeochemistry*, 86(1), 19–31. <http://doi.org/10.1007/s10533-007-9140-0>
- Sudar, R.A., Saxton, K.E., Spomer, R.G. (1981). A predictive model of water stress in corn and soybeans. *Transactions of the ASAE*, 97–102.
- Suliman, W., Harsh, J.B., Abu-lail, N.I., Fortuna, A., Dallmeyer, I., Garcia-Pérez, M. (2017). The role of biochar porosity and surface functionality in augmenting hydrologic properties of a sandy soil. *Science of the Total Environment*, 574, 139–147. <http://doi.org/10.1016/j.scitotenv.2016.09.025>
- Sun, H., Brewer, C.E., Masiello, C.A., Zygourakis, K. (2015). Nutrient transport in soils amended with biochar: A transient model with two stationary phases and intraparticle diffusion. *Industrial and Engineering Chemistry Research*, 54(16), 4123–4135. <http://doi.org/10.1021/ie503893t>
- Sun, H., Hockaday, W.C., Masiello, C.A., Zygourakis, K. (2012). Multiple controls on the chemical and physical structure of biochars. *Industrial and Engineering Chemistry Research*, 51(9), 3587–3597. <http://doi.org/10.1021/ie201309r>
- Sun, Z., Moldrup, P., Elsgaard, L., Arthur, E., Bruun, E.W., Hauggaard-Nielsen, H., de Jonge, L.W. (2013). Direct and indirect short-term effects of biochar on physical characteristics of an arable sandy

- loam. *Soil Science*, 178(9), 465–473. <http://doi.org/10.1097/SS.0000000000000010>
- Swift, L.W. (1984). Gravel and grass surfacing reduces soil loss from mountain roads. *Forest Science*, 30(30), 657–670.
- Switalski, T.A., Bissonette, J.A., DeLuca, T.H., Luce, C.H., Madej, M.A. (2004). Benefits and impacts of road removal. *Frontiers in Ecology and the Environment*, 2(1), 21–28. [http://doi.org/10.1890/1540-9295\(2004\)002\[0021:BAIORR\]2.0.CO;2](http://doi.org/10.1890/1540-9295(2004)002[0021:BAIORR]2.0.CO;2)
- Tammeorg, P., Simojoki, A., Mäkelä, P., Stoddard, F.L., Alakukku, L., Helenius, J. (2014). Biochar application to a fertile sandy clay loam in boreal conditions: Effects on soil properties and yield formation of wheat, turnip rape and faba bean. *Plant and Soil*, 374, 89–107. <http://doi.org/10.1007/s11104-013-1851-5>
- Taylor, B.R., Parsons, P., Parsons, W.F.J. (1989). Nitrogen and lignin content as predictors of litter decay rates: A microcosm test. *Ecological Society of America*, 70(1), 97–104.
- Thomazini, A., Spokas, K., Hall, K., Ippolito, J., Lentz, R., Novak, J. (2015). GHG impacts of biochar: Predictability for the same biochar. *Agriculture, Ecosystems and Environment*, 207, 183–191. <http://doi.org/10.1016/j.agee.2015.04.012>
- Throop, H.L., Archer, S.R., Monger, H.C., Waltman, S. (2012). When bulk density methods matter : Implications for estimating soil organic carbon pools in rocky soils. *Journal of Arid Environments*, 77, 66–71. <http://doi.org/10.1016/j.jaridenv.2011.08.020>
- Trumbore, S., Schiff, S., Aravena, R., Elgood, R. (1992). Sources and transformation of dissolved organic carbon in the Harp Lake forested catchment: The role of soils. *Radiocarbon*, 34(3), 626-635. doi:10.1017/S0033822200063918
- Trombulak, S.C., Frissell, CA. (2001). Review of ecological effects of roads on terrestrial and aquatic communities. *Conservation Biology*, 14(1), 18–30. <http://doi.org/10.1046/j.1523-1739.2000.99084.x>
- Turner, P.A., Griffis, T.J., Mulla, D.J., Baker, J.M., Venterea, R.T. (2016). A geostatistical approach to identify and mitigate agricultural nitrous oxide emission hotspots. *Science of the Total Environment*, 572, 442–449. <http://doi.org/10.1016/j.scitotenv.2016.08.094>
- van Zwieten, L., Singh, B.P., Kimber, S.W.L., Murphy, D.V., Macdonald, L.M., Rust, J., Morris, S. (2014). An incubation study investigating the mechanisms that impact N₂O flux from soil following biochar application. *Agriculture, Ecosystems and Environment*, 191, 53–62. <http://doi.org/10.1016/j.agee.2014.02.030>
- van Zwieten, L., Kimber, S., Morris, S., Downie, A., Berger, E., Rust, J., Scheer, C. (2010). Influence of biochars on flux of N₂O and CO₂ from Ferrosol. *Australian Journal of Soil Research*, 48(6–7), 555–568. <http://doi.org/10.1071/SR10004>
- Vasquez, E., Sheley, R., Svejcar, T. (2008). Creating invasion resistant soils via nitrogen management, *Invasive Plant Science and Management*, 1, 304–314. <http://doi.org/10.1614/IPSM-07-059.1>
- Veihmeyer, F.J., Hendrickson, A.H. (1949). Methods of measuring field capacity and permanent wilting percentage of soils. *Soil Sci.* 68 (1), 75–94.
- Venner, K.H., Prescott, C.E., Preston, C.M. (2009). Leaching of nitrogen and phenolics from wood waste and co-composts used for road rrehabilitation. *Journal of Environment Quality*, 38(1), 281.

<http://doi.org/10.2134/jeq2007.0595>

- Venterea, R.T., Halvorson, A.D., Kitchen, N., Liebig, M.A., Cavigelli, M.A., Del Grosso, S.J., Collins, H. (2012). Challenges and opportunities for mitigating nitrous oxide emissions from fertilized cropping systems. *Frontiers in Ecology and the Environment*, 10(10), 562–570. <http://doi.org/10.1890/120062>
- Verhoeven, E., Pereira, P., Decock, C., Suddick, E., Angst, T., Six, J. (2017). Toward a Better Assessment of Biochar– Nitrous Oxide Mitigation Potential at the Field Scale. *Journal of Environment Quality*, 46, 237–246. <http://doi.org/10.2134/jeq2016.10.0396>
- Viall, E. M., Gentry, L. F., Hopkins, D. G., Ganguli, A. C., & Stahl, P. (2014). Legacy effects of oil road reclamation on soil biology and plant community composition. *Restoration Ecology*, 22(5), 625–632. <http://doi.org/10.1111/rec.12115>
- Wada, Y., Bierkens, M.F.P. (2014). Sustainability of global water use: Past reconstruction and future projections. <http://doi.org/10.1088/1748-9326/9/10/104003>
- Wang, J., Xiong, Z., Kuzyakov, Y. (2016). Biochar stability in soil: Meta-analysis of decomposition and priming effects. *GCB Bioenergy*, 8(3), 512–523. <http://doi.org/10.1111/gcbb.12266>
- Wang, Z., Zong, H., Zheng, H., Liu, G., Chen, L., Xing, B. (2015). Reduced nitrification and abundance of ammonia-oxidizing bacteria in acidic soil amended with biochar. *Chemosphere*, 138(3), 576–583. <http://doi.org/10.1016/j.chemosphere.2015.06.084>
- Wells, N.S., Baggs, E.M. (2014). Char amendments impact soil nitrous oxide production during ammonia oxidation. *Soil Science Society of America Journal*, 78(5), 1656–1660. <http://doi.org/10.2136/sssaj2013.11.0468n>
- Whitman, T., Scholz, S.M., Lehmann, J. (2014). Biochar projects for mitigating climate change: An investigation of critical methodology issues for carbon accounting Biochar projects for mitigating climate change : an investigation of critical methodology issues for carbon accounting, 3004. <http://doi.org/10.4155/cmt.10.4>
- Wiedemeier, D.B., Abiven, S., Hockaday, W.C., Keiluweit, M., Kleber, M., Masiello, C.A., Schmidt, M.W.I. (2015). Aromaticity and degree of aromatic condensation of char. *Organic Geochemistry*, 78, 135–143. <http://doi.org/10.1016/j.orggeochem.2014.10.002>
- Woolf, D., Amonette, J.E., Street-Perrott, F.A., Lehmann, J., Joseph, S. (2010). Sustainable biochar to mitigate global climate change. *Nature Communications*, 1(56), 1–19. <http://doi.org/10.1038/ncomms1053>
- You, C., Wu, F., Gan, Y., Yang, W., Hu, Z., Xu, Z., Ni, X. (2017). Grass and forbs respond differently to nitrogen addition: A meta-analysis of global grassland ecosystems. *Scientific Reports*, 7(1), 1–10. <http://doi.org/10.1038/s41598-017-01728-x>
- Yu, L., Tang, J., Zhang, R., Wu, Q., Gong, M. (2013). Effects of biochar application on soil methane emission at different soil moisture levels. *Biology and Fertility of Soils*, 49, 119–128. <http://doi.org/10.1007/s00374-012-0703-4>
- Zeng, Z., Zhang, S., Li, T., Zhao, F., He, Z., Zhao, H., Rafiq, M.T. (2013). Sorption of ammonium and phosphate from aqueous solution by biochar derived from phytoremediation plants. *Journal of Zhejiang University. Science. B*, 14(12), 1152–61. <http://doi.org/10.1631/jzus.B1300102>

- Zhang, D., Hui, D., Luo, Y., Zhou, G. (2018). Rates of litter decomposition in terrestrial ecosystems: Global patterns and controlling factors, *1*(2), 85–93. <http://doi.org/10.1093/jpe/rtn002>
- Zhang, A., Bian, R., Hussain, Q., Li, L., Pan, G., Zheng, J., Zheng, J. (2013). Change in net global warming potential of a rice-wheat cropping system with biochar soil amendment in a rice paddy from China. *Agriculture, Ecosystems and Environment*, *173*, 37–45. <http://doi.org/10.1016/j.agee.2013.04.001>
- Zhang, A., Liu, Y., Pan, G., Hussain, Q., Li, L., Zheng, J., Zhang, X. (2012). Effect of biochar amendment on maize yield and greenhouse gas emissions from a soil organic carbon poor calcareous loamy soil from Central China Plain. *Plant and Soil*, *351*(1–2), 263–275. <http://doi.org/10.1007/s11104-011-0957-x>
- Zheng, J., Stewart, C. E., Cotrufo, M. F. (2012). Biochar and nitrogen fertilizer alters soil nitrogen dynamics and greenhouse gas fluxes from two temperate soils. *Journal of Environmental Quality*, *41*(5), 1361–70. <http://doi.org/10.2134/jeq2012.0019>
- Zhou, M., Butterbach-Bahl, K. (2014). Assessment of nitrate leaching loss on a yield-scaled basis from maize and wheat cropping systems. *Plant and Soil*, *374*, 977–991. <http://doi.org/10.1007/s11104-013-1876-9>
- Zimmerman A.R., Gao B. (2013). The stability of biochar in the environment. In: *Biochar and Soil Biota* (eds Ladygina N., Rineau F.). CRC Press, Boca Raton, FL.

APPENDICES

Appendix 1. Chapter 2 Supplementary Information

Table A1: Mean value (avg) and standard error (SE) of soil properties for each treatment sampled at the end of the 60-day incubation, including soil organic carbon (SOC), total nitrogen (TN), and soil pH.

Soil	Fertilizer	Amendment	SOC (%C)		TN (%N)		pH (pH)	
			avg	SE	avg	SE	avg	SE
CO	Unfertilized	Control	0.79%	0.01%	0.13%	0.00%	8.36	0.08
CO	Unfertilized	Biochar	2.61%	0.17%	0.13%	0.00%	8.53	0.10
CO	Fertilized	Control	0.79%	0.01%	0.14%	0.00%	8.09	0.02
CO	Fertilized	Biochar	2.45%	0.16%	0.15%	0.00%	8.14	0.03
ID	Unfertilized	Control	5.13%	0.06%	0.50%	0.01%	5.21	0.02
ID	Unfertilized	Biochar	7.70%	0.21%	0.49%	0.01%	5.29	0.02
ID	Fertilized	Control	4.95%	0.16%	0.50%	0.02%	4.66	0.01
ID	Fertilized	Biochar	7.42%	0.66%	0.49%	0.01%	4.75	0.01
ND	Unfertilized	Control	2.30%	0.01%	0.24%	0.00%	7.16	0.08
ND	Unfertilized	Biochar	5.46%	0.77%	0.25%	0.00%	7.36	0.02
ND	Fertilized	Control	2.40%	0.08%	0.26%	0.00%	6.69	0.02
ND	Fertilized	Biochar	5.08%	0.29%	0.27%	0.01%	6.73	0.04
TX	Unfertilized	Control	0.87%	0.00%	0.11%	0.00%	7.99	0.05
TX	Unfertilized	Biochar	3.00%	0.16%	0.11%	0.00%	8.11	0.03
TX	Fertilized	Control	0.88%	0.00%	0.12%	0.00%	7.60	0.04
TX	Fertilized	Biochar	2.93%	0.11%	0.12%	0.01%	7.55	0.04

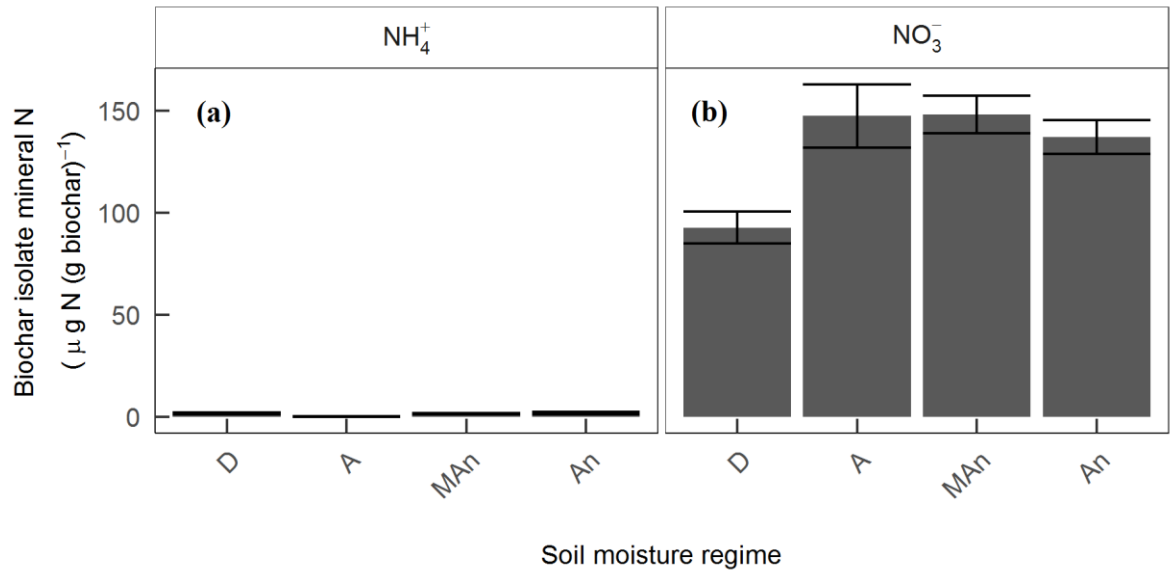


Fig. A1: Biochar isolate mineral nitrogen (N) from the biochar soils separated by mineral N type (ammonium (NH_4^+), Fig. A1a; nitrate (NO_3^-), Fig. A1b) across the four soil moisture regimes (dry (D), aerobic (A), moderately anaerobic (MAAn), anaerobic (AN); see text for details) measured at the end of the 28-day, fertilized, CO soil incubation (E2). Error bars display standard error.

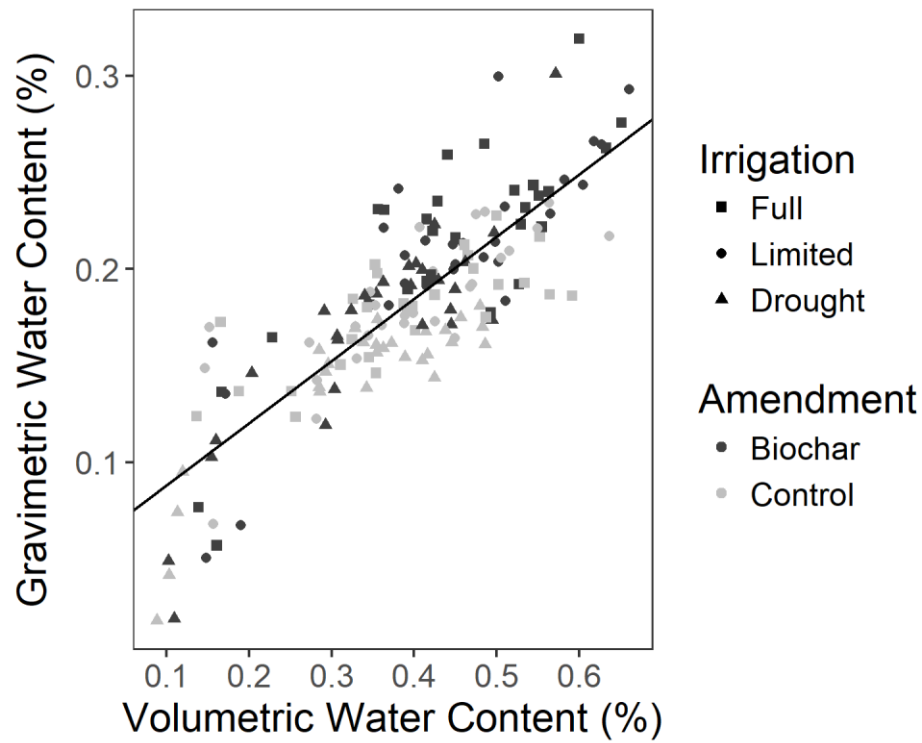


Fig. A2: Calibration of gravimetric water content measured from soil samples against volumetric water content measured on the same soils in the field using a TDR probe

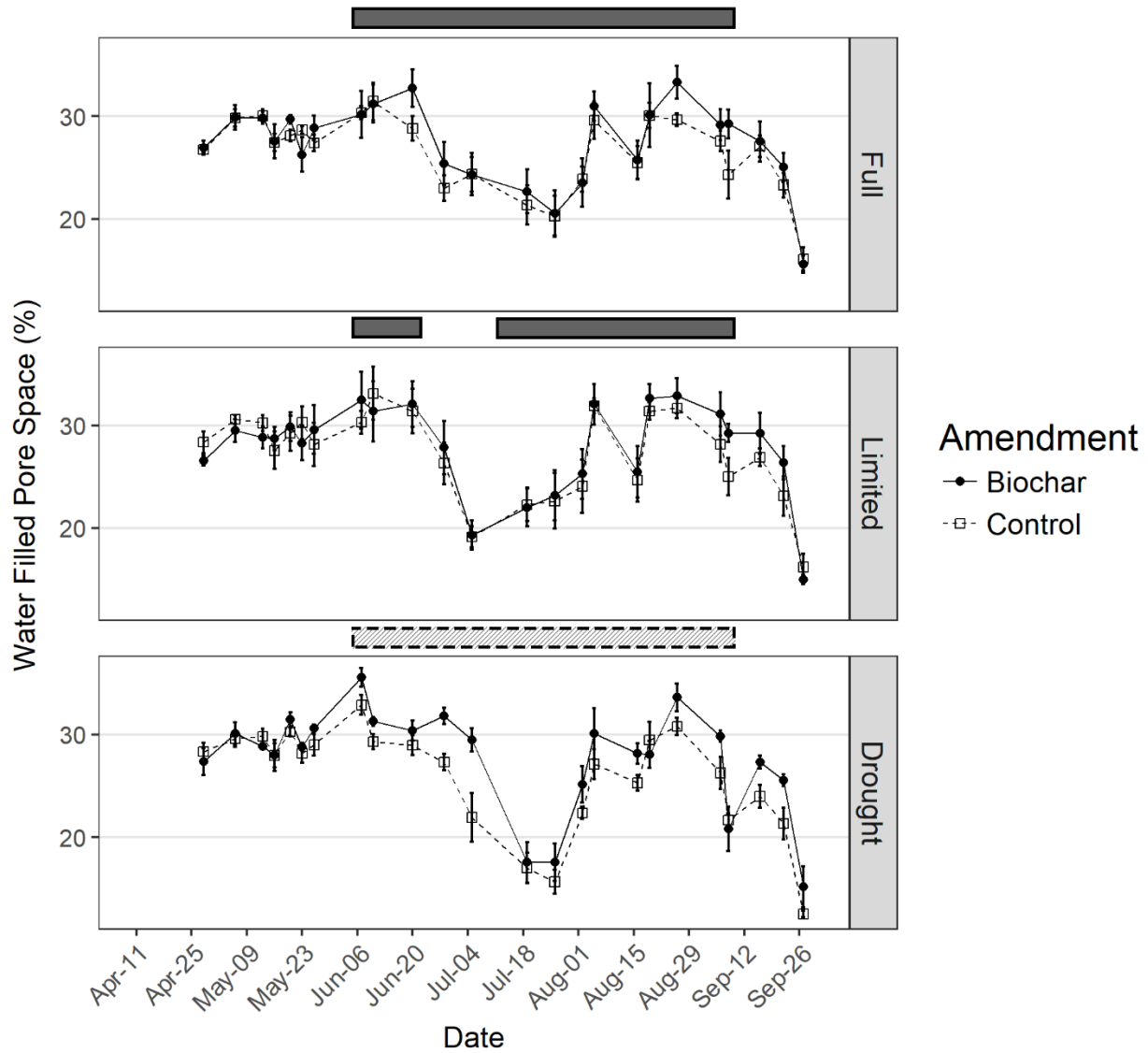


Fig. A3: Water-filled pore space dynamics throughout the 2016 growing season in the biochar (closed circles) and control (open squares) treatments, across the three irrigation regimes (Full, Limited and Drought). Bars above the plots represent the period of weekly irrigation water application with darker shading representing conventional irrigation rates and lighter shading indicating half such rates. Data are presented as means ± 1 SE (n=4).

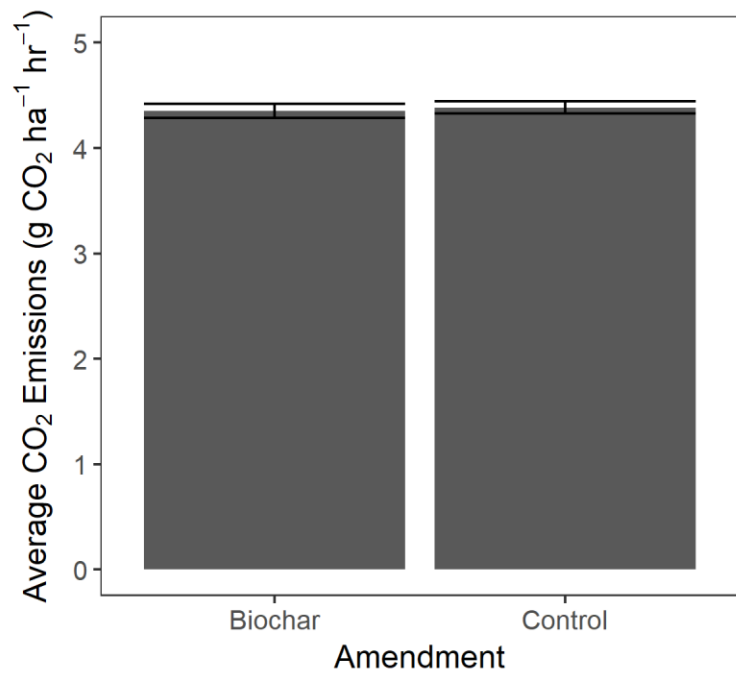


Fig. A4: Average carbon dioxide fluxes from sampled using automated chambers and cavity ring down spectroscopy in one plot per treatments throughout the 2016 growing season in the biochar and control soils averaged across the growing season and irrigation treatments.

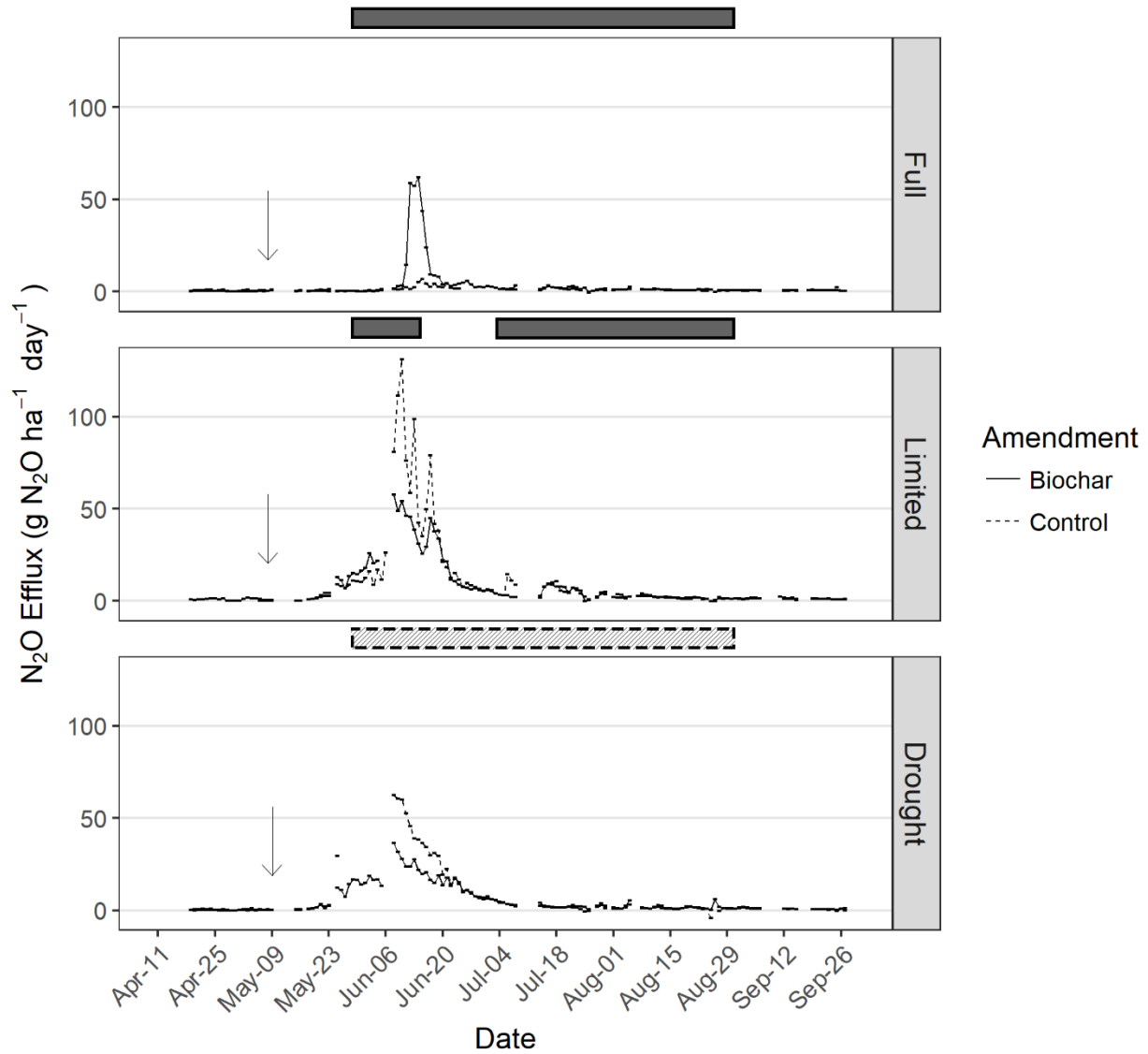


Fig. A5: Nitrous oxide fluxes sampled using automated chambers and cavity ring down spectroscopy in one plot per treatments throughout the 2016 growing season in the biochar (solid line) and control (dotted line) treatments, across the three irrigation regimes (Full, Limited and Drought). Arrows indicate fertilizer application, while bars above the plots represent the period of weekly irrigation water application with darker shading representing conventional irrigation rates and lighter shading indicating half such rates.

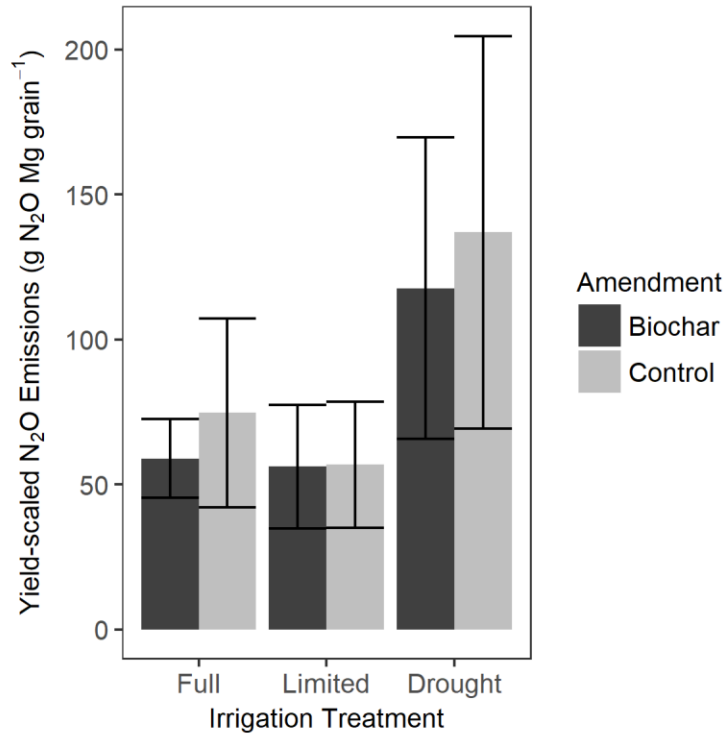


Fig. A6: Yield-scaled cumulative nitrous oxide emissions interpolated over the growing season using static chamber data in the biochar (black) and control (light grey) treatments, across the three irrigation regimes (Full, Limited and Drought). Data are presented as means \pm 1 SE (n=4).

Appendix 3. Chapter 4 Supplementary Information

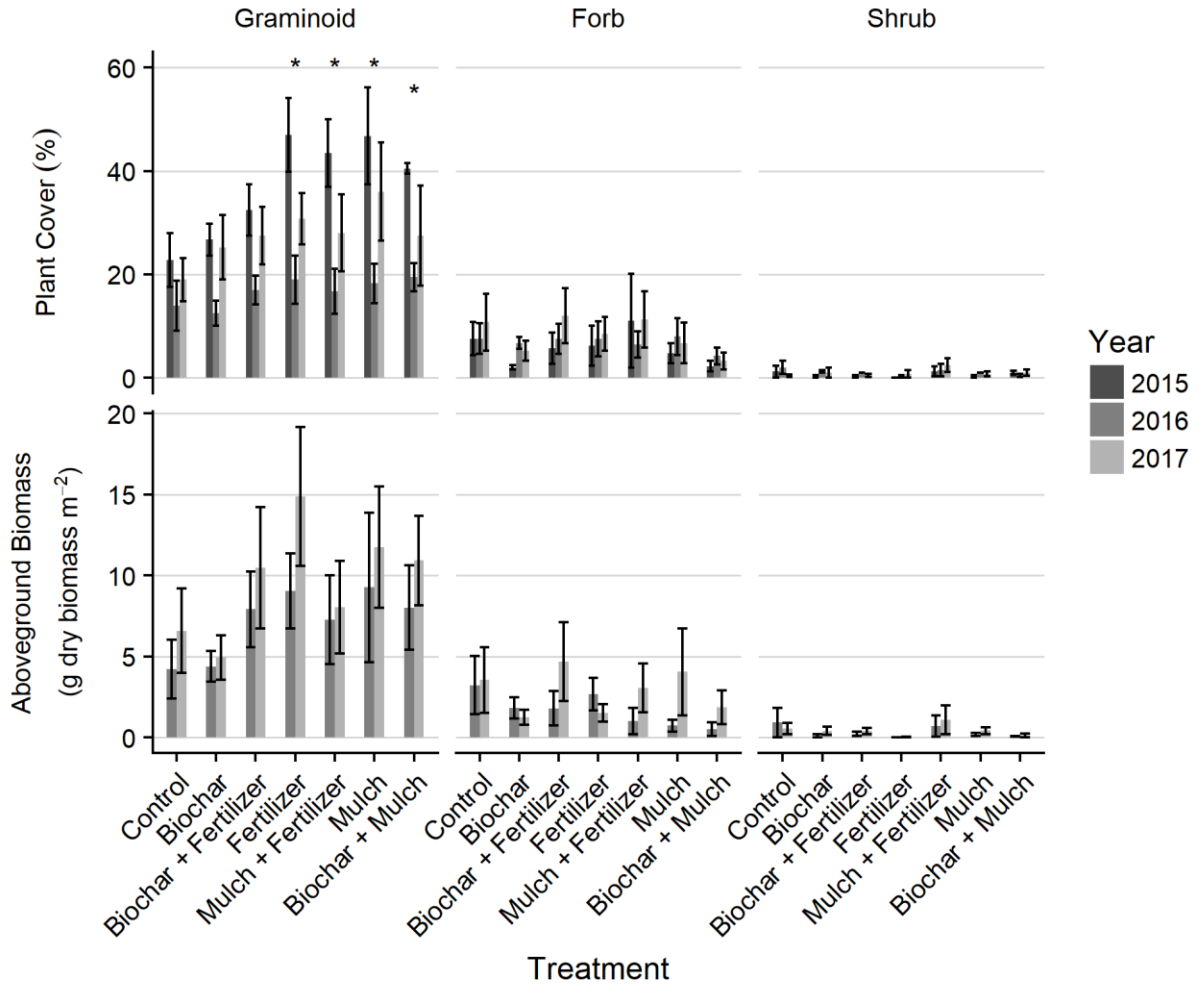


Fig. A7: Mean plant cover and aboveground biomass for each of the treatments by year for each plant functional group (graminoids, forbs, and shrubs). Error bars display one standard error, with significance effects across the three years denoted by * relative to the control treatment.

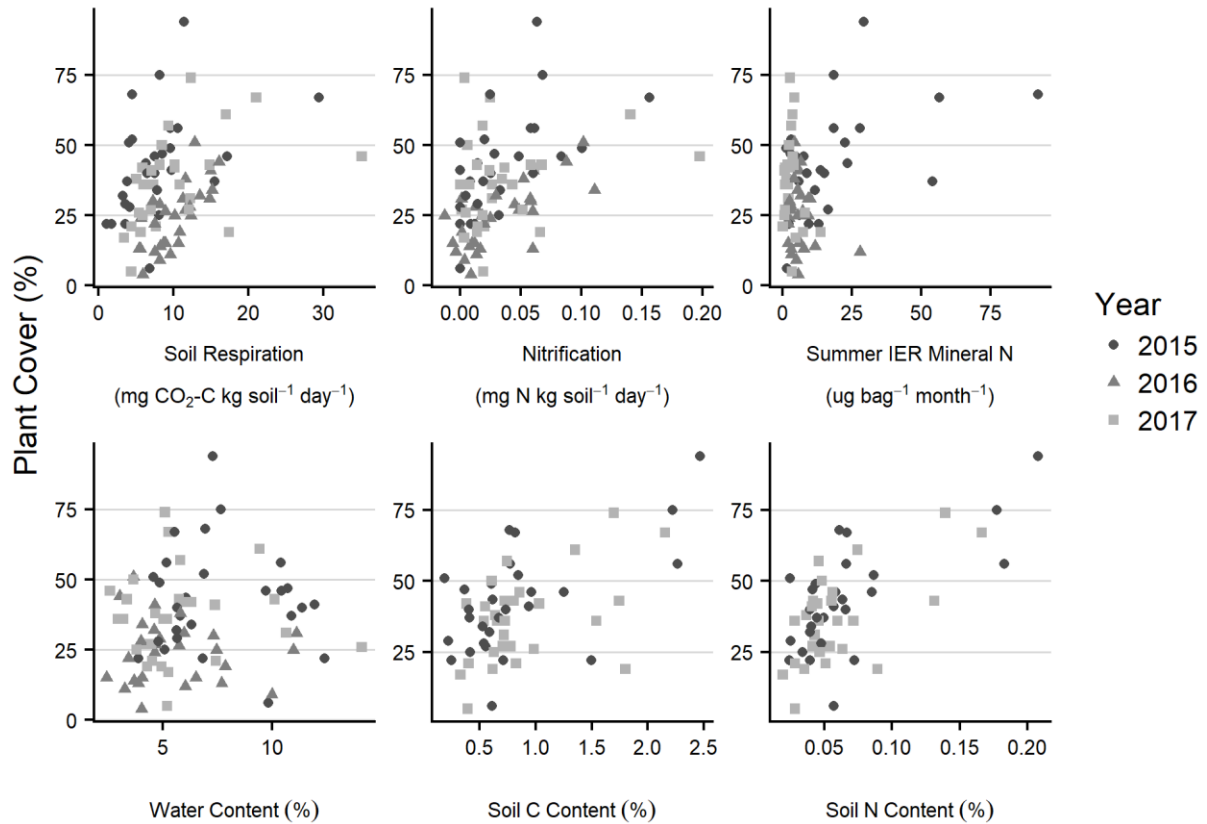


Fig. A8: Total plant cover responses to the best soil predictors of revegetation used in the multiple linear regression models. Predictors include soil respiration and potential nitrification from aerobic mineralization assay conducted in the fall of each year; ion exchange resin (IER) mineral N deployed in the field from May to Oct each year; mean gravimetric water content for each year; and soil C and N content from the 0-15 cm mineral soil depth sampled in 2015 and 2017.

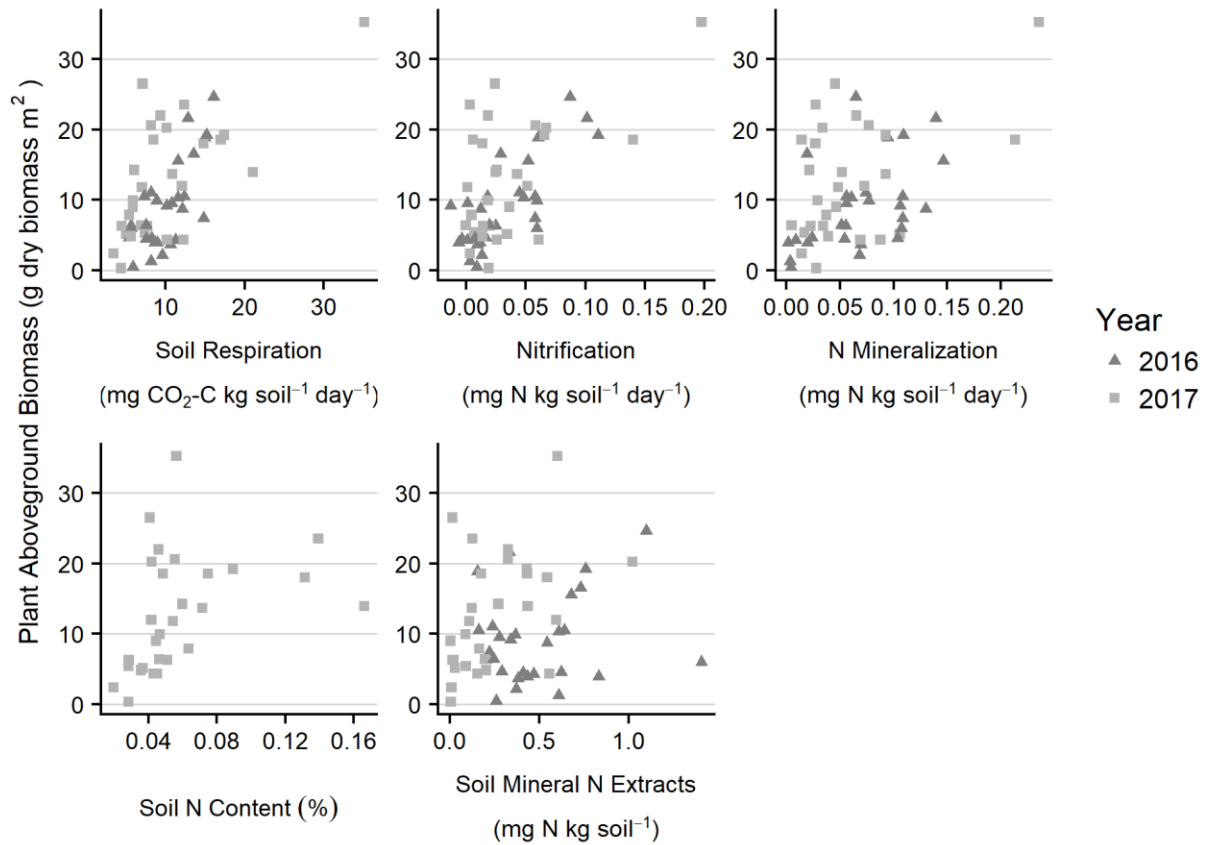


Fig. A9: Total plant aboveground biomass responses to the best soil predictors of revegetation used in the multiple linear regression models. Predictors include soil respiration, potential nitrification and potential N mineralization from aerobic mineralization assay conducted in the fall of each year; soil N content from the 0-15 cm mineral soil depth sampled in 2017; and mineral N extracted from soils sampled in the fall of each year.

Appendix 4. Chapter 5 Supplementary Information

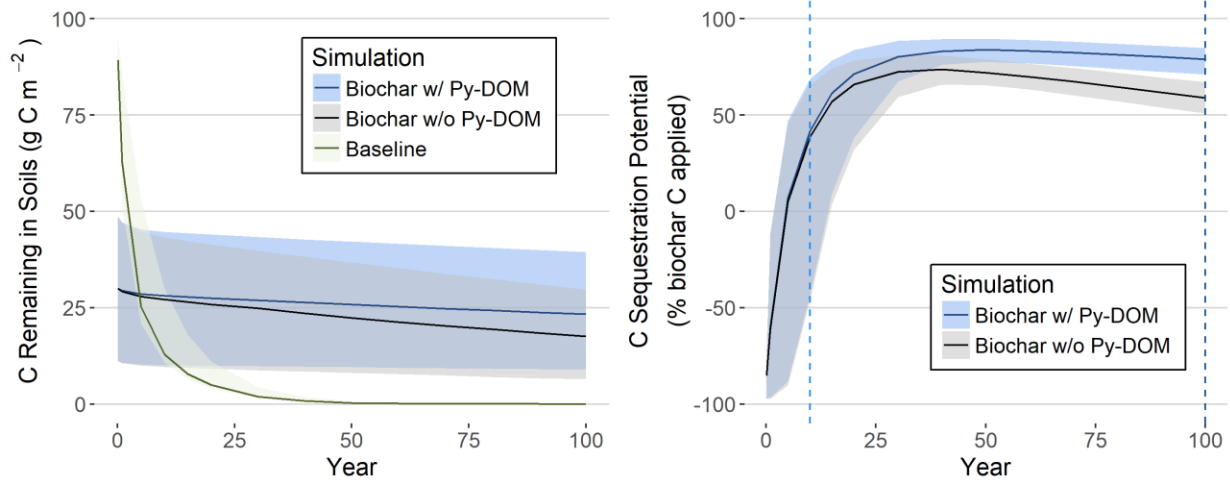


Fig. A10: 100-year MEMS-PyOM model run displaying the carbon remaining in soils for the biochar simulation including Py-DOM, biochar simulation not including Py-DOM and baseline simulation (left panel) and resulting biochar C sequestration potential including Py-DOM vs not including Py-DOM (biochar scenario – baseline scenario; right panel) over time. Shaded area displays the 95% confidence interval.